LA-13773-MS

Approved for public release;
distribution is unlimited.

Toward a General Theory for Multiphase Turbulence Part I: Development and Gauging of the Model Equations

Los Alamos
NATIONAL LABORATORY

Los Alamos National Laboratory is operated by the University of California for the United States Department of Energy under contract W-7405-ENG-36.

This work was supported by the U.S. Department of Energy, Office of Industrial Technologies.

An Affirmative Action/Equal Opportunity Employer

LA-13773-MS

Issued: December 2000

Toward a General Theory for Multiphase Turbulence Part I: Development and Gauging of the Model Equations

B. A. Kashiwa
W. B. VanderHeyden

Los Alamos
NATIONAL LABORATORY
Los Alamos, New Mexico 87545

Contents

Toward a General Theory for Multiphase Turbulence

Part I: Development and Gauging of the Model Equations

B. A. Kashiwa and W. B. VanderHeyden

Abstract

A formalism for developing multiphase turbulence models is introduced by analogy to the phenomenological method used for single–phase turbulence. A sample model developed using the formalism is given in detail. The procedure begins with ensemble averaging of the exact conservation equations, with closure accomplished by using a combination of analytical and experimental results from the literature. The resulting model is applicable to a wide range of common multiphase flows including gas–solid, liquid–solid and gas–liquid (bubbly) flows. The model is positioned for ready extension to three–phase turbulence, or for use in two–phase turbulence in which one phase is accounted for in multiple size classes, representing polydispersivity. The formalism is expected to suggest directions toward a more fundamentally based theory, similar to the way that early work in single–phase turbulence has led to the spectral theory.

The approach is unique in that a portion of the total energy decay rate is ascribed to each phase, as is dictated by the exact averaged equations, and results in a transport equation for energy decay rate associated with each phase. What follows is a straightforward definition of a turbulent viscosity for each phase, and accounts for the effect of exchange of fluctuational energy among phases on the turbulent shear viscosity. The model also accounts for the effect of slip momentum transfer among the phases on the production of turbulence kinetic energy and on the tensor character of the Reynolds stress. Collisional effects, when appropriate, are included by superposition.

The model reduces to a standard form in limit of a single, pure material, and is expected to do a credible job of describing multiphase turbulent flows in a wide variety of regimes using a single set of coefficients.

1. Introduction

The goal of this report is to take a step toward a general useful theory of multiphase turbulence. By general we mean a theory that has a wide range of applicability – so wide that one might be bold enough to apply it to circumstances for which there are no experimental data. By useful we mean a theory that can be applied readily by the practitioner possessing reasonable skill – and having an adequate need for doing so. Even the casual observer in this area will appreciate immediately the proliferation of both theories and of experimental correlations that have been devised, primarily motivated by engineering needs, for very specific problems in multiphase turbulence. Whereas this

large collection of data does serve to satisfy the "useful" part of the foregoing goal, one can argue that the knowledge as a whole fails to satisfy the "general" part of the goal.

In light of the well–known fact that single–phase turbulence theory currently falls far short of being sufficiently mature for the needs of many scientific and engineering problems, one could argue that the goal of the present work simply cannot be achieved. Such a position is easily defended. Nevertheless the pressures for making progress, exerted from all sectors, are sufficiently great to serve as inspiration to push forward; and we do so taking great satisfaction for having taken at least a small step toward an impossible goal.

To begin we need to clarify what we mean by multiphase turbulence, which requires us first to define what we mean by multiphase, and then what it means to say the flow is turbulent. For simplicity we do so by means of example, as follows.

Multiphase flow arises when the averaged motion of one material is distinctly different from that of another: droplets of rain falling in air, sand moving along a stream bed under the force of running water, or products of combustion forced through fractures between propellant grains in a modern high explosive are a few common examples. Typically we are interested only in the averaged behavior of the flow system, as opposed to wanting to know the exact history of a particular grain of sand, or of a particular rain drop. In the case of individual grains or drops, we can readily write down the equations of motion (complete with initial and boundary conditions) and solve them, yielding a full solution for their history. Unfortunately the solution for a single particle is generally inadequate for saying how the system works as a whole. Hence we can characterize the multiphase flow problem as one for which we want to know the averaged behavior of a system having a large number of degrees of freedom, knowing the behavior of one (or a small number) of the components making up the system. Such a problem is quite akin to that of determining the properties of a gas made up of a great many molecules, armed with only the knowledge of how one molecule behaves (or possibly two molecules).

The problem of fluid turbulence is similar to that of multiphase flow, in that we are likewise interested in the averaged dynamics of a system having a large (in fact infinite) number of degrees of freedom. In the case of a pure fluid we can likewise write down the equations of motion, and solve them, for a given region of space. The obvious difficulty is

that one may be interested in a region of space that is very large compared to the smallest scales of motion that the fluid will exhibit; and the averaged motion may be greatly influenced by the details of these small scales. So once again the practitioner interested in the average must devise a means of connecting the exact motion, which is known on a small scale, to the averaged motion on a larger scale. *Turbulence* is typically the name given to the small scale motions.

So small scale motions in multiphase flows and turbulence in a pure fluid share a common feature. They are both the well–defined dynamics that ultimately determine the averaged motion. This leads us to our working definition of *multiphase turbulence*: the small scale, fully determined dynamics having a significant influence on the large–scale motion of interest, in a system for which there are distinctly different averaged material velocities.

Given the foregoing definition it is obvious to ask, "What multiphase flow does not exhibit multiphase turbulence?" The practical answer is none, although we can cite a case for which the answer is debatable: namely the slow gravitational settling of a single sphere in an ocean of quiescent fluid (or the slow rise of a small bubble). If the settling speed is sufficiently slow, the small–scale motion is identical to the large–scale motion (provided Brownian motion is negligible). There is no difference between the mean and local motions, so there are no statistical fluctuations. However, if the settling speed is such that separation of the boundary layer can occur, and the wake becomes unstable, then a vortex street will ensue and small–scale motions in the fluid will begin to influence the averaged settling speed. Hence even a single perfect sphere can exhibit multiphase turbulence.

If we now add a second sphere to the foregoing thought experiment, the flow becomes even more turbulent, particularly if the separation is close enough for particle–fluid–particle interactions to develop, in which case the settling speed can be greatly affected. Because the motions at scales smaller than the spheres influence the mean motion, we shall call the small–scale motion multiphase turbulence.

Clearly our definition of multiphase turbulence is fuzzy, and intentionally so; after all, what is meant by *significant influence* depends on what the observer regards as being

important; just as with single–phase turbulence it depends on how closely the observer is looking. From the viewpoint of the Space Shuttle an astronaut might conclude that the motion of the earth's atmosphere, as indicated by the cloud motion, is changing slowly and smoothly: it is perfectly laminar. The simultaneous observer aboard a fishing boat in a gulf hurricane might conclude the opposite. Hence one persons's turbulence could be another person's idea of perfect serenity. What is absolutely wonderful about this fuzziness is that it makes no difference from the standpoint of the formalism used to develop models for describing this thing called turbulence – which can change if information is added. (Suppose further that the astronaut speaks via radio to her brother aboard the fishing boat. Her attitude toward the laminar nature of the atmosphere is likely to change substantially, owing only to a change in what it is that is of significance.)

In order to work, the formalism does require a strict adherence to a policy of consistency; as long as each part of the model equations are represented with the same attitude toward what is significant, then the result is one that is perfectly self–consistent. The full meaning of this will emerge by example later on, as the model equations are developed. By the end of the discussion it should be quite evident, however, that the consistency policy has powerful consequences. (Note: We avoid using the term *universality* with respect to this report because at this stage it would be presumptuous – and not because the authors think it has no relevance.)

We emphasize these semantical issues here because this terminology, and more important this line of thinking, is in contrast to some of the prior work. For example others have referred to the motions of the interacting spheres in the foregoing case as "pseudo–turbulence" precisely because the motions can exist no matter how slow is the flow (Lhuillier 1996, Buyevich 1999). The fact that the fluctuations (no matter how slow) can have a significant influence on the mean motion is precisely why we elect to call it multiphase turbulence. Furthermore, that being the case, the general theory used to describe the averaged motions (which is the subject of this report) must be capable of describing these slow fluctuations.

The implications of this broad line of thinking are both good and bad. For one thing it increases the difficulty of reaching the goal, but at the same time it opens up the

investigation to a wide range of high–quality (and available) experimental data against which to test (and to help guide) the developing theory. For example, some of the finest data for fluctuational energies and integral length scales, are to be found for dense slowly settling suspensions in the Stokes flow regime (Segrè et al. 1997).

In what follows, we develop a set of model equations which generally describe the averaged consequences of multiphase turbulence. In a subsequent report, we demonstrate the accuracy and scope of the model by applying it to the quantitative description of a wide array of prototypical turbulent flows including gas–solid flows in various geometries, liquid fluidized beds of solid grains, and bubble columns. This report is devoted to the formal development, and closure, of the model equations.

To make matters perfectly clear we emphasize that the developments here are of the phenomenological sort. That is, we permit the exact equations to furnish the general form of certain unknown terms in the model – and to these terms a physical interpretation is given on the basis of general conservation principles. This means that closures are determined in functional form from physical and mathematical arguments and are finally gauged by the available experimental data. This approach by itself is not expected to furnish the general theory, but is expected to lead in the right direction – as it has already done for the problem of single–fluid turbulence. In the meantime we hope that the range of applicability of the half–baked theory is wide enough to be of value to engineers and scientists whose unsolved problems continue to provide the motivation to get a better theory.

The report is laid out in eight sections. In § 2 the relevant, and accessible, literature is reviewed in a context specific to this work. The labor begins in § 3 where the exact equations for multiple materials are displayed, and then averaged using well–known methods. Whenever possible, a standard closure is utilized as soon as one appears to be necessary. In that way we can devote the entire § 4 to a discourse on the closures that are unique to the present work, where we obtain the closures in functional form, leaving the final determination of coefficients for a later section. Then in § 5 the so–called "structural equilibrium approximation" is made, and a perturbation method used to find a low–order solution for the multiphase Reynolds stress. In § 6 we address the problem of finding

the undetermined coefficients that arise from the phenomenological closure method, and which are consistent with the structural equilibrium approximation. For this we focus on the problems of isotropic decay and homogeneous sedimentation. In § 7 we finish the modeling tasks by introducing a necessary generalization to the boundary condition on material dissipation, at a solid wall. Finally § 8 is a summary of the work, a discussion which includes comments on the range of validity for the theory, and suggestions for follow up work.

In order to avoid any possible future confusion (or appearance of ambiguity), it is important to address two more semantical issues before getting started. First, we will use the terms *phase*, *field* and sometimes *fluid* interchangeably. This is because the multiple fields that may be considered are not always distinctly different phases of matter, and the materials may or may not behave as fluids. Second, we shall find it convenient to make use of the term *particle* in reference to selected kinds of bodies submerged in a fluid. The dialogue just flows better by using it. Unfortunately, the word particle is probably the one most overused word in all of physics. In atomic physics it is used synonymously with *molecule, atom, ion, electron, neutrino, quark*, and so on ad infinitum. In other disciplines it may mean *dust, droplet, bubble, grain, cotton ball, whisp, string, cluster, streamer, cannonball*, or *blob*. For this work we use particle in reference to some definite body, defined by the observer to be discrete, and submerged in an otherwise continuous fluid. (By this definition your Volkswagen, swept up by a tornado, is a particle.)

2. Relation to prior work

There are two distinct classes of prior work that furnish the foundation upon which the present results have been built. The first class is made up of works that can be considered phenomenological single–phase turbulence theories. The second class is made up of those works that have made a direct assault on the problem of multiphase turbulence. Both classes are huge. We make reference here to a subset in both classes not because the full set is unimportant, but rather because it is just too large to cover in a finite space. Hence we attempt to make reference to the most recent pieces of work that are relevant. The interested reader will find that the references to the literature given here, each have

important references themselves (and so on) which should be consulted in order to obtain a full appreciation of the long and varied history of this subject.

The formalism espoused here is largely adopted from the collection of single–phase turbulence works summarized nicely between Reynolds (1987), and Launder (1990). These two pieces form the tip of an iceberg that is the phenomenological approach to single–phase turbulence. They teach the basic method of averaging, interpretation of physical effects implied by the exact terms resulting from the averaging, and methods for modeling those terms on a physical basis. It is those methods that are used here, and extended for the multiphase case, to form what we are calling the formalism within which the model is developed. Of particular importance to the present work is the process of obtaining an approximate solution for the Reynolds stress, for which we have relied heavily on the so–called structural equilibrium approximation. This approximation is used by Gatski and Speziale (1993) whose work led us directly to the notion of using a perturbation expansion method shown later.

The multiphase extensions made to the foregoing single–phase turbulence approach can be split into two kinds: (1) extension from one material to multiple materials without regard to the turbulence, and (2) extension specifically to multiphase turbulence. Extension to multiple materials takes on the form of creating a whole discipline by itself, called *multiphase flow*. Helpful recent references in this area are the books by Drew & Passman (1999); Fan & Zhu (1998); Crowe et al. (1998); Gidaspow (1994); Roco (ed. 1993); and Soo (1990). For the purposes of teaching multiphase flow to the uninitiated reader, the lectures by Lhuillier (1996) should be considered mandatory. Lhuillier gives a full and concise treatment of multiphase flow for suspensions of particles in a way that covers mixture theory, continuum theory, and statistical theory – using a common and unifying language (which is something that all of the standard texts have failed to accomplish.)

Extension of the single–phase turbulence formalism to a specifically multiphase one is summarized, roughly, in the recent review article by Crowe et al. (1996). This review covers a broad range of both theoretical and experimental works that have collectively offered a substantial thrust toward the present status of the multiphase turbulence knowledge. The

experimental works include a large number of so–called "numerical experiments" that seek to perform a direct simulation of the exact dynamics underlying the averages of interest in this report. Specific reference to the experimental literature will be postponed until later, when we shall have occasion to need some data for gauging purposes.

For the theoretical part of extending the turbulence formalism to a multiphase one, there have been two basic approaches. By far the most common approach is to first get a set of multiphase equations by means of volume averaging the exact equations for a specific instantaneous topology. These volume–averaged equations are then decomposed into mean and fluctuating parts, and then averaged again (either by invoking the idea of an ensemble, or by time averaging). This technique was used recently by Crowe & Gillandt (1998); long ago by Elghobashi & Abou–Arab (1983); and in between times by a fairly large array of others (for example, Besnard & Harlow 1988, Viollet et al. 1992, Hwang & Shen 1993, Dasgupta et al. 1994, Cao & Ahmadi 1995). The double–averaging method is closely aligned with a continuum–mechanical approach. The opposing approach has been to use a statistical average of the exact equations, thereby obtaining the turbulent multiphase equations directly (in a single averaging step); shown in elegant fashion by Lhuillier (1996). Surprisingly there have been very few attempts to model these statistically averaged equations directly, even though it would appear to be the most natural way to extend the single–phase turbulence formalism to the multiphase one (Kashiwa 1987, Kashiwa & Gore 1991); this report is all about doing just that.

The fact that few works have been set forth that make a one–step jump to multiphase turbulence *for all fields* does not mean that the statistical (ensemble) methods are foreign to multiphase flow as a whole. Quite the contrary is true. Key contributions have been made to the first part of the extension (getting multiple material effects, but ignoring the turbulence) using the statistical average. Notable are the pioneering works of Saffman (1971) and Lundgren (1971) who established the crucial means by which the multiple materials could be identified and isolated in the averaging process. We make heavy use of their methods in the next section.

There has been of course, a successful but limited mixed approach to the problem of extending to the multiphase turbulence formalism. This has been in the granular flow

of solids, with a gaseous interstitial fluid. In this special case the interaction of the two phases is so weak that the dynamics of the fluctuating grains is largely unaffected by the surrounding gas, whose turbulence can be neglected altogether. The approach is mixed because a statistical average has been used for describing the dynamics of the grains, and a continuum method used for the weakly interacting (and typically nonturbulent) gas. A complete anthology of the work in this area beginning with Savage & Jeffrey (1981) is cataloged in the book by Gidaspow (1994). Other notable contributions to the mixed approach have been made by Ma & Ahmadi (1988) who attempted to bring in the finite effects of the interstitial fluid. In a less dense system where the grain–grain collision rate may be much lower, the fundamental work of Koch (1990) is notable; the work provides a potential link to some of the missing data for homogeneous sedimentation, and will be discussed more in § 6.

Finally there are certainly a host of other significant contributions from the prior work, some of which have a direct impact on the present work. These will be mentioned at the appropriate time in the body of the text in the sections that follow.

3. Averaged equations

The purpose of this section is to set the stage for later developments by selecting a closed set of conservation equations considered to describe the exact dynamics of multiple materials, any *one* of which can occupy a given point at an instant. These exact equations will be averaged using standard techniques and sample closures given whenever a reliable one is known to exist; for some parts closures do not exist. Nevertheless, it will be shown that both multiphase and turbulence features emerge naturally in the (single–step) averaging process, and some of those features will be discussed prior to going forward with closure procedures for the newly uncovered terms.

For illustration, we begin by considering a set of N materials, whose dynamics exclude a change in phase, and whose state may be fully described at a point in space and time $(\mathbf{x}, t)$, by the vector $(v_{\rm o}, \mathbf{u}_{\rm o}, \boldsymbol{\sigma}_{\rm o}, \alpha_{\rm r})$. The state vector represents, respectively, the volume occupied by a unit of mass, velocity, material stress, and $\mathbf{H}$ function for material r, with $1 \leq {\rm r} \leq N$. The function $\alpha_{\rm r}(\mathbf{x}, t)$ is a generalization of the $\mathbf{H}$ used by Saffman (1971). It

has a value of one if material r is at $(\mathbf{x}, t)$, and is zero otherwise. This generalized $\mathbf{H}$ is exactly the "phase function" adopted by Drew (1983), as well as the "function of presence" used by Lhuillier (1996), and has certainly been called other things by other authors – all having identically the same meaning; it provides a unique material identifier. Note that we use a subscript o to denote the state at a space–time point, and further that we have elected to describe the state by only those items that vary continuously in space, except for the generalized $\mathbf{H}$ function. Hence we ignore (for now) surface tension effects, and any other prestressing effects such as thermally induced internal stress. The variable $v_{\rm o}$ can be thought of as a state relation; it defines the volume that a unit mass of material would occupy if it were to exist at the local conditions of stress – and it is defined everywhere, whether or not r–material is at $(\mathbf{x}, t)$.

Let us further consider materials for which the stress is well represented by the sum of an isotropic pressure, and a (traceless) deviator. For many materials this decomposition is not possible, but for now it makes a helpful idealization, which can be improved at a later time. We shall suppose that the deviatoric part of the stress can be expressed as a simple function of the known state. In general we could, of course, consider materials whose stress is history dependent, rather than just state dependent, but such additional complexity does not offer anything substantive to the present discussion. (Furthermore, after making one small point, we shall very soon limit consideration to two incompressible materials, to simplify matters even more and, hopefully, increase the clarity at the same time.)

Before beginning, we make use of the kinematic relation for any volume (regardless of what may be in it), $(\partial v_{\rm o}/\partial t) + \mathbf{u}_{\rm o} \cdot \boldsymbol{\nabla} v_{\rm o} = v_{\rm o} \boldsymbol{\nabla} \cdot \mathbf{u}_{\rm o}$, and define $\rho_{\rm o} = 1/v_{\rm o}$. Accordingly we change the state vector into these terms $(\rho_{\rm o}, \mathbf{u}_{\rm o}, \boldsymbol{\sigma}_{\rm o}, \alpha_{\rm r})$ while remembering that $\rho_{\rm o}$ varies continuously in space. As a reminder we shall keep a functional equation on the side that relates the known specific volume to the pressure, $v_{\rm ro} = V_{\rm r}(p_{\rm o})$, so there will be one function $V_{\rm r}$ for each for our N materials.

The conservation equations describing the dynamics of foregoing set of materials are

$$\frac{\partial \alpha_{\rm r}}{\partial t} + \mathbf{u}_{\rm o} \cdot \boldsymbol{\nabla} \alpha_{\rm r} = 0 \qquad [3.1]$$

$$\frac{\partial \rho_{\rm o}}{\partial t} + \boldsymbol{\nabla} \cdot \rho_{\rm o} \mathbf{u}_{\rm o} = 0 \qquad [3.2]$$

$$\rho_{\rm o} \left(\frac{\partial \mathbf{u}_{\rm o}}{\partial t} + \mathbf{u}_{\rm o} \cdot \boldsymbol{\nabla} \mathbf{u}_{\rm o} \right) = \boldsymbol{\nabla} \cdot \boldsymbol{\sigma}_{\rm o} + \rho_{\rm o} \mathbf{g} \; . \qquad [3.3]$$

Equation [3.1] is simply the statement that a point originally associated with material r, is always associated with material r; it says that $\alpha_{\rm r}$ is a Lagrangian invariant. Equations [3.2] and [3.3] express volume conservation and momentum conservation for whatever material resides at $(\mathbf{x}, t)$. The stress in [3.3] requires evaluation of a state relation for the hydrodynamic pressure $p_{\rm o}$. Using our collection of side expressions, such a relation may be written

$$1 - \rho_{\rm o} \textstyle\sum_{\rm r=1}^{N} \alpha_{\rm r} V_{\rm r}(p_{\rm o}) = 0 \; , \qquad [3.4]$$

where the $\mathbf{H}$ function has once again been used to select the appropriate state relation for whatever material resides at the point. The statement made by [3.4] is, simply, to evaluate the state relation associated with the *one* nonzero $\mathbf{H}$ function, using the local hydrodynamic pressure given by $p_{\rm o}$. Similarly we can write $\nu_o = \sum_{\rm r=1}^{N} \alpha_{\rm r} \nu_{\rm r}$ to select the appropriate viscosity $\nu_{\rm r}$; and use $\mathbf{S}_{\rm o}$ for the symmetric, traceless rate of strain, so that the stress may finally be expressed $\boldsymbol{\sigma}_{\rm o} = -p_{\rm o}\mathbf{I} + \nu_{\rm o}\mathbf{S}_{\rm o}$. Because the rate of strain in a rigid body is locally zero, we can simply set $\nu_{\rm r} = 0$ for any material whose behavior can be idealized as rigid (Joseph & Lundgren 1990), and compute the motion accordingly (which just places velocity boundary conditions on the inside of a fluid domain, for example).

So the system is fully closed in the usual sense of having as many equations as there are unknowns. Given a proper set of initial and boundary conditions they can be, and are very frequently, solved numerically. Because the domain over which the equations can be solved for practical cases is limited, and because we are mainly interested large–scale averaged behavior anyway, we shall resort to averaging these equations knowing that solutions to the averaged equations over a comparatively large domain can be found with considerably less computational effort.

Before proceeding to conduct our ensemble averaging operations, we are obliged to inject a remark concerning Eq. [3.1] for the generalized $\mathbf{H}$, which is a discontinuous function. In the mathematical sense the variable $\alpha_{\rm r}(\mathbf{x}, t)$ is a "weak solution" satisfying

the differential equation (Kevorkian 1974). (Such a function is piecewise continuous and at least once differentiable). We shall regard the differential equation itself as a shorthand expression for the integral form (over some finite volume of space), which is always valid, even in the presence of discontinuities in the state. In what follows we use the variable $\alpha_{\rm r}$ as a placeholder that reminds us where it is that additional physics must be inserted, and then we proceed to insert what is needed to make the *averaged* equations complete in a way that reflects the exact nature of the unknown terms (a process called closure).

The average we prefer is the ensemble average, mainly because of its conceptual simplicity, not to mention the operational simplicity when compared to volume or time averages. Like most authors following Saffman (1971) we use angle brackets $\langle\ \rangle$ to denote the ensemble average, which formally is thought of as an integral over an appropriate probability function, weighted by a some function of the independent variables making up the phase space of the probability function. In what follows we will simply use the ensemble average as an operator, so we just need to know the rules of operation. First, the operations of averaging and *partial* time differentiation commute because the time is an independent variable in the averaging operator. Hence

$$\left\langle \frac{\partial \phi}{\partial t} \right\rangle = \frac{\partial}{\partial t} \langle \phi \rangle$$

where ϕ is any variable (or product of variables), continuous or not. Second, the averaging operator commutes with spatial differentiation only for smooth functions (like the averages themselves); for discontinuous functions there is a remainder called a jump density. We shall isolate these jump densities by using a trick that apparently is due to Lundgren (1971), whereby we manipulate the weighting functions using the product rule from calculus, prior to commuting the operations of averaging and differentiation. Hence we will use

$$\left\langle \alpha_{\rm r} \frac{\partial q_{\rm o}}{\partial x} \right\rangle = \frac{\partial}{\partial x} \langle \alpha_{\rm r} q_{\rm o} \rangle - \left\langle q_{\rm o} \frac{\partial \alpha_{\rm r}}{\partial x} \right\rangle \ ;$$

whose second part on the right is the jump density; it represents a conservative exchange of $q_{\rm o}$ among the fields (Lundgren 1971).

We shall be interested in the mean mass density, and mean momentum density, defined

$$\rho_{\rm r} = \langle \alpha_{\rm r} \rho_{\rm o} \rangle \equiv \text{mean r–material total mass density}$$

$$\rho_{\rm r}\mathbf{u}_{\rm r} = \langle \alpha_{\rm r}\rho_{\rm o}\mathbf{u}_{\rm o}\rangle \equiv \text{mean r–material momentum density}$$

whose evolution equations will be conveniently expressed in terms of the averages

$$\boldsymbol{\sigma} = \langle \boldsymbol{\sigma}_{\rm o}\rangle \equiv \text{mean mixture stress}$$

$$\theta_{\rm r} = \langle \alpha_{\rm r}\rangle \equiv \text{mean r–material } \mathbf{H} \text{ function}$$

$$\theta_{\rm r}\boldsymbol{\sigma}_{\rm r} = \langle \alpha_{\rm r}\boldsymbol{\sigma}_{\rm o}\rangle \equiv \text{mean r–material stress}$$

with associated fluctuational parts defined

$$\mathbf{u}'_{\rm r} = \mathbf{u}_{\rm o} - \mathbf{u}_{\rm r} \equiv \text{r–material velocity fluctuation}$$

$$\boldsymbol{\sigma}' = \boldsymbol{\sigma}_{\rm o} - \boldsymbol{\sigma} \equiv \text{stress fluctuation}$$

with averages of the velocity fluctuation giving the all–important multiphase Reynolds stress density, and its corresponding fluctuational energy density

$$\rho_{\rm r}\mathbf{R} = \langle \alpha_{\rm r}\rho_{\rm o}\mathbf{u}'_{\rm r}\mathbf{u}'_{\rm r}\rangle \equiv \text{r–material Reynolds stress density}$$

$$\rho_{\rm r}k_{\rm r} = \left\langle \alpha_{\rm r}\rho_{\rm o}\tfrac{1}{2}u'^2_{\rm r}\right\rangle \equiv \text{r–material fluctuational energy density.}$$

In these we make use of dyadic notation, so that $\mathbf{uu}$ is a second order tensor. The equations for the various densities are found by taking the time derivative of the ensemble average and rearranging, making use of the exact equations [3.1–3.4]. For example,

$$\begin{aligned}\frac{\partial \rho_{\rm r}}{\partial t} = \frac{\partial}{\partial t}\langle \alpha_{\rm r}\rho_{\rm o}\rangle &= \left\langle \rho_{\rm o}\frac{\partial \alpha_{\rm r}}{\partial t} + \alpha_{\rm r}\frac{\partial \rho_{\rm o}}{\partial t}\right\rangle \\ &= -\boldsymbol{\nabla}\langle \alpha_{\rm r}\rho_{\rm o}\mathbf{u}_{\rm o}\rangle \\ &= -\boldsymbol{\nabla}\rho_{\rm r}\mathbf{u}_{\rm r}\ ,\end{aligned}$$

which is the multiphase mass conservation equation. In similar fashion, we have

$$\frac{\partial \rho_{\rm r}\mathbf{u}_{\rm r}}{\partial t} + \boldsymbol{\nabla}\cdot\rho_{\rm r}\mathbf{u}_{\rm r}\mathbf{u}_{\rm r} = -\boldsymbol{\nabla}\cdot\langle \alpha_{\rm r}\rho_{\rm o}\mathbf{u}'_{\rm r}\mathbf{u}'_{\rm r}\rangle + \langle \alpha_{\rm r}\boldsymbol{\nabla}\cdot\boldsymbol{\sigma}_{\rm o}\rangle + \rho_{\rm r}\mathbf{g}\ .$$

In this, we have made use of the identity $\langle \alpha_{\rm r}\rho_{\rm o}\mathbf{u}'_{\rm r}\rangle \equiv 0$, which is implied by the definitions of $\mathbf{u}_{\rm r}$ and its associated fluctuational velocity. The mass conservation equation is fully determined as a result of our choice of using a mass–weighted ensemble average, now commonly referred to as the "Favre" average (Besnard and Harlow 1988). The first term

on the right of the mean momentum equation is the acceleration due to what we have called the multiphase Reynolds stress. The second term will be immediately reconfigured using mean and fluctuating stresses, and Lundgren's trick:

$$\begin{aligned}\langle \alpha_{\rm r} \boldsymbol{\nabla} \cdot \boldsymbol{\sigma}_{\rm o} \rangle &= \langle \alpha_{\rm r} \rangle \, \boldsymbol{\nabla} \cdot \boldsymbol{\sigma} + \langle \alpha_{\rm r} \boldsymbol{\nabla} \cdot \boldsymbol{\sigma}' \rangle \\ &= \langle \alpha_{\rm r} \rangle \, \boldsymbol{\nabla} \cdot \boldsymbol{\sigma} + \boldsymbol{\nabla} \cdot \langle \alpha_{\rm r} \boldsymbol{\sigma}' \rangle + \langle \boldsymbol{\sigma}' \cdot \boldsymbol{\nabla} \alpha_{\rm r} \rangle \\ &= \theta_{\rm r} \boldsymbol{\nabla} \cdot \boldsymbol{\sigma} + \boldsymbol{\nabla} \cdot \theta_{\rm r} (\boldsymbol{\sigma}_{\rm r} - \boldsymbol{\sigma}) + \mathbf{F}_{\rm r}\end{aligned}$$

which extracts the momentum exchange force density denoted simply by $\mathbf{F}_{\rm r}$ (and frequently modeled by an empirical coefficient times the difference in mean material velocities). The foregoing arrangement also neatly displays the acceleration due to the mean mixture stress $\boldsymbol{\sigma}$ (first term) as well as the acceleration due to r–averaged deviations from the mean mixture stress (second term).

Before going on to display specific closures for the mixture stress, material stress, and the force density, it is worthwhile to pause and examine what we have so far, with certain approximations. That is, let us just suppose that the effects of Reynolds stress and deviatoric part of the mixture stress are negligible for a given problem (or said another way, suppose we want to find out *if* those effects may be negligible). Furthermore, suppose that there is negligible difference between the mixture stress (pressure) and the r–averaged stress. What is left? If we let $-p\mathbf{I}$ denote the isotropic part of the mixture stress, then the equations boil down to simply

$$\frac{\partial \rho_{\rm r}}{\partial t} + \boldsymbol{\nabla} \rho_{\rm r} \mathbf{u}_{\rm r} = 0 \qquad [3.5]$$

$$\frac{\partial \rho_{\rm r} \mathbf{u}_{\rm r}}{\partial t} + \boldsymbol{\nabla} \cdot \rho_{\rm r} \mathbf{u}_{\rm r} \mathbf{u}_{\rm r} = -\theta_{\rm r} \boldsymbol{\nabla} p + \mathbf{F}_{\rm r} + \rho_{\rm r} \mathbf{g} \qquad [3.6]$$

so the equations are nearly closed; they just lack relations for $\theta_{\rm r}$ and p. To complete the job, take the ensemble average of the state relation [3.4]

$$1 - \textstyle\sum_{\rm r=1}^{N} \langle \alpha_{\rm r} \rho_{\rm o} V_{\rm r}(p_{\rm o}) \rangle = 0 \; .$$

Now suppose that the averaged function $\alpha_{\rm r}$, which represents the expectation that r–material will reside at $(\mathbf{x}, t)$, is identical to the volume fraction. This means that

$\theta_{\rm r} \equiv \rho_{\rm r} V_{\rm r}(p)$, which is a closure assumption, and one that is frequently (but not always) made. Having made this assumption, however, means that the state relation becomes simply

$$1 - \sum_{\rm r=1}^{N} \rho_{\rm r} V_{\rm r}(p) = 0 \ , \qquad [3.7]$$

and we have a closed set of equations. The averaged state relation, in this approximation, says "find the one value of p, which when used in the collection of functions $V_{\rm r}(p)$ will yield a unit sum of volume fractions". This is an equilibrium assumption, and so we shall refer to p as the equilibration pressure: it is the pressure that permits masses $\rho_{\rm r}\mathtt{V},\ 1 \leq {\rm r} \leq N$, to fill an arbitrary volume $\mathtt{V}$.

In order to appreciate the full meaning of the equilibration pressure, let us place the state relation in rate form, by taking the partial time derivative, making use of the mean mass equation, and using the differential expansion $dv_{\rm r} = (\partial v_{\rm r}/\partial p)dp$, where $v_{\rm r} = V_{\rm r}(p)$. The result is

$$\sum_{\rm r=1}^{N} (\theta_{\rm r} v_{\rm r}/c_{\rm r}^2) \left(\frac{\partial p}{\partial t} + \mathbf{u}_p \cdot \boldsymbol{\nabla} p \right) + \boldsymbol{\nabla} \cdot \sum_{\rm r=1}^{N} \theta_{\rm r} \mathbf{u}_{\rm r} = 0 \ , \qquad [3.8]$$

in which the transport velocity is $\mathbf{u}_p = \sum_{\rm r=1}^{N} (\mathbf{u}_{\rm r} \theta_{\rm r} v_{\rm r}/c_{\rm r}^2) / \sum_{\rm r=1}^{N} (\theta_{\rm r} v_{\rm r}/c_{\rm r}^2)$, and where we use $-(c_{\rm r}/v_{\rm r})^2 = (\partial v_{\rm r}/\partial p)$ for the r–material compressibility. This is still the state relation, which is to be thought of as the equation that determines p. In the limit that all material compressibilities go to zero, it says that the volume–averaged mean velocity $\mathbf{u} = \sum_{\rm r=1}^{N} \theta_{\rm r} \mathbf{u}_{\rm r}$ is solenoidal. (As will be seen shortly, the mean deviatoric stress is also conveniently expressed in terms of the solenoidal velocity, so it is given here the special symbol $\mathbf{u}$.) The equation for the pressure is found by multiplying each momentum equation by the corresponding (constant) specific volume of the material, and adding. The time–derivative is eliminated by using the mass equations and the solenoidality condition. This yields a boundary value problem (that is, a Poisson equation) for p, whose solution determines p up to an additive constant (unless one of the boundaries has a fixed pressure, thereby gauging p). The foregoing character of the system is well known, and has been used for years for the study of multiphase dynamics of incompressible materials.

To summarize so far Eqs. [3.1–3.4] are supposed to be an exact representation of the dynamics of multiple compressible materials; their ensemble averaged form, in the

nonturbulent limit, reduces to a closed set given by Eqs. [3.5–3.7], or equivalently by [3.5, 3.6, 3.8], plus a model for a force density. If one were to express the exchange force density in terms of only the nonviscous (potential flow) effects, then these could be called the multiphase Euler equations; this is essentially the starting place assumed in much of the early multiphase turbulence work (Besnard and Harlow 1988, for example). The starting place used here is already established, and to go forward one needs only to follow through with the development of the equation for the multiphase Reynolds stress. First, however we need to finish the business of managing the other stress terms in the mean momentum equation, so we need expressions for the exact term $\langle \alpha_{\rm r} \boldsymbol{\nabla} \cdot \boldsymbol{\sigma}_{\rm o} \rangle$ (which contains the mixture stress, material stress, and momentum force jump density).

Fortunately, very reasonable closures for the mixture stress, material stress, and the force density all exist, and are even classical by now. The mixture stress is approximated by making use of Einstein's well–known result

$$\boldsymbol{\sigma} = -p\mathbf{I} + \mu_{\rm r}(1 + \tfrac{5}{2}\theta_{\rm s})\mathbf{S} \ ,$$

where it is assumed that the r–field is continuous and the s–field is dispersed, and where the symmetric traceless rate of strain is based on the solenoidal velocity $\mathbf{u}$ (Lhuillier 1996).

The material stress due to direct collisional interaction between elastic solid grains has been fully developed by analogy to the kinetic theory of gases, and by neglecting the intermediary role of the fluid in which the grains are immersed. Results are summarized nicely in the book by Gidaspow (1994) and are displayed here in Appendix A, for the convenience of the reader. For the present discussion it is sufficient to know that a recipe exists for our use, valid in some approximation not too far from practical conditions, when we need it. What is important here, however, is that we shall find it convenient to consider the multiphase Reynolds stress as the thing that represents all the consequences of fluctuational processes, including direct grain–grain collisions, in the special case for which such effects are nonnegligible. We shall model grain–grain effects by superposition, a matter that is discussed more fully in § 4.

The momentum exchange (drag) force density $\mathbf{F}_{\rm r}$ is probably the single most widely researched aspect of multiphase flow as a discipline. Significant contributions date clear

back to the time of Kelvin and the legion of subsequent workers who engaged in the study of potential flow around fixed bodies; work whose relevance to the present endeavor must have been completely unknown to Kelvin. Later the viscous flow contributions of Stokes, and many other followers, provided a long list of analytical and experimental results that form an important cornerstone of this field. Current workers consider such things as the "Stokes drag coefficient for a sphere" as being elementary common knowledge. (Rather than to recapitulate the standard results for a momentum exchange force density, we refer the interested reader to any of the many texts mentioned in the Introduction for extensive discussion of the matter.)

For the purposes of this work it will suffice nicely to use only the simplest of all possible expressions for the drag force density, that is

$$\mathbf{F}_{\rm r} = \sum_{{\rm s}=1}^{N} K_{\rm rs}(\mathbf{u}_{\rm s} - \mathbf{u}_{\rm r})$$

where the scalar coefficient $K_{\rm rs}$, having dimensions of mass density per unit of time, gives the rate at which fields r and s exchange momentum due processes of viscous shear and flow separation. To be sure there are many other physical effects that could be considered, and must be for some applications. For example the coefficient is surely a second–order tensor, in general, that must depend on mean flow gradients and which gives rise to a force perpendicular to the mean relative flow (lift). A resistance to relative acceleration is also known to be an important part of the full force, especially for bubbly flows. For the developments of this section and the next, the foregoing form is adequate. In fact, we really only need to consider the case of two materials, so we can dispense with the summation and will do so from this point forward. Thus the subscript r will always refer to one material, and where necessary s will be used to denote the material that is not r.

If we assume that the drag force on a single sphere with diameter d of r–material, whose mean velocity relative to that of s–material is $\mathbf{u}_{\rm r} - \mathbf{u}_{\rm s}$, then it is a straightforward matter to deduce that the force density of a collection of such spheres all of which experience the same drag force, would be given by $\mathbf{F}_{\rm r} = K_{\rm rs}(\mathbf{u}_{\rm s} - \mathbf{u}_{\rm r})$ where

$$K_{\rm rs} = \theta_{\rm r}\theta_{\rm s}\tfrac{3}{4}C_d\rho^{\rm o}_{\rm rs}|\mathbf{u}_{\rm s} - \mathbf{u}_{\rm r}|/d \ ,$$

which could be called the "standard form" for the force density, with fluid density $\rho^{\rm o}_{\rm rs}$ and drag coefficient C_d. The coefficient $K_{\rm rs}$ is a characteristic density, times a characteristic rate (inverse time scale). Many other embellishments can be made to improve the correlation to experimental data, and are typically invoked on a case–by–case basis. The important thing to note is that the turbulence model developed here depends mainly on the force density $\mathbf{F}_{\rm r}$ itself – whatever it may be for the particular physical conditions of interest. The model does *not* specifically depend on a having a certain configuration, such as a monodispersed, dilute suspension of spheres. The model does depend on a knowledge of the length scale associated with the momentum exchange process, which can be determined from the rate part of $K_{\rm rs}$; in this case it is a constant and is called d. (In general this length scale can be space–time varying in ways that depend on the turbulence itself.)

We are now ready to complete the unfinished matter of expressing the full multiphase Reynolds stress equation, a process that is greatly facilitated by first rewriting [3.3] using the definition of the r–material velocity fluctuation as follows:

$$\rho_{\rm o}\left(\frac{\partial \mathbf{u}_{\rm r}}{\partial t}+\mathbf{u}_{\rm r}\cdot\boldsymbol{\nabla}\mathbf{u}_{\rm r}\right)+\rho_{\rm o}\left(\frac{\partial \mathbf{u}_{\rm r}}{\partial t}+\mathbf{u}_{\rm r}\cdot\boldsymbol{\nabla}\mathbf{u}'_{\rm r}+\mathbf{u}'_{\rm r}\cdot\boldsymbol{\nabla}\mathbf{u}_{\rm r}+\mathbf{u}'_{\rm r}\cdot\boldsymbol{\nabla}\mathbf{u}'_{\rm r}\right)=\boldsymbol{\nabla}\cdot\boldsymbol{\sigma}_{\rm o}$$

or equivalently, using component (indicial) notation with summation implied,

$$\rho_{\rm o}\left(\frac{\partial u_{{\rm r}i}}{\partial t}+u_{{\rm r}k}\nabla_k u_{{\rm r}i}\right)+\rho_{\rm o}\left(\frac{\partial u_{{\rm r}i}}{\partial t}+u_{{\rm r}k}\nabla_k u'_{{\rm r}i}+u'_{{\rm r}k}\nabla_k u_{{\rm r}i}+u'_{{\rm r}k}\nabla_k u'_{{\rm r}i}\right)=\nabla_j\sigma_{{\rm o}ij}$$

which can then be multiplied by $\alpha_{\rm r}\mathbf{u}'_{\rm r}$ and averaged. This is identical to taking the time derivative of, for example, $\langle\alpha_{\rm r}\rho_{\rm o}\frac{1}{2}\mathbf{u}_{\rm o}\cdot\mathbf{u}'_{\rm r}\rangle=\left\langle\alpha_{\rm r}\rho_{\rm o}\frac{1}{2}u'^2_{\rm r}\right\rangle=\rho_{\rm r}k_{\rm r}$, which again makes use of the fact that $\langle\alpha_{\rm r}\rho_{\rm o}\mathbf{u}'_{\rm r}\rangle=0$, by definition. This procedure was shown by Lhuillier (1996) and minimizes the steps in the development, providing a very useful way of avoiding mistakes in the algebra. Following this method, we readily find the exact equation for fluctuational energy. To make things a bit more compact we also use the mean r–material mass equation to express the time derivative in Lagrangian form using the overdot to represent differentiation relative to the mean r–material motion. That is $\dot{a}_{\rm r}=\partial a_{\rm r}/\partial t+\mathbf{u}_{\rm r}\cdot\boldsymbol{\nabla}a_{\rm r}$. With this convention, the fluctuational energy equation is

$$\rho_{\rm r}\dot{k}_{\rm r}+\rho_{\rm r}\mathbf{R}_{\rm r}:\boldsymbol{\nabla}\mathbf{u}_{\rm r}=-\boldsymbol{\nabla}\cdot\left\langle\alpha_{\rm r}\rho_{\rm o}\mathbf{u}'_{\rm r}\tfrac{1}{2}u'^2_{\rm r}\right\rangle+\langle\alpha_{\rm r}\mathbf{u}'_{\rm r}\cdot\boldsymbol{\nabla}\cdot\boldsymbol{\sigma}_{\rm o}\rangle\ .$$

The first right side term is obviously the fluctuational transport of mean fluctuational energy, typically modeled with a diffusion term by analogy to a heat flux. The second right side term can be expanded to extract the jump density. That is

$$\begin{aligned}\langle \alpha_{\rm r} \mathbf{u}'_{\rm r} \cdot \boldsymbol{\nabla} \cdot \boldsymbol{\sigma}_{\rm o} \rangle &= \langle \alpha_{\rm r} \mathbf{u}'_{\rm r} \rangle \cdot \boldsymbol{\nabla} \cdot \boldsymbol{\sigma} + \langle \alpha_{\rm r} \mathbf{u}'_{\rm r} \cdot \boldsymbol{\nabla} \cdot \boldsymbol{\sigma}' \rangle \\ &= \langle \alpha_{\rm r} \mathbf{u}'_{\rm r} \rangle \cdot \boldsymbol{\nabla} \cdot \boldsymbol{\sigma} + \boldsymbol{\nabla} \cdot \langle \alpha_{\rm r} \mathbf{u}'_{\rm r} \cdot \boldsymbol{\sigma}' \rangle - \langle \alpha_{\rm r} \boldsymbol{\sigma}' : \boldsymbol{\nabla} \mathbf{u}'_{\rm r} \rangle - \langle \mathbf{u}_{\rm r} \cdot \boldsymbol{\sigma}' \cdot \boldsymbol{\nabla} \alpha_{\rm r} \rangle\end{aligned}$$

where the first line is used to decompose the stress into mean and fluctuating parts, and the second is used to expose the jump density. The first right side term of the second line appears to be a fluctuational work term; it goes to zero in the incompressible limit whereby $\langle \alpha_{\rm r} \mathbf{u}'_{\rm r} \rangle = 0$. Our first closure simplification will be to assume incompressiblity of all materials so that we can neglect the first right side term. The second right side term of line two is identified with pressure–velocity fluctuational correlations; it is in conservation form (an average, under the gradient operator) and will ultimately be modeled as part of a diffusion–like term. The third right side term is clearly nonconservative (considered by itself). Recall that the stress is composed of both pressure and deviator parts: the third term then appears to represent, in effect, the dissipation of fluctuational energy plus the effect of pressure–velocity fluctuational correlations. The last right side term is the jump density and will be the dominant subject of discussion shortly; it is the only term in the equation for fluctuational energy that does not have a single–field counterpart. The last term represents strictly multiphase turbulence, and this is the payoff for having gone about the business of finding the multiphase and turbulence equations simultaneously. The payoff is that we can focus nearly all of our attention on the modeling of this one term, because the entire rest of the equation system has been addressed in one way or another by prior workers in the area of single–phase turbulence.

The equation for $\mathrm{R}_{{\rm r}ij}$ is found by adding $\alpha_r u'_{{\rm r}i}$ times the equation for $\rho_{\rm o} u_{{\rm o}j}$ to $\alpha_r u'_{{\rm r}j}$ times the equation for $\rho_{\rm o} u_{{\rm o}i}$, and averaging. The result, having already extracted the jump density (and having passed to the incompressible limit), is

$$\rho_{\rm r} \dot{\mathrm{R}}_{{\rm r}ij} + \rho_{\rm r} \mathrm{R}_{{\rm r}(ik} \nabla_k u_{{\rm r}j)} = -\nabla_k \mathrm{J}_{{\rm r}kij} - \rho_{\rm r} \varepsilon_{\rm r} \tfrac{2}{3} \delta_{ij} + \Pi_{{\rm r}ij} - \left\langle u'_{{\rm r}(i} \sigma'_{j)k} \nabla_k \alpha_{\rm r} \right\rangle \ . \qquad [3.9]$$

Here we use the subscript parentheses to indicate symmetrization with respect to the enclosed indices (that is, $A_{(ij)} = A_{ij} + A_{ji}$.) In the manner of Launder (1990) we also use

$$\left\langle \alpha_{\rm r} u'_{{\rm r}i} \sigma'_{jk} - \alpha_{\rm r} \rho_{\rm o} u'_{{\rm r}k} u'_{{\rm r}(i} u'_{{\rm r}j)} \right\rangle = -{\rm J}_{{\rm r}kij}$$

for the triple correlations, and

$$-\left\langle \alpha_{\rm r} \sigma'_{(ik} \nabla_k u'_{{\rm r}j)} \right\rangle = -\rho_{\rm r} \varepsilon_{\rm r} \tfrac{2}{3} \delta_{ij} + \Pi_{{\rm r}ij}$$

to define the r–material dissipation rate $\varepsilon_{\rm r}$ and its partner the so–called traceless isotropization tensor $\Pi_{{\rm r}ij}$, a model that implicitly ignores the deviatoric part of the dissipation tensor.

In anticipation of our next steps, we shall model triple correlations in standard fashion. That is, in the section that follows we find an approximate solution to [3.9] whereby we ignore the $\nabla_k {\rm J}_{{\rm r}kij}$ term altogether, meaning that only the contraction is required for use in the $k_{\rm r}$ equation. The contraction is modeled by a diffusive form in which the flux is

$$\mathbf{J}_{\rm r}^{(k)} = -\rho_{\rm r} (\nu_{\rm r}/\sigma_k) \boldsymbol{\nabla} k_{\rm r}$$

(Launder & Spalding 1974) where, as usual, σ_k is a coefficient expected to be near one. This is often called a gradient approximation; the turbulent viscosity $\nu_{\rm r}$ will be defined in the next section.

By way of an interim summary, in addition to [3.9] and the sample closures given previously for $\boldsymbol{\sigma}, \boldsymbol{\sigma}_{\rm r}$, and $\mathbf{F}_{\rm r}$, we have so far

$$\dot{\rho}_{\rm r} + \rho_{\rm r} \boldsymbol{\nabla} \cdot \mathbf{u}_{\rm r} = 0 \qquad [3.10]$$

$$\rho_{\rm r} \dot{\mathbf{u}}_{\rm r} + \boldsymbol{\nabla} \cdot \rho_{\rm r} \mathbf{R}_{\rm r} - \theta_{\rm r} \boldsymbol{\nabla} \cdot \boldsymbol{\sigma} - \boldsymbol{\nabla} \cdot \theta_{\rm r} (\boldsymbol{\sigma}_{\rm r} - \boldsymbol{\sigma}) - \mathbf{F}_{\rm r} - \rho_{\rm r} \mathbf{g} = 0 \qquad [3.11]$$

$$\boldsymbol{\nabla} \cdot \mathbf{u} = 0 \qquad [3.12]$$

$$\rho_{\rm r} \dot{k}_{\rm r} + \rho_{\rm r} \mathbf{R}_{\rm r} : \boldsymbol{\nabla} \mathbf{u}_{\rm r} + \boldsymbol{\nabla} \cdot \mathbf{J}_{\rm r}^{(k)} = -\rho_{\rm r} \varepsilon_{\rm r} - \langle \mathbf{u}_{\rm r} \cdot \boldsymbol{\sigma}' \cdot \boldsymbol{\nabla} \alpha_{\rm r} \rangle \qquad [3.13]$$

where we have intentionally placed the terms for which closure assumptions are yet to be made, on the right sides of each equation. (Recall that we have passed to the incompressible limit, and that $\mathbf{u} = \sum_{{\rm r}=1}^{N} \theta_{\rm r} \mathbf{u}_{\rm r}$, which can be thought of as the mixture volume flux.) We suppose that [3.9] yields a solution for $\mathbf{R}_{\rm r}$, at least in some approximation; [3.10]

determines the r–mass density; [3.11] determines the r–velocity; [3.12] determines the mixture equilibration pressure; and [3.13] determines the r–fluctuational energy. So we are missing closures for the dissipation $\varepsilon_{\rm r}$, the isotropization tensor $\mathbf{\Pi}_{\rm r}$, and the Reynolds stress jump density, $-\left\langle u'_{{\rm r}(i}\sigma'_{j)k}\nabla_k\alpha_{\rm r}\right\rangle$. Those items are all made definite in the next sections. Before going on, however, it is worthwhile to comment on what is displayed in [3.9–3.13], for the set of N materials under consideration.

These averaged equations have been found by a straightforward application of the ensemble averaging operator onto some strategically selected quantities for mass, momentum, and stress. The only modeling done so far has been to make a wholesale adoption of standard results that have been used for a fairly long time and with varying degrees of success; so things are not any better or worse off, as yet. What we have done, in very large part, is to engage in a perfectly legitimate accounting (bookkeeping) game that permits us to place parts of the state vector into a collection of N "bins", so to speak. Each bin represents a place to put a system of equations for one of the N materials. This has all been tidy work that is required in order to keep things neatly in order so that when we do finally launch off into the matters that follow, we stand a better chance of keeping our energies directed toward the pieces of the theory that are unique to the multiphase problem – rather than to become entangled in the (still unsettled) issues of single–phase turbulence.

Of particular significance relative to the foregoing accounting game is that a part of the total fluctuational energy dissipation rate has turned out the be present in the each of the N equations for the Reynolds stress, and consequently in each of the equations for $k_{\rm r}$. And this is so, whether or not material r has any real capacity for viscous dissipation in its pure form. The term referred to here is, of course, the one involving $\varepsilon_{\rm r}$ in [3.9] (or its counterpart in [3.13]). This term has emerged precisely because of our uniform (symmetric) treatment of all materials – regardless of their physical nature; it arises because *every* material has an equal *right* to occupy a point at an instant. It will be seen that the practice of adhering to a uniform treatment of materials has a substantial reward in the end, when an approximate solution for the Reynolds stress is finally obtained. The reward is that the effective shear viscosity that emerges from the approximate solution feels the effect of energy exchange

among the materials, which can have a profound influence on the averaged behavior in some cases of very practical importance.

Finally we comment that this bookkeeping method is analogous, but not identical to, a method used for separating scales used in single–phase turbulence work, in which the energy spectrum itself is subdivided into accounting bins that each hold part of the fluctuational energy associated with the field (see for example, Schiestl 1987 or Kim & Chen 1989). In the present work we have elected to stay with an individual spectrum for each field, which differs from (and is somewhat simpler than) dividing up the spectrum for a single field. One can easily imagine potential advantages to subdividing our fieldwise energy bins that we have here, but until we see what happens with a single bin per field it would seem unreasonable to encumber ourselves with the added complexity of multiscale turbulence methods.

4. Closure approximations in functional form

In this section the closure process is continued by developing models for (1) the Reynolds stress jump density $\left\langle -u'_{\mathrm{r}(i}\sigma'_{j)k}\nabla_k\alpha_{\mathrm{r}}\right\rangle$; (2) the r–material dissipation rate ε_{r}; and (3) for the r–material collisional contribution to the stress, for which the collisional temperature Θ_{r} is required. (The models for the r–isotropization $\mathbf{\Pi}_{\mathrm{r}}$, and for the turbulent r–viscosity ν_{r} are closely tied to the approximate solution for $\mathbf{R}_{\mathrm{r}}$. Discussion of those items is reserved for § 5.) So there are three items on the shopping list for this section, and we will pick them up in order. We must emphasize that the means by which this task is approached here, is to bear down heavily on the *physical* modeling of the processes observed to be represented by the exact term that resulted from the averaging, rather than modeling the term itself, as we are duly warned against by Reynolds (1987).

As is always the case this endeavor must be undertaken with considerable care, in order to avoid certain pitfalls that may be devastating. To make the point in this regard, we begin by considering the scalar part of the Reynolds stress jump density (as it would appear on the right side of the r–fluctuational energy equation)

$$-\left\langle \mathbf{u}'_{\mathrm{r}}\cdot\boldsymbol{\sigma}'\cdot\boldsymbol{\nabla}\alpha_{\mathrm{r}}\right\rangle = -\left\langle \mathbf{u}_{\mathrm{o}}\cdot\boldsymbol{\sigma}'\cdot\boldsymbol{\nabla}\alpha_{\mathrm{r}}\right\rangle + \mathbf{u}_{\mathrm{r}}\cdot\left\langle \boldsymbol{\sigma}'\cdot\boldsymbol{\nabla}\alpha_{\mathrm{r}}\right\rangle$$

where we have used the definition of the r–velocity fluctuation to express the jump density in two parts. The first part, evidently, is a kind of work term that clearly represents a conservative exchange of energy; the sum over all materials is zero. The second part is known exactly because the expectation is just the (negative) r–material force density. If we take the two–material case, and sum the energy jump terms the result is, exactly,

$$
\begin{aligned}
-\left\langle \mathbf{u}_{\mathrm{r}}' \cdot \boldsymbol{\sigma}' \cdot \boldsymbol{\nabla}\alpha_{\mathrm{r}} \right\rangle &= -(\mathbf{u}_{\mathrm{r}} \cdot \mathbf{F}_r + \mathbf{u}_{\mathrm{s}} \cdot \mathbf{F}_{\mathrm{s}}) \\
&= K_{\mathrm{rs}}(u_{\mathrm{s}} - u_{\mathrm{r}})^2
\end{aligned}
$$

which is always positive. This is a fluctuational energy production rate, and is exactly the rate at which mean flow kinetic energy of the mixture is destroyed due to momentum interaction between materials. So the temptation would be to model the energy jump term as the sum of a conservative exchange rate and a positive creation rate, whose sum (for materials r and s) is $K_{\mathrm{rs}}(u_{\mathrm{s}} - u_{\mathrm{r}})^2$. We find that a slightly more general model is required, and is managed according to the following discussion.

The main idea is this: the mean flow kinetic energy deficit represented by $K_{\mathrm{rs}}(u_{\mathrm{s}} - u_{\mathrm{r}})^2$ may turn up in forms other than the mixture fluctuational energy – there are other energy modes that could vie equally for a part of that energy flow. Heat energy and potential energy of surrounding fields (like magnetic or gravitational ones) have an equal opportunity to get some of the mean flow kinetic energy loss. To see this we appeal to the well–known (elementary) fact that the only energy principle we can really depend on is the first law of thermodynamics. That is, the total mixture energy E is fixed. Hence if we use e_{r} for the r–material internal (heat) energy, $\mathtt{V}$ for an arbitrary volume, and Φ for the sum of all potential energies, we can express the first–law

$$
\dot{E} = \left[\Phi + \textstyle\sum_{\mathrm{r}=1}^{N} \rho_{\mathrm{s}} \mathtt{V}(\frac{1}{2}u_{\mathrm{r}}^2 + k_{\mathrm{r}} + e_{\mathrm{r}})\right]^{\cdot} = 0 \ ,
$$

where the overdot is used to mean the time rate of change along the mixture center–of–mass motion. The dilemma here arises as follows. For a single fluid, the usual way of finding the correct equation for heat energy is to subtract the equation for mean kinetic energy from that of the known total energy, and it always works. In the multiphase case, we again have a known total energy conservation principle, and we wish to subtract away

the mean kinetic energy of multiple materials and right away we are stuck: there is no way to generate N heat energy equations. Now add the further complexity of wanting to subtract away the fluctuational energy, and we are hopelessly stuck. Ishii (1975) recognized this dilemma early on, and resolved it by lumping the turbulence energy with the internal energy. We are forced to keep internal and turbulence modes separate, simply because the internal energy determines the averaged material temperature and, in general, the material temperature enters into the equations of state and can play an important role in other parts of the physics (like finite–rate chemistry and phase change).

This means that as we proceed to model the energy jump density term, total energy conservation requires that our model equations for all of the energy forms must add up to satisfy the first law. Besides that we are free to invoke whatever imagination is needed to get the job done, and we do so as follows.

Let $\mathcal{P}^S_{\rm rs} = K_{\rm rs}(u_{\rm s} - u_{\rm r})^2$ be the mixture mean flow kinetic energy loss rate. That much we know for sure; now we need to identify where it goes, for which we propose to ignore any direct flow into the potential fields and simply subdivide the flow into the fluctuational and internal energy modes *on a material–by–material basis*. Thus we shall have to *partition* $\mathcal{P}^S_{\rm rs}$ not only among the N materials, but between fluctuational and heat modes. In making such a subdivision, we are undoubtedly going to do so with some uncertainty – although we hope not too much. In order to maintain the functional form of the exact equations, and to remedy some of the uncertainty associated with which material gets the energy (as opposed to which mode), we shall provide for an r–s conservative exchange of the energy.

The foregoing partitioning is expressed functionally, for two materials, as

$$-\langle \mathbf{u}'_{\rm r} \cdot \boldsymbol{\sigma}' \cdot \boldsymbol{\nabla}\alpha_{\rm r}\rangle = \beta_{\rm r} f_{\rm r} \mathcal{P}^S_{\rm rs} + K_{\rm rs}(c_{\rm s}k_{\rm s} - c_{\rm r}k_{\rm r})$$

in which the partitioning coefficient between materials is $\beta_{\rm r}$ such that $\beta_{\rm r} + \beta_{\rm s} = 1$, and the partitioning between r–modes is $f_{\rm r}$ such that $(1 - f_{\rm r})\mathcal{P}^S_{\rm rs}$ of the energy deficit goes into the internal mode associated with r–material. The internal mode does not have to be accounted for in our isothermal, incompressible, approximation. For general materials, of course, the term $(1 - f_{\rm r})\mathcal{P}^S_{\rm rs}$ would be a source in the equation for $e_{\rm r}$, which already would have a rearrangement (exchange) term arising from a heat flow jump density. Notice that

we use the mean momentum exchange rate K_{rs} in the foregoing energy exchange term. The rationale is that the same processes determining the mean flow momentum exchange rate (viscous and pressure forces) will ultimately determine the energy exchange rate; the potential multiplying that rate is given by a difference in material fluctuational energies, multiplied by undetermined coefficients c_{s}. The c_{s} can be thought of as specific heats or fluctuational energy capacities; they permit the material fluctuational energies to take on different values in some equilibrium state. Thus one might expect the c_{s} to be related to the partition functions β_{s}.

For the mode partitioning function f_{r} consider the following. Let us refer to the energy removed from the mean flow and distributed to the fluctuational energy and heat energy as the slip production energy; it is only nonzero if there is a finite fluid viscosity in the presence of a velocity difference (slip) between r and s, on average. Let us suppose that the energy produced by the slip production process is created at a scale comparable to the scale of dispersed entities (the grain size, for example). If this scale is small compared to the integral scale, and so small that it may be closer to the Kolmogorov scale, then it is reasonable to further assume that much of the energy is lost to dissipation before it has a chance to cascade upward into the integral scale of the spectrum.

The foregoing can be made definite, at least in a functional way, by supposing that the energy spectra have some idealized form. Let that form be one whose fluctuational energy per unit of mass is

$$\frac{4E_0}{\pi}\int_0^\infty \frac{x}{1+x^4}dx \ ,$$

where $x = \mathrm{k}\lambda$ is the wave number k nondimensionalized by the integral scale λ. This gives a -3 slope to the distribution of energy for large x (in log–log space), and is roughly characteristic of the measured spectra for isotropic two–phase turbulence (Kulick et al. 1994, Sundaram & Collins 1999). We use a specific exponent here just to make the calculus easier, and not necessarily because it matches any particular physical situation (recall that we are only looking for the functional form here.) Now let us ask what fraction of the

spectrum is characteristic of the scales larger than some specific value, say δ. That fraction will be

$$\frac{4}{\pi}\int_0^{\lambda/\delta}\frac{x}{1+x^4}dx = \frac{2}{\pi}\tan^{-1}\left(\frac{\lambda}{\delta}\right)^2 ,$$

which is the fraction of the slip energy that we expect to be lost rapidly. Hence a functional model for the fraction of the energy characteristic of scales smaller than δ would be the complement. If we use a series approximation to the inverse tangent, this result is

$$f_{\rm r} = C_f\left(\frac{\delta}{\delta+\lambda_{\rm r}}\right)^n , \qquad [4.1]$$

where the exponent would be exactly two if the spectrum had the foregoing form; we expect the exponent to be less than two (because some of the some slip energy can go up the spectrum, via vortex pairing in the wake, say). Further, provision is made for a general nondimensional multiplier C_f in order to achieve proper scaling. The specific scale δ, the exponent, and the scaling function are determined in § 6.

Partitioning of $\mathcal{P}^S_{\rm rs}$ among materials is expected to be largely controlled by the inertia of the interacting materials; a marble falling in air is less likely to wiggle because of an unsteady wake than is a feather (of comparable size to the marble) falling in air. Thus one would expect that our partition functions $\beta_{\rm s}$ should vary like the ratio of the material specific volumes – when the separation between dispersed entities is large enough to preclude the collective effects of multiple bodies in the flow. To account for these collective effects, we note some well–known facts concerning multiphase flows. That is, for example, that the sedimentation speed of a suspension is highly susceptible to nonhomogeneity of the phase distribution (Weiland et al. 1984) caused by the very nonlinear dynamical behavior of so–called particle–fluid–particle interactions. These multibody interactions result in an instability driven by a drag force density that is larger if two bodies fall side–by–side, and smaller if they fall one behind the other, both of which vary inversely with the spacing in between them. The reasons for this are obvious: the fluid squeezing between the side–by–side bodies moves faster as the bodies get closer; and the trailing body is just in the wake of the leading one making the two look like a single body that is heavier. This spacing–plus–orientation dependent force density leads directly to what Joseph (1993) calls "Drafting, Kissing, and Tumbling" of solid objects levitated by an upward fluid flow.

(This multiphase instability is so far unnamed; we propose to call it the DKT instability in honor of D. D. Joseph who always reminds us that "kissing comes before tumbling".) As the number of objects increases the behavior intensifies and eventually leads to the creation of so–called fingers and channels that strongly resemble the bubbles and spikes that appear in the classical Rayleigh–Taylor instability due to acceleration of separated fluids having different density. Because of the creation of multibody structures by means of the DKT instability one can expect that the partitioning of slip production energy will potentially change greatly from one based on the inertia of the interacting materials alone. In particular one would expect that the partitioning could become more or less equal, owing to the fact that the newly organized multibody structures are composed of both materials.

To make the foregoing qualitative argument into a quantitative one, consider the following. Let us suppose that the microscopic motions whose average we have carefully obtained, tend to emulate the averaged motions themselves. (This line of thinking is not entirely uncommon in the single–phase turbulence literature.) This would permit us to explore the likely response of the microphysical system, to some microphysical perturbation. Hence we consider the scalar system of momentum equations

$$\rho_1 \dot{u}_1 = -\theta_1 p_x + K(u_2 - u_1) + B(\dot{u}_2 - \dot{u}_1)$$

$$\rho_2 \dot{u}_2 = -\theta_2 p_x + K(u_1 - u_2) + B(\dot{u}_1 - \dot{u}_2)$$

where p_x is the component of a pressure gradient in the direction of the scalar component. The coefficient B is supposed to represent virtual mass effects. With drag coefficient K and B constant, this is a linear system for the fluctuating velocities u_1 and u_2 associated with their respective material fields, with forcing function p_x. In system form this is

$$\begin{pmatrix} \dot{u}_1 \\ \dot{u}_2 \end{pmatrix} = -\begin{pmatrix} \rho_1 + B & -B \\ -B & \rho_2 + B \end{pmatrix}^{-1} \begin{pmatrix} \theta_1 \\ \theta_2 \end{pmatrix} p_x - \begin{pmatrix} \rho_1 + B & -B \\ -B & \rho_2 + B \end{pmatrix}^{-1} \begin{pmatrix} K & -K \\ -K & K \end{pmatrix} \begin{pmatrix} u_1 \\ u_2 \end{pmatrix} .$$

The early time response is given by the p_x term and the late time response is determined by the K term. The inertia of the system is carried by the vector

$$\begin{pmatrix} \rho_1 + B & -B \\ -B & \rho_2 + B \end{pmatrix}^{-1} \begin{pmatrix} \theta_1 \\ \theta_2 \end{pmatrix} = \frac{1}{A} \begin{pmatrix} \rho_2^{\circ} + \frac{1}{2}\rho_{12}^{\circ} \\ \rho_1^{\circ} + \frac{1}{2}\rho_{12}^{\circ} \end{pmatrix}$$

where A is the determinant of the matrix, and we have used the virtual mass coefficient $B = \theta_1\theta_2\frac{1}{2}\rho_{12}^{\circ}$. The partitioning suggested by the inertia vector is just the ratio of the response of the various components to the forcing. Let us use $1/v_{\rm r} = \rho_{\rm r}^{\circ}$ to denote the density of pure r–material. Also let $\rho_{\rm rs}^{\circ}$ be the density that is used in momentum exchange rate coefficient $K_{\rm rs}$ ($1/v$ of the continuous phase). The inertial response implied is

$$\frac{\beta_1}{\beta_2} \sim \frac{\dot{u}_1}{\dot{u}_2} = \frac{\rho_2^{\circ} + \frac{1}{2}\rho_{12}^{\circ}}{\rho_1^{\circ} + \frac{1}{2}\rho_{12}^{\circ}} \ ,$$

which meets the physical expectations mentioned above for the very dilute case – and makes good intuitive sense even in the case of bubbles rising in a liquid, because the virtual mass now appears. The late time inertial response is controlled by the eigenvalues of the matrix premultiplying the velocities on the right of the linear system. There is a single eigenvalue proportional to $\rho_1 + \rho_2$, the mixture mass density, suggesting that $(\beta_1/\beta_2) \sim 1$ for late times. This also meets our physical expectations associated with dense suspensions, in which multibody effects take over and produce structures in the flow that linger long enough to be observed on time scales large compared to the mean motion. In order to bridge the gap between these two limiting cases, we consider an integral of the foregoing system over a finite time τ; a time that we shall associate with the mean flow. The result in terms of the expected energy partitioning is

$$\frac{\beta_1}{\beta_2} \sim \frac{u_1(\tau)}{u_2(\tau)} = \frac{\rho_2^{\circ} + (\frac{1}{2} + \tau/\tau_x)\rho_{12}^{\circ}}{\rho_1^{\circ} + (\frac{1}{2} + \tau/\tau_x)\rho_{12}^{\circ}} \ ,$$

where τ_x is the time scale associated with the local–instantaneous momentum exchange process. Note that if $\tau/\tau_x \ll 1$, then the dilute case is recovered, and if $\tau/\tau_x \to \infty$ then $(\beta_1/\beta_2) \to 1$ which is the dense case. We expect the local–instantaneous process for velocity relaxation due to fluctuations to be characterized by the size of the fluctuations themselves, and the entity scale d. Hence $1/\tau_x \sim k^{\frac{1}{2}}/d$. The relative mean flow time scale varies like $\tau \sim \lambda/w$ so that $\tau/\tau_x \sim (k^2/\varepsilon)/(wd)$, which is like an inverse particle Reynolds number, based on the *turbulent* viscosity. Let $Re_{\lambda p}^{-1}$ denote this Reynolds number, in which the energy and dissipation rate are the mass–mean for materials s and r. Because the $\beta_{\rm r}$ must sum to one, the foregoing results become

$$\beta_{\rm r} = \frac{a_{\rm s}}{a_{\rm r} + a_{\rm s}} \quad \text{where} \quad a_{\rm r} = \rho_{\rm r}^{\circ} + [\tfrac{1}{2} + Re_{\lambda p}^{-1}]\rho_{\rm rs}^{\circ} \ . \qquad [4.2]$$

Equations [4.1–4.2] respectively express the consequences of modewise partitioning, and materialwise partitioning of the slip production rate. Equation [4.1] is a rough subdivision of the energy spectra resulting in a model for $f_{\rm r}$; [4.2] represents a low–order solution to the dynamical equations using rates that are suggested by the turbulence intensities of the interacting materials. Using these the energy jump density can be expressed in functional form by further assuming that the heat capacities are in fact the inverse of the material partition functions; the idea is that if we have partitioned $\mathcal{P}^S_{\rm rs}$ among materials reasonably well to start with, then that is the partitioning that should remain. This means that $k_{\rm r}/k_{\rm s} \approx \beta_{\rm r}/\beta_{\rm s}$. The only uncertainty concerning the energy exchange rate is whether or not the rate is similar to the relaxation rate for mean velocity differences. We expect there to exist some kind of proportionality between the two rates because they represent the same physical process; that proportionality being expressed by another unknown coefficient, C_β, to be determined in § 6. Hence we have, finally, the model for the fluctuational energy jump density.

$$-\langle \mathbf{u}'_{\rm r} \cdot \boldsymbol{\sigma}' \cdot \boldsymbol{\nabla}\alpha_{\rm r}\rangle = f_{\rm r}\beta_{\rm r}\mathcal{P}^S_{\rm rs} + K_{\rm rs}C_\beta(\beta_{\rm r}k_{\rm s} - \beta_{\rm s}k_{\rm r}) \; . \qquad [4.3]$$

By analogy the corresponding Reynolds stress jump density is

$$-\left\langle u'_{{\rm r}(i}\sigma'_{j)k}\nabla_k\alpha_{\rm r}\right\rangle = f_{\rm r}\beta_{\rm r}P_{{\rm rs}ij} + K_{\rm rs}C_\beta(\beta_{\rm r}R_{{\rm s}ij} - \beta_{\rm s}R_{{\rm r}ij}) \qquad [4.4]$$

where now the full stress production term is

$$P_{{\rm rs}ij} = K_{\rm rs}U_{{\rm rs}(i}U_{{\rm rs}j)} \qquad [4.5]$$

in which the r–s relative velocity is $U_{{\rm rs}i} = u_{{\rm s}i} - u_{{\rm r}i}$. One–half the trace of [4.4] is supposed to equal [4.3], which can be verified by inspection. With these we can now rewrite [3.13] for the r–fluctuational energy

$$\rho_{\rm r}\dot{k}_{\rm r} = -\boldsymbol{\nabla}\cdot\mathbf{J}^{(k)}_{\rm r} - \rho_{\rm r}\mathbf{R}_{\rm r} : \boldsymbol{\nabla}\mathbf{u}_{\rm r} - \rho_{\rm r}\varepsilon_{\rm r} + f_{\rm r}\beta_{\rm r}\mathcal{P}^S_{\rm rs} + K_{\rm rs}C_\beta(\beta_{\rm r}k_{\rm s} - \beta_{\rm s}k_{\rm r}) \; , \qquad [4.6]$$

whose right side terms represent, respectively, energy transport by fluctuational velocities; energy production by mean flow gradients, r–material dissipation (decay); material– and

mode–partitioned $\mathcal{P}^S_{\rm rs}$ (called slip production); and energy exchange. Equation [4.6] supplies the first item on our shopping list.

The second item on our closure shopping list is the r–material dissipation rate $\varepsilon_{\rm r}$. In order to represent flows with varying length (and time) scales we seek to develop transport equations for the decay variables that include not only the local processes but also diffusion and history effects. For this, numerous avenues have been considered in the (single–phase) turbulence literature. One is to develop a closure model for a rigorously derived transport equation for the dissipation and to close each term with microphysical models. This would not only be extremely difficult, but it also potentially overemphasizes processes at the small dissipation scales compared with those occurring at the integral scales (Launder 1990). Another avenue has been to develop equations for ε_k based on similarity arguments concerning integral scale processes (Launder & Spalding 1974, Reynolds 1987), and that is what we shall do here.

The similarity argument goes approximately like this. Suppose the statistics of the microphysical processes are all contained in the energy spectrum, which is like a two–point probability distribution for velocities. The total energy and its rate of dissipation are just two different moments of that energy spectrum. Now suppose that as fluctuational energy is gained or lost, as a result of production and dissipative processes, the energy spectrum adjusts so rapidly that some relationship between total energy and total dissipation remains fairly fixed. For illustration consider the integral scale $\lambda = k^{\frac{3}{2}}/\varepsilon$. A fixed relationship would mean that $d(k^{\frac{3}{2}}/\varepsilon) \sim 0$, which if it were true would correspond to $d\varepsilon \sim \frac{3}{2}(\varepsilon/k)dk$. (If instead the time scale, or viscosity scale were preserved, then the coefficient would be one or two, respectively.)

Now suppose it is known that the relationship between the the fluctuational energy and its dissipation rate is somehow known to be changing. This would correspond to a changing energy spectrum, rather than one which is tending to remain self–similar. Just to make the point in a relevant way, let us suppose that the integral scale of the spectrum

is influenced by some microphysical process; in our case this would be like the process of turbulence creation due to slip production. The differential relation would then be

$$\frac{d\lambda}{\lambda} = \frac{3}{2}\frac{dk}{k} - \frac{d\varepsilon}{\varepsilon}$$

and the model would be completed by devising an evolution expression for the rate of change of λ.

In reference to [4.6] there are six physical processes that are to be reconciled in the similarity equation for ε: diffusion, gradient production, dissipation, positive exchange, negative exchange, and slip production. For the diffusive flux, at least as an initial proposition, we shall make a wholesale theft of the closure that is used for single–phase turbulence

$$\mathbf{J}_{\mathrm{r}}^{(\varepsilon)} = -\rho_{\mathrm{r}}(\nu_{\mathrm{r}}/\sigma_{\varepsilon})\boldsymbol{\nabla}\varepsilon_{\mathrm{r}} \ ,$$

where σ_ε is the turbulence Prandtl number for diffusion of decay rate. Similarly we do the same for the gradient production and dissipation terms. For the positive part of the exchange we assume a fixed scale as well, but we elect to model the rate based upon the rate controlled by the turbulence of the opposite field (the field donating the energy); for the negative exchange part we again elect to keep a fixed scale, and use the rate from the r–field (which is donating energy to the s–field in the negative part). These approximations all, in effect, assume $\dot{\lambda} = 0$.

For the slip production term we shall introduce the relaxation rate model

$$\rho_{\mathrm{r}}\left(\frac{\dot{\lambda}_{\mathrm{r}}}{\lambda_{\mathrm{r}}}\right) = \frac{\mathcal{P}_{\mathrm{r}}^{S}}{k_{\mathrm{r}}}\left(a - b\frac{\lambda_{\mathrm{r}}}{D}\right) \qquad [4.7]$$

where the rate is given by $\mathcal{P}_{\mathrm{r}}^{S}/k_{\mathrm{r}}$, the parameters a, b are nonnegative numbers of order one, and the logarithmic potential is scaled by the separation distance $D = d(\theta_{\mathrm{r}}\theta_{\mathrm{s}})^{-\frac{1}{3}}$. With this, the ε_{r} equation becomes, in functional form,

$$\begin{aligned}\rho_{\mathrm{r}}\dot{\varepsilon}_{\mathrm{r}} &= -\boldsymbol{\nabla}\cdot\mathbf{J}_{\mathrm{r}}^{(\varepsilon)} \\ &\quad + \frac{\varepsilon_{\mathrm{r}}}{k_{\mathrm{r}}}\left[C_{\varepsilon 1}\mathcal{P}_{\mathrm{r}}^{G} - C_{\varepsilon 2}\rho_{\mathrm{r}}\varepsilon_{\mathrm{r}} + (\lambda_{\mathrm{r}}/D - C_{\varepsilon 3})\mathcal{P}_{\mathrm{r}}^{S}\right] + K_{\mathrm{rs}}C_{\beta}(C_{\varepsilon 4}\beta_{\mathrm{r}}\varepsilon_{\mathrm{s}} - C_{\varepsilon 5}\beta_{\mathrm{s}}\varepsilon_{\mathrm{r}}) \qquad [4.8]\end{aligned}$$

where $C_{\varepsilon 3}$ is a combination of the parameters a, b. Also, we use $\mathcal{P}_{\mathrm{r}}^{G} = -\rho_{\mathrm{r}}\mathbf{R}_{\mathrm{r}} : \boldsymbol{\nabla}\mathbf{u}_{\mathrm{r}}$, and $\mathcal{P}_{\mathrm{r}}^{S} = f_{\mathrm{r}}\beta_{\mathrm{r}}\mathcal{P}_{\mathrm{rs}}^{S}$ for the r–material gradient production and r–material net slip production,

respectively. Observe on the second line that $C_{\varepsilon 1}$ multiplies the gradient production rate; $C_{\varepsilon 2}$ multiplies the decay rate; $(\lambda_{\mathrm{r}}/D - C_{\varepsilon 3})$ multiplies the slip production rate; $C_{\varepsilon 4}$ multiplies the positive exchange part; and $C_{\varepsilon 5}$ multiplies the negative exchange part.

Consider the exchange terms for a moment. To construct models for these terms, it has been useful to think about what happens as turbulent kinetic energy is transferred from or to a given phase. We can imagine that as a field donates turbulence energy, it does so across the spectrum of turbulent scales roughly in proportion to the amount of energy at each scale. Thus, roughly speaking, we can expect that the integral scale is somewhat preserved during the turbulent kinetic energy donation process. On the other hand, as a field receives energy, we can expect that it roughly receives energy at the scale of the field which is donating it. Thus, the receiving field will tend to see its scale change toward the length scale of the recipient field. In order to capture these effects in a smooth fashion, we have found it advantageous to separately treat the positive and negative parts of the exchange term; so each part gets its own proportionality coefficient (rather than a single coefficient for the difference). So the incoming and outgoing rates are different from one another, yielding the foregoing functional form.

Before moving on we emphasize that the coefficients C_ε are fully developed in § 6 where we take into account the interaction of the various energy spectra. As a result the coefficients are not just fixed numbers, but functions of the turbulence quantities and other measures of the state of the system. For now the reader should regard the C_ε as placeholders for those functions. We postpone their full development in order to permit getting on with the approximate solution for the stress, which is of more global significance to the model framework developed here.

The third and last item to be discussed in this section is the collisional temperature Θ_{r}, which we have chosen to define as the part of the fluctuational energy spectrum that is accessible to direct grain–grain collisions. Hence it will be necessary to compute Θ_{r} only for one of our two fields; the one associated with the special case of dispersed solid grains, which we shall refer to as the particle field as opposed to the fluid field. The idea, again, is that the fluctuational part of the material stress (for all fields) is characterized fully by $\mathbf{R}_{\mathrm{r}}$ and its attendant models; in the case of solid grains we shall superimpose a

second part associated with direct grain–grain collisions, called the collisional part. The physical origin of the collisional part is a finite grain size, and has a direct analog in the kinetic theory of gases whereby consideration if finite molecule size leads to a modified gas viscosity. Momentum can be transferred rapidly over a distance much greater than a single grain dimension, compared to the fluctuational transport rate, provided that the grains are not too far apart – and provided that they collide frequently enough. The collisional temperature $\Theta_{\rm r}$ is used to estimate how frequent, and with what intensity, the collisions occur.

To find a model for $\Theta_{\rm r}$ we again visualize a set of turbulent kinetic energy spectra, as we have done earlier in connection with modewise slip energy partitioning, and also in connection with modeling the exchange part the dissipation equation. Hence we suppose that there is an integral scale for the turbulence which is the scale of the largest, energy containing structures (eddies). Superimposed on the large eddies, is a continuous spectrum of fluctuational motion which reaches down to the sizes of the smallest eddies at the Kolmogorov scale of the fluid. We further suppose that the collisional temperature is equal to the grain field turbulence kinetic energy at the scale similar to the separation of the grains and smaller. The idea here is that turbulence energy associated with eddies much larger than the mean separation does not significantly drive collisions between individual grains. Instead the grains in a large eddy move more or less coherently when viewed from the integral scale perspective. Another way to look at this is that the grain field fluctuational motion is composed of clusters of grains moving about in a random fashion with the integral scale turbulence energy. Inside these clusters, the grains collide with a lower energy, namely, the collisional temperature.

Referring to the earlier discussion of the modewise energy partitioning, we model the collisional temperature by analog to $f_{\rm r}$ given by [4.1], that functional form is

$$\Theta_{\rm r} = k_{\rm r} \left(\frac{D}{D + \lambda_{\rm r}} \right)^{\eta} \qquad [4.9]$$

where again $D = d(\theta_{\rm r}\theta_{\rm s})^{-\frac{1}{3}}$ is a length scale that corresponds to something like the mean separation path, and the exact value of the exponent being left open for final determination in a subsequent report. The collisional temperature given by Eq. [4.9] is to be used in the

formulas given in Appendix A for the collisional contribution to the stress – for only those fields (solid grains) capable of transmitting such a stress. The important qualitative feature of the model is that as the integral scale of the turbulence gets large compared to the separation of the grains, the granular temperature becomes a smaller and smaller fraction of the total turbulent kinetic energy. Thus, for turbulent multiphase flows with large integral length scales, the collisional terms from the kinetic theory will tend to become less important compared to the fluctuational phenomena associated with the Reynolds stress.

We comment that the foregoing method of estimating the collisional temperature is, of course, only one way to accomplish the task. Clearly one could use a so–called multiscale model to subdivide the particle field energy spectrum into large–scale and small–scale parts, and then to associate the small–scale parts with the collisional temperature. Such a model would represent the full multiphase analog of the single–field, multiscale method mentioned earlier, and has been explored in the limited context of a turbulent gas with suspended solid grains (Bolio & Sinclair 1995). It is not yet clear whether such a practice has an adequate payoff for general purposes, so again we elect to stick with the simpler procedure of retaining a single bin for fluctuational energy, for each material in the problem.

Before leaving this section we offer a final remark concerning the partitioning of energy sources between fluctuational energy and heat energy; the physical process which is modeled by our Eq. [4.1] in connection with slip energy. It should be clear that a similar (implicit) line of thinking applies to the manner in which the gradient production term is modeled (the second right side term of [4.6]). The typical approach is to assume that all of the energy produced by this term is fluctuational in nature, but that need not be so. One could just as well suppose that some of the gradient production occurs at scales near the Kolmogorov scale, and is therefore much more likely to dissipate immediately into heat energy. The implication of including 100% of the gradient production term as a source in the fluctuational energy equation is to establish one's meaning of "turbulence" in a very quantitative way. The obvious corollary to this is that if we wish to exclude some portion of the kinetic energy spectrum as being *resolved* rather than *modeled*, then a factor like [4.1] could be applied to the gradient production term as well. For example, suppose that

we expect to account for the full dynamics of the motion at scales larger than a specified value, say, Δx. Then it would be perfectly consistent to place the fraction

$$f = \left(\frac{\Delta x}{\Delta x + \lambda_{\rm r}} \right)$$

in front of the gradient production term in the $k_{\rm r}$ equation, and add $1-f$ of that rate to the r–heat energy equation. This would redefine turbulence to be the unresolved fluctuational motions occurring at scales less than Δx; it furnishes a turbulence model for so–called Large–Eddy–Simulation, whereby the fluctuational dynamics of scales larger than Δx (a grid size) are contained explicitly in the mean flow equation for linear momentum conservation. LES problems are not the subject of this report, but the foregoing concept clearly establishes a commonality that will be pursued elsewhere.

5. Approximate solution for the stress

In this section we find an approximate solution to the r–material Reynolds stress equation, again taking extensive guidance from our single–field turbulence predecessors. In particular we make the usual decomposition of the stress into isotropic and (traceless) deviatoric parts, invoke the so–called *structural equilibrium approximation*, and generalize the Launder isotropization model for our r–material stress equation. The result of these approximations is an implicit algebraic model for the stress, a sort of state relationship, which is inverted by means of a perturbation expansion. In the single–phase limit the stress is simply given by the so–called Boussinesq approximation, with turbulent viscosity proportional to k^2/ε, replete with the usual set of undetermined coefficients. Most of the coefficients have single–field counterparts, and are already determined. We shall see that the additional undetermined coefficients are kept to a minimum in the framework adopted in this report. Furthermore it will be shown (in § 6) that the new coefficients can be determined using a small set of the available data – by using the standard values of the single–field coefficients; from which we infer that the theory permits the peaceful coexistence of fluctuational energy from both gradient production, and slip production sources. We further infer that this vindicates the definition of multiphase turbulence given in the Introduction.

The first step is to let $R_{rij} = 2k_r b_{rij} + \frac{2}{3}k_r\delta_{ij}$, which immediately defines the r–field (traceless) anisotropy

$$b_{rij} = (R_{rij}/2k_r) - \tfrac{1}{3}\delta_{ij} \ .$$

The structural equilibrium approximation is $\dot{b}_{rij} = 0$ in which the overdot again represents the r–material Lagrangian derivative. The assumption is that the anisotropic structure of r–material statistical correlations adjusts rapidly as the material moves along its Favre–averaged trajectory. Clearly this is an assumption that can be easily challenged, but nevertheless one that we will make, followed in a subsequent report by an exploration of its limits of validity by way of comparing numerical results to a large collection of experimental data. Hence

$$\rho_r \dot{R}_{rij} = (R_{rij}/k_r)\rho_r \dot{k}_r$$

can be used to reduce the equation for $\mathbf{R}_r$ to an algebraic one involving the known right side of the k_r equation. In addition it is customary to ignore the diffusive flux, so that the algebraic equation is

$$\begin{aligned}(R_{rij}/k_r)[- \rho_r \mathbf{R}_r : \boldsymbol{\nabla}\mathbf{u}_r - \rho_r\varepsilon_r + \mathcal{P}_r^S + K_{rs}C_\beta(\beta_r k_s - \beta_s k_r)] = \\ - \rho_r R_{r(ik}\nabla_k u_{rj)} - \rho_r\varepsilon_r \tfrac{2}{3}\delta_{ij} + \Pi_{rij} + \mathcal{P}_{rij}^S + K_{rs}C_\beta(\beta_r R_{sij} - \beta_s R_{rij}) \ , \quad [5.1]\end{aligned}$$

where we have combined [3.9], [4.4], and [4.5], and let $\mathcal{P}_{rij}^S = f_r\beta_r K_{rs}U_{rs(i}U_{rsj)}$ which is just the r–material part of the tensor slip production term, one–half the trace of which is $\mathcal{P}_r^S$. Because the term on the left in brackets is just $[\rho_r\dot{k}_r]$ we can simply leave it as such symbolically, knowing that it represents a total scalar rate, which is known (and is displayed in [4.6]). In terms of the anisotropy [5.1] is

$$\begin{aligned}(2b_{rij} + \tfrac{2}{3}\delta_{ij})[\rho_r\dot{k}_r] &= -\rho_r R_{r(ik}\nabla_k u_{rj)} - \rho_r\varepsilon_r\tfrac{2}{3}\delta_{ij} + \Pi_{rij} + \mathcal{P}_{rij}^S + K_{rs}C_\beta(\beta_r R_{sij} - \beta_s R_{rij}) \\ &= \left[-\rho_r 2k_r b_{r(ik}\nabla_k u_{rj)} + K_{rs}C_\beta(\beta_r 2k_s b_{sij} - \beta_s 2k_r b_{rij})\right] + \Pi_{rij} + \mathcal{P}_{rij}^S \\ &\quad + \tfrac{2}{3}\delta_{ij}\left[-\rho_r k_r b_{r(ik}\nabla_k u_{rj)} + K_{rs}C_\beta(\beta_r k_s - \beta_s k_r)\right] - \rho_r\varepsilon_r\tfrac{2}{3}\delta_{ij} \ .\end{aligned}$$

The equation for $[\rho_r\dot{k}_r]$ can be used to eliminate the last line. In addition the notation becomes more economical if we use dyadic notation, and more so if we drop the material

subscripts on K, because we consider the two–material case. Let the bullet $\bullet$ denote the symmetric inner product of two second order tensors, so that

$$b_{(ik}\nabla_k u_{j)} = [\mathbf{b}\cdot\boldsymbol{\nabla}\mathbf{u} + (\boldsymbol{\nabla}\mathbf{u})\cdot\mathbf{b}] = \mathbf{b}\bullet\boldsymbol{\nabla}\mathbf{u}$$

and we have

$$\begin{aligned} 2\mathbf{b}_{\rm r}[\rho_{\rm r}\dot{k}_{\rm r}] + \tfrac{2}{3}\mathbf{I}[-\rho_{\rm r}2k_{\rm r}\mathbf{b}_{\rm r}:\boldsymbol{\nabla}\mathbf{u}_{\rm r} + \mathcal{P}^S_{\rm r}] = \\ [-\rho_{\rm r}2k_{\rm r}\mathbf{b}_{\rm r}\bullet\boldsymbol{\nabla}\mathbf{u}_{\rm r} + KC_\beta(\beta_{\rm r}2k_{\rm s}\mathbf{b}_{\rm s} - \beta_{\rm s}2k_{\rm r}\mathbf{b}_{\rm r})] + \boldsymbol{\Pi}_{\rm r} + \underline{\underline{\mathcal{P}}}^{\mathbf{S}}_{\rm r}\ . \end{aligned}$$

As a final preparatory step, let us combine the diagonal second term on the left with the corresponding terms of like kind on the right, and also replace the velocity gradient dyadic with the usual sum of symmetric and antisymmetric parts: $\boldsymbol{\nabla}\mathbf{u} = \mathbf{S} + \mathbf{W}$, with $\mathbf{S} = \frac{1}{2}(\boldsymbol{\nabla}\mathbf{u} + \boldsymbol{\nabla}\mathbf{u}^{\rm T})$ and $\mathbf{W} = \frac{1}{2}(\boldsymbol{\nabla}\mathbf{u} - \boldsymbol{\nabla}\mathbf{u}^{\rm T})$. (Some helpful identities are: $\mathbf{I}\bullet\mathbf{S} = 2\mathbf{S}$, $\mathbf{I}\cdot\mathbf{W} = \mathbf{I}\bullet\mathbf{W} = 0$, $\mathbf{b}:\mathbf{W} = 0$, and $\mathbf{I}:\mathbf{S} = \boldsymbol{\nabla}\cdot\mathbf{u} = \Delta$.) With these conventions [5.1] becomes

$$\begin{aligned} \boldsymbol{\Pi}_{\rm r} = 2\mathbf{b}_{\rm r}[\rho_{\rm r}\dot{k}_{\rm r}] + \tfrac{4}{3}\rho_{\rm r}k_{\rm r}[\mathbf{S}_{\rm r} - \tfrac{1}{3}\mathbf{I}\Delta_{\rm r}] + 2\rho_{\rm r}k_{\rm r}[\mathbf{b}_{\rm r}\bullet\mathbf{S}_{\rm r} - \tfrac{2}{3}\mathbf{I}(\mathbf{b}_{\rm r}:\mathbf{S}_{\rm r})] + 2\rho_{\rm r}k_{\rm r}\mathbf{b}_{\rm r}\bullet\mathbf{W}_{\rm r} \\ - [\underline{\underline{\mathcal{P}}}^S_{\rm r} - \tfrac{2}{3}\mathbf{I}\mathcal{P}^S_{\rm r}] - KC_\beta(\beta_{\rm r}2k_{\rm s}\mathbf{b}_{\rm s} - \beta_{\rm s}2k_{\rm r}\mathbf{b}_{\rm r})\ , \end{aligned} \qquad [5.2]$$

where each term can be verified symmetric traceless, by inspection. This is still [5.1], just written in terms of the unknown anisotropy, and in a different order.

Now perhaps the biggest leap of all comes as we elect to model the isotropization tensor following the collective genius of our forbears (Reynolds 1987, Launder 1990, Gatski & Speziale 1993). That is to say, we let

$$\begin{aligned} \boldsymbol{\Pi}_{\rm r} = -C_1\mathbf{b}_{\rm r}[\rho_{\rm r}\varepsilon_{\rm r}] + C_2\rho_{\rm r}k_{\rm r}[\mathbf{S}_{\rm r} - \tfrac{1}{3}\mathbf{I}\Delta_{\rm r}] + C_3\rho_{\rm r}k_{\rm r}[\mathbf{b}_{\rm r}\bullet\mathbf{S}_{\rm r} - \tfrac{2}{3}\mathbf{I}(\mathbf{b}_{\rm r}:\mathbf{S}_{\rm r})] + C_4\rho_{\rm r}k_{\rm r}\mathbf{b}_{\rm r}\bullet\mathbf{W}_{\rm r} \\ - C_5[\underline{\underline{\mathcal{P}}}^S_{\rm r} - \tfrac{2}{3}\mathbf{I}\mathcal{P}^S_{\rm r}] - KC_\beta[C_6\beta_{\rm r}2k_{\rm s}\mathbf{b}_{\rm s} - C_7\beta_{\rm s}2k_{\rm r}\mathbf{b}_{\rm r}]\ , \end{aligned} \qquad [5.3]$$

in which the first line is all straight from the single–phase turbulence line of thinking, whereby the C_1 term is called the "rapid" part of the isotropization rate, and the C_2–C_4 terms make up the "slow" part. The second line is multiphase only, and written by analogy to the first line. We express the equations in this way in order to permit a term by term

association of the isotropization model [5.3] with the Reynolds stress equation [5.2] itself. The physical rationale behind this model is made evident when [5.3] is inserted into the Reynolds stress equation. The result is,

$$
\begin{aligned}
2[\rho_{\rm r}\dot{k}_{\rm r}]\mathbf{b}_{\rm r} + C_1\rho_{\rm r}\varepsilon\mathbf{b}_{\rm r} &= (C_2 - \tfrac{4}{3})\rho_{\rm r}k_{\rm r}[\mathbf{S}_{\rm r} - \tfrac{1}{3}\mathbf{I}\Delta_{\rm r}] \\
&\quad + (C_3 - 2)\rho_{\rm r}k_{\rm r}[\mathbf{b}_{\rm r}\bullet\mathbf{S}_{\rm r} - \tfrac{2}{3}\mathbf{I}(\mathbf{b}_{\rm r} : \mathbf{S}_{\rm r})] + (C_4 - 2)\rho_{\rm r}k_{\rm r}\mathbf{b}_{\rm r}\cdot\mathbf{W}_{\rm r} \\
&\quad + (1 - C_5)[\underline{\underline{\mathcal{P}}}^S_{\rm r} - \tfrac{2}{3}\mathbf{I}\mathcal{P}^S_{\rm r}] \\
&\quad + 2KC_\beta[(1 - C_6)\beta_{\rm r}k_{\rm s}\mathbf{b}_{\rm s} - (1 - C_7)\beta_{\rm s}k_{\rm r}\mathbf{b}_{\rm r}] \ .
\end{aligned}
$$

In this form, the genius behind the Launder–Reynolds–Speziale isotropization model equation can now be observed. Consider the single–phase case, and divide through by the factor ρk so the left side becomes $\mathbf{b}[2(\dot{k}/k) + (\varepsilon/k)]$; this can be viewed as relaxation model for isotropy, with a rate given by the turbulence time scale.

In general the solution to this tensor algebraic equation is quite complicated, but can nevertheless be accomplished. The method of solution involves the identification of the tensor integrity bases and then the use of all the invariant scalar coefficients required to satisfy the equation (Gatski & Speziale 1993). In the present case, however, a low–order solution can in fact be found by means of expansion in a small parameter. This is because in the absence of mean velocity gradients the equation takes on a particularly simple form and is easily solved. We therefore look for an approximate perturbation series solution, which should be accurate for small departures from the zero velocity gradient case.

The appropriate expansion parameter emerges naturally upon dividing through by the factor $2\rho_{\rm r}\varepsilon_{\rm r}$ (which is clearly not the only choice, but turns out to be a good one). In doing so, we let the time scale $k_{\rm r}/\varepsilon_{\rm r}$ serve to nondimensionalize all of the r–material rates. Let the superscript $*$ denote the nondimensional rates so that $\mathbf{S}^*_r = (k_{\rm r}/\varepsilon_{\rm r})\mathbf{S}_{\rm r}$, $K^*_{\rm r} = (Kk_{\rm r}/\rho_{\rm r}\varepsilon_{\rm r})$, and $[\underline{\underline{\mathcal{P}}}^S_{\rm r} - \frac{2}{3}\mathbf{I}\mathcal{P}^S_{\rm r}]^* = [\underline{\underline{\mathcal{P}}}^S_{\rm r} - \frac{2}{3}\mathbf{I}\mathcal{P}^S_{\rm r}]/(\rho_{\rm r}\varepsilon_{\rm r})$. Accordingly, the nondimensional algebraic equation is

$$
\begin{aligned}
[\dot{k}_{\rm r}/\varepsilon_{\rm r}]\mathbf{b}_{\rm r} + [\tfrac{1}{2}C_1 + K^*_{\rm r}(1 - C_7)C_\beta\beta_{\rm s}]\mathbf{b}_{\rm r} - [K^*_{\rm r}(1 - C_6)C_\beta\beta_{\rm r}(k_{\rm s}/k_{\rm r})]\mathbf{b}_{\rm s} &= \\
+ \tfrac{1}{2}(C_3 - 2)[\mathbf{b}_{\rm r}\bullet\mathbf{S}^*_{\rm r} - \tfrac{2}{3}\mathbf{I}(\mathbf{b}_{\rm r} : \mathbf{S}^*_{\rm r})] + \tfrac{1}{2}(C_4 - 2)\mathbf{b}_{\rm r}\bullet\mathbf{W}^*_{\rm r} \\
+ \tfrac{1}{2}(C_2 - \tfrac{4}{3})[\mathbf{S}^*_{\rm r} - \tfrac{1}{3}\mathbf{I}\Delta^*_{\rm r}] + \tfrac{1}{2}(1 - C_5)[\underline{\underline{\mathcal{P}}}^S_{\rm r} - \tfrac{2}{3}\mathbf{I}\mathcal{P}^S_{\rm r}]^* \ . \qquad [5.4]
\end{aligned}
$$

In this, the last right side term represents the effect of slip production on the anisotropy; for multiphase flow it is always nonzero, which furnishes a substantive difference between the single– and multiphase cases. In system form [5.4] can be expressed

$$\begin{pmatrix} g_{\rm r} & -\xi_{\rm r} \\ -\xi_{\rm s} & g_{\rm s} \end{pmatrix} \begin{pmatrix} \mathbf{b}_{\rm r} \\ \mathbf{b}_{\rm s} \end{pmatrix} = \begin{pmatrix} \boldsymbol{\Omega}_{\rm r} + \boldsymbol{\kappa}_{\rm r} \\ \boldsymbol{\Omega}_{\rm s} + \boldsymbol{\kappa}_{\rm s} \end{pmatrix} ,$$

where the nondimensional r–equation coefficients are defined

$$g_{\rm r} = [\dot{k}_{\rm r}/\varepsilon_{\rm r}] + \tfrac{1}{2}C_1 + K^*_{\rm r}(1 - C_7)C_\beta\beta_{\rm s}$$

$$\xi_{\rm r} = K^*_{\rm r}(1 - C_6)C_\beta\beta_{\rm r}(k_{\rm s}/k_{\rm r})$$

$$\boldsymbol{\Omega}_{\rm r} = \tfrac{1}{2}(C_3 - 2)[\mathbf{b}_{\rm r} \bullet \mathbf{S}^*_{\rm r} - \tfrac{2}{3}\mathbf{I}(\mathbf{b}_{\rm r} : \mathbf{S}^*_{\rm r})] + \tfrac{1}{2}(C_4 - 2)\mathbf{b}_{\rm r} \cdot \mathbf{W}^*_{\rm r}$$

$$\boldsymbol{\kappa}_{\rm r} = \tfrac{1}{2}(C_2 - \tfrac{4}{3})[\mathbf{S}^*_{\rm r} - \tfrac{1}{3}\mathbf{I}\Delta^*_{\rm r}] + \tfrac{1}{2}(1 - C_5)[\underline{\underline{\mathcal{P}}}^S_{\rm r} - \tfrac{2}{3}\mathbf{I}\mathcal{P}^S_{\rm r}]^*$$

and where the coefficients for the s equation are found by interchanging the material indices r and s. The zeroth–order solution is $\mathbf{b}^{(0)}_{\rm r}$; it is found by letting the coefficients $\boldsymbol{\Omega}_{\rm r} = 0$; the second–order solution $\mathbf{b}^{(1)}_{\rm r}$ is found by using $\boldsymbol{\Omega}_{\rm r}(\mathbf{b}^{(0)}_{\rm r})$, and so on. Let us denote the cofactors of the coefficient matrix with a superscript prime, for example,

$$g'_{\rm r} = g_{\rm r}/(g_{\rm r}g_{\rm s} - \xi_{\rm r}\xi_{\rm s}) .$$

Then we can write the zeroth–order solution

$$\begin{pmatrix} \mathbf{b}^{(0)}_{\rm r} \\ \mathbf{b}^{(0)}_{\rm s} \end{pmatrix} = \begin{pmatrix} g'_{\rm s} & \xi'_{\rm r} \\ \xi'_{\rm s} & g'_{\rm r} \end{pmatrix} \begin{pmatrix} \boldsymbol{\kappa}_{\rm r} \\ \boldsymbol{\kappa}_{\rm s} \end{pmatrix} , \qquad [5.5]$$

and in general for any order i,

$$\begin{pmatrix} \mathbf{b}^{(i)}_{\rm r} \\ \mathbf{b}^{(i)}_{\rm s} \end{pmatrix} = \begin{pmatrix} g'_{\rm s} & \xi'_{\rm r} \\ \xi'_{\rm s} & g'_{\rm r} \end{pmatrix} \begin{pmatrix} \boldsymbol{\Omega}^{(i-1)}_{\rm r} + \boldsymbol{\kappa}_{\rm r} \\ \boldsymbol{\Omega}^{(i-1)}_{\rm s} + \boldsymbol{\kappa}_{\rm s} \end{pmatrix} . \qquad [5.6]$$

Observe that the expansion parameters correspond to the nondimensional rates of strain $\mathbf{S}^*$ and $\mathbf{W}^*$, which are independent of the $\mathbf{b}$. The coefficients ξ and $\boldsymbol{\kappa}$ are also independent of the $\mathbf{b}$. Only the coefficients g vary between the zeroth and first approximations, because $[\dot{k}/\varepsilon]$ does depend on the anisotropy. Suppose, however, that the $[\dot{k}/\varepsilon]$ are in

fact negligible compared to $\frac{1}{2}C_1$, due to closeness of the system to a equilibrium point (production equals dissipation). Then the coefficients are all essentially fixed, and the expansion solution is guaranteed convergent, which is the fundamental virtue of the linear model used for the isotropization. If instead, however, the coefficients vary as a result of strong nonequilibrium, then the g will vary from approximation to approximation, in which case all convergence bets are off. Hence the modeler has to choose their own poison here: use the more robust equilibrium model – and accept the potential inaccuracy, or use the fully nonequilibrium model – and accept the numerical fact that there will be cases for which a solution may be unreliable. In the single–phase turbulence venue the jury is out on this matter. Thus we shall comment that the nonequilibrium model has been developed and presented in [5.6]. A substantial exercise remains to be done; it needs extensive testing in a wide range of practical applications.

(For applications in which a numerical solution method is employed that evolves the full system state forward in a sequence of discrete time steps, one can easily use a common trick for obtaining robustness while getting at the same time the greatest accuracy from the model equations. The trick is to evaluate $[\dot{k}/\varepsilon]$ using data from the previous time step, whereby the coefficients g will be fixed relative to the anisotropy at the previous time. This permits evaluating the new anisotropy to any desired accuracy with complete confidence of convergence. When a steady state is finally reached, the approximate solution to [5.4] will be exact.)

Equation [5.6] is our final solution for the anisotropy, and we recommend extending the expansion to $i = 1$ mainly because we see no great advantage in going to higher approximations, at least until the low–order one is checked out, and because a steady state is frequently the item of interest. Hence the Reynolds stress is given by $\mathbf{R}_\mathrm{r} = 2k_\mathrm{r}(\mathbf{b}_\mathrm{r}^{(1)} + \frac{1}{3}\mathbf{I})$, which can be written out in full dimensional terms

$$\begin{aligned}
\mathbf{R}_\mathrm{r} &= \tfrac{2}{3}k_\mathrm{r}\mathbf{I} + 2g'_\mathrm{s}k_\mathrm{r}[\boldsymbol{\Omega}_\mathrm{r}^{(0)} + \boldsymbol{\kappa}_\mathrm{r}] + 2\xi'_\mathrm{r}k_\mathrm{r}[\boldsymbol{\Omega}_\mathrm{s}^{(0)} + \boldsymbol{\kappa}_\mathrm{s}] \\
\mathbf{R}_\mathrm{s} &= \tfrac{2}{3}k_\mathrm{s}\mathbf{I} + 2g'_\mathrm{r}k_\mathrm{s}[\boldsymbol{\Omega}_\mathrm{s}^{(0)} + \boldsymbol{\kappa}_\mathrm{s}] + 2\xi'_\mathrm{s}k_\mathrm{s}[\boldsymbol{\Omega}_\mathrm{r}^{(0)} + \boldsymbol{\kappa}_\mathrm{r}]
\end{aligned} \qquad [5.7]$$

and which, unfortunately, is not in a very handy form for observing what it contains. It is instructive to look at the result in a few special limiting cases.

First consider the case for which the momentum interaction between fields is weak, and the velocity gradients are zero. This corresponds to a homogeneous sedimentation in which the falling field has a long velocity relaxation time (loose coupling). Quantitatively this means that the $[\dot{k}/\varepsilon]$ are zero, and the ξ are negligible compared to the g. It also means that $\mathbf{b}^{(0)}$ and $\mathbf{b}^{(1)}$ are the same, because there are no gradients. Now suppose that the coordinate system is such that the gravitational direction is aligned the $\mathbf{e}_3$ axis, so the relative velocity looks like $(0, 0, w)$. There will be exactly one nonzero component in the slip production tensor $[\underline{\underline{\mathcal{P}}}_{\mathrm{r}}^{S} - \frac{2}{3}\mathbf{I}\mathcal{P}_{\mathrm{r}}^{S}]^{*}$, namely the (3,3) component; it is $\frac{4}{3}\mathcal{P}_{\mathrm{r}}^{*}$. Let b_{r} stand for the corresponding nonzero anisotropy component. The result of these approximations is

$$b_{\mathrm{r}} = \left(\frac{\frac{1}{2}(1 - C_5)\frac{4}{3}\mathcal{P}_{\mathrm{r}}^{*}}{\frac{1}{2}C_1 + K_{\mathrm{r}}^{*}(1 - C_7)C_\beta \beta_{\mathrm{s}}} \right) .$$

Recall that the coefficients K_{r}^{*}, $\mathcal{P}_{\mathrm{r}}^{*}$, and β_{s} are all positive. So this component of the anisotropy tensor is some positive multiple of the mean relative velocity magnitude, provided of course that $C_5 < 1$, and $C_7 < 1$. The stress is

$$\mathbf{R}_{\mathrm{r}} = \begin{pmatrix} \frac{2}{3}k_{\mathrm{r}} & 0 & 0 \\ 0 & \frac{2}{3}k_{\mathrm{r}} & 0 \\ 0 & 0 & 2k_{\mathrm{r}}(b_{\mathrm{r}} + \frac{1}{3}) \end{pmatrix} ,$$

so the (3,3) component is an amount $2k_{\mathrm{r}}b_{\mathrm{r}}$ larger than the others, which is certainly in qualitative agreement with experiment (Parthasarathy and Faeth 1990). In general the fields experience finite coupling so the $\mathbf{b}$'s wind up coupled as well, which is indicated by [5.5]. To make this quantitatively in agreement with experiment requires setting specific values for the C's, which is undertaken in the next section.

Now consider the simple case of a single fluid, where the slip production and exchange parts of the stress are zero, and the components of $\mathbf{b}^{(0)}$ are zero. The anisotropy turns out to be

$$\mathbf{b}^{(1)} = -\left[\frac{\frac{1}{2}(\frac{4}{3} - C_2)}{[\dot{k}/\varepsilon] + \frac{1}{2}C_1} \right] \frac{k}{\varepsilon} [\mathbf{S} - \tfrac{1}{3}\mathbf{I}\Delta]$$

and the stress is

$$\mathbf{R} = \tfrac{2}{3}k\mathbf{I} - \left[\frac{(\frac{4}{3} - C_2)}{[\dot{k}/\varepsilon] + \frac{1}{2}C_1} \right] \frac{k^2}{\varepsilon} [\mathbf{S} - \tfrac{1}{3}\mathbf{I}\Delta]$$

which in the equilibrium approximation, $[\dot{k}/\varepsilon] = 0$, is the classical Boussinesq formula, with the coefficient given from experiment by

$$(\tfrac{4}{3} - C_2)/\tfrac{1}{2}C_1 = C_\mu^{\rm o} \approx 0.09 \ ,$$

(so for the classical k–ε model and C_1 given an arbitrary value of two, $C_2 = 1.24$).

Finally consider the weakly coupled case, with two materials and finite gradients. Again the coefficients ξ are negligible making expression of the anisotropy relatively simple, and there is a single nonzero component in the $\mathbf{b}^{(0)}$, which was displayed above; it is used to multiply the C_3 and C_4 terms in the coefficients $\mathbf{\Omega}^{(0)}$. The anisotropy is now

$$\mathbf{b}_{\rm r}^{(1)} = -\left[\frac{\frac{1}{2}(\frac{4}{3} - C_2)}{[\dot{k}_{\rm r}/\varepsilon_{\rm r}] + \frac{1}{2}C_1 + K_{\rm r}^*(1 - C_7)C_\beta\beta_{\rm s}}\right]\frac{k_{\rm r}}{\varepsilon_{\rm r}}[\mathbf{S}_{\rm r} - \tfrac{1}{3}\mathbf{I}\Delta_{\rm r}] + \mathcal{O}(\mathbf{b}_{\rm r}^{(0)}) \ ,$$

where the last term represents all the terms of order $\mathbf{b}^{(0)}$. At multiphase equilibrium, where the $[\dot{k}_{\rm r}/\varepsilon_{\rm r}] = 0$, the stress can be written

$$\mathbf{R}_{\rm r} = \tfrac{2}{3}k_{\rm r}\mathbf{I} - \left[\frac{C_\mu^{\rm o}}{1 + C_7^+ K_{\rm r}^*\beta_{\rm s}}\right]\frac{k_{\rm r}^2}{\varepsilon_{\rm r}}[\mathbf{S}_{\rm r} - \tfrac{1}{3}\mathbf{I}\Delta_{\rm r}] + 2k_{\rm r}[\mathcal{O}(\mathbf{b}_{\rm r}^{(0)})] \ , \qquad [5.8]$$

where we define the combined coefficient $C_7^+ = (1 - C_7)C_\beta/\frac{1}{2}C_1$. Clearly there are two modifications to the single–phase stress, in this approximation. One is due to the zeroth–order term, which comes from sedimentation, and is multiplied by the velocity gradients; it is expressed symbolically in the last term. The other modification is an apparent reduction in the single–phase coefficient $C_\mu^{\rm o}$, evidently as a result of the physical process of energy exchange between fields; we conclude that increasing the rate of isotropization manifests itself as a reduction in the turbulent shear viscosity, as would be expected. In general there would be a slip production term added to both the numerator and to the denominator of the turbulent viscosity in [5.8] (the $\boldsymbol{\kappa}\xi$ parts of [5.6]), so that the viscosities are themselves fully coupled. We display [5.8] only to make the point that the coefficient $C_\mu^{\rm o}$ gets reduced in the process.

In summary our straightforward extension of the most popular model for isotropization has led us to introduce three new coefficients, C_5–C_7. The structural equilibrium approximation has allowed us to find an approximate solution for the stress, and it appears

to make qualitative sense. We have two remaining chores; one is to establish specific values for the new coefficients, while using standard values for the old ones; and the second is to see how widely the model can be applied in practice.

6. Determination of the coefficients

It is our good fortune that there exists a high–quality experimental data set that can be used to gauge the values of the coefficients left undetermined in § 4-5, thereby producing a "finished" model. The purpose of this section is to make an initial determination of those coefficients, by considering only a small subset of the available data. The obvious hope in this regard is that the finished model will yield reasonable results for problems far different than the ones used for gauging in this section – lending some indication of success relative to the general part of the goal mentioned in the Introduction. To begin the task we take an inventory of what needs to be done by displaying the model equations, again for the case of two incompressible materials. First recall that the partitioning between energy modes was expressed by the coefficient $f_{\rm r}$, and given functionally by [4.1]

$$f_{\rm r} = C_f \left(\frac{\delta}{\delta + \lambda_{\rm r}} \right)^n \ , \qquad [4.1]$$

where the function C_f, scale δ, and the exponent n are to be determined here. Second, recall our postulate that there is a basic tendency for the available slip production energy $\mathcal{P}^S_{\rm rs}$ to be partitioned according to the inverse mass density of the pure materials. That was expressed by [4.2]

$$\beta_{\rm r} = \frac{a_{\rm s}}{a_{\rm r} + a_{\rm s}} \quad \text{where} \quad a_{\rm r} = \rho^{\rm o}_{\rm r} + [\tfrac{1}{2} + Re^{-1}_{\lambda p}]\rho^{\rm o}_{\rm rs} \ . \qquad [4.2]$$

With these, [4.6] and [4.8] are the model equations for k and ε

$$\rho_{\rm r}\dot{k}_{\rm r} = -\boldsymbol{\nabla}\cdot\mathbf{J}^{(k)}_{\rm r} + [\mathcal{P}^G_{\rm r} - \rho_{\rm r}\varepsilon_{\rm r} + \mathcal{P}^S_{\rm r}] + KC_\beta(\beta_{\rm r}k_{\rm s} - \beta_{\rm s}k_{\rm r}) \ , \qquad [4.6]$$

$$\rho_{\rm r}\dot{\varepsilon}_{\rm r} = -\boldsymbol{\nabla}\cdot\mathbf{J}^{(\varepsilon)}_{\rm r} + \frac{\varepsilon_{\rm r}}{k_{\rm r}}\left[C_{\varepsilon 1}\mathcal{P}^G_{\rm r} - C_{\varepsilon 2}\rho_{\rm r}\varepsilon_{\rm r} + (\lambda_{\rm r}/D - C_{\varepsilon 3})\mathcal{P}^S_{\rm r}\right] + KC_\beta(C_{\varepsilon 4}\beta_{\rm r}\varepsilon_{\rm s} - C_{\varepsilon 5}\beta_{\rm s}\varepsilon_{\rm r}) \qquad [4.8]$$

where, again, we use $\mathcal{P}^G_{\rm r} = -\rho_{\rm r}\mathbf{R}_{\rm r} : \boldsymbol{\nabla}\mathbf{u}_{\rm r}$, and $\mathcal{P}^S_{\rm r} = f_{\rm r}\beta_{\rm r}\mathcal{P}_{\rm rs}$ for the r–material gradient production and r–material net slip production, respectively; and where the Reynolds stress

is $\mathbf{R}_\mathrm{r} = 2k_\mathrm{r}(\mathbf{b}_\mathrm{r}^{(1)} + \frac{1}{3}\mathbf{I})$ with anisotropy $\mathbf{b}_\mathrm{r}$ given by [5.6]. Finally recall that if the media is capable of transmitting a force via direct grain–grain collisions, we superimpose a collisional contribution that is driven by the collisional temperature. The connection between the fluctuational energy k and the collisional temperature was established in § 4, Eq. [4.9], and will be examined in detail in future work; for now we shall consider only those problems for which the collisional contribution is negligible. An inventory of the remaining coefficients needed to finish the model is provided in Table 6.1.

	$\mathbf{\Pi}$	$\dot{\varepsilon}$	$\dot{k}$
Single–phase	C_1, C_2, C_3, C_4	$C_{\varepsilon 1}$, $C_{\varepsilon 2}$	σ_k, σ_ε
Typical Values:	2.00, 1.24, 2.00, 2.00	1.44, 1.92	1.00, 1.30
New two–phase	C_5, C_6, C_7	$C_{\varepsilon 3}$, $C_{\varepsilon 4}$, $C_{\varepsilon 5}$	C_β, C_f

Table 6.1. Inventory of proportionality coefficients.

In Table 6.1 the line denoted "Typical Values" corresponds to the values used here, taken (in effect) from Launder & Spalding (1974). The columns represent, respectively, coefficients for the isotropization tensor, ε equation, and k equation. The last line is the collection of items to be found in this section; they are new to the multiphase turbulence world. We remark that the headcount of proportionality coefficients is eight for the single–phase theory, and eight more for the theory extended to the two–phase case; which does *not* mean the coefficients increase linearly with the number of materials. In fact we have constructed a formalism that has a fixed set of coefficients – for N materials, something that will stand as a prediction, until sufficient experimental data for $N > 2$ are furnished, against which to test the theory.

Note that if the system is homogeneous (no mean flow gradients so the Lagrangian derivative is just the partial time derivative), and with no gravitational acceleration to furnish a separation potential, the system is simply

$$\rho_\mathrm{r}\dot{k}_\mathrm{r} = -\rho_\mathrm{r}\varepsilon_\mathrm{r} + KC_\beta(\beta_\mathrm{r}k_\mathrm{s} - \beta_\mathrm{s}k_\mathrm{r}) \,, \qquad [6.1]$$

$$\rho_\mathrm{r}\dot{\varepsilon}_\mathrm{r} = \frac{\varepsilon_\mathrm{r}}{k_\mathrm{r}}\left[-C_{\varepsilon 2}\rho_\mathrm{r}\varepsilon_\mathrm{r}\right] + KC_\beta(C_{\varepsilon 4}\beta_\mathrm{r}\varepsilon_\mathrm{s} - C_{\varepsilon 5}\beta_\mathrm{s}\varepsilon_\mathrm{r}) \qquad [6.2]$$

which is a model for the decay of isotropic two–material turbulence; for some specified initial value of the k's, and the $\dot{k}$'s, these equations specify the rate at which the initial

energies decay to zero. Clearly this is an enormous idealization, but is also the two–phase analog of the canonical starting place for gauging coefficients in single–phase turbulence theory. We shall use this model for the first step here as well. As will be seen shortly, it is a way to find C_β, $C_{\varepsilon 4}$, and $C_{\varepsilon 5}$.

If instead we suppose there is a gravitational acceleration, then there will ensue a mean relative motion which would otherwise have been zero. If the system is still free of gradients, but at steady state, then the equations become

$$0 = -\rho_{\rm r}\varepsilon_{\rm r} + \mathcal{P}_{\rm r}^S + KC_\beta(\beta_{\rm r}k_{\rm s} - \beta_{\rm s}k_{\rm r}) \ , \qquad [6.3]$$

$$0 = \frac{\varepsilon_{\rm r}}{k_{\rm r}}\left[-C_{\varepsilon 2}\rho_{\rm r}\varepsilon_{\rm r} + (\lambda_{\rm r}/D - C_{\varepsilon 3})\mathcal{P}_{\rm r}^S\right] + KC_\beta(C_{\varepsilon 4}\beta_{\rm r}\varepsilon_{\rm s} - C_{\varepsilon 5}\beta_{\rm s}\varepsilon_{\rm r}) \qquad [6.4]$$

which expresses the less idealized situation of a homogeneous sedimentation. The experimental data for homogeneous sedimentation will provide the means of gauging C_f: the coefficient connected with slip production partitioning among energy modes (fluctuational and heat). If that were to be all that is of interest, we would be done. However we are fundamentally interested in the anisotropy, and we are lucky to find that experimenters have carefully reported velocity fluctuations in the various component directions – which permits us to complete the job by gauging C_5, C_6, and C_7 for the isotropization tensor.

In principle these two cases are all that are necessary to establish values for the needed coefficients, and we shall do so starting with isotropic decay, which is a test of the (isolated) time–dependent behavior of the model. Homogeneous sedimentation tests the balance among energy production by slip between fields, exchange, and decay, at the steady state. This leaves testing the model representation of nonhomogeneous velocity fields in the presence of slip production, energy exchange, and multiphase dissipation, which is the subject of our next report.

6.1. Isotropic decay

The data for isotropic decay of two–material turbulence is relatively new, and is only made possible by computer simulation. The work of Sundaram & Collins (1999) appears

to be the first attempt to report a full collection of data for fluctuational energies of the two materials (along with some juicy statistical correlations for integral scales and energy spectra). Sundaram and Collins used a so–called pseudospectral method to compute the motion of a viscous fluid containing a large collection of identical rigid solid grains. The motion of each individual solid grain was followed "exactly" in the sense that the interaction force was approximated by a drag law; with an equal and opposite thrust force added to the fluid as a momentum source. Grains are represented by point masses (zero volume), but permitted to undergo elastic collisions by assuming a finite size, and assuming that the grain–grain contact lasts for an infinitesimally short time (hard spheres). It is difficult to characterize this as a Direct Numerical Simulation because the viscous boundary layer at the surface of each and every grain is not resolved. Thus some modeling is already present. Nevertheless we shall utilize the data as if it came from a DNS, while assuming that the errors are no greater than what would arise from a comparable physical experiment (in fact the errors are infinitely smaller because there is no physical experiment for this case). Before proceeding it is worthwhile noting that it was a spectacular stroke of genius (or serendipity) for Sundaram and Collins to permit only elastic collisions, thereby eliminating any doubt as to the physical origin of the dissipation in their system. If they had permitted finite elasticity of the grains the picture would have become muddled, and would have required us to consider a collisional dissipation in this section; because of their choice we don't have that added complexity, at least not right now.

To see what this section is all about, consider [6.1–6.2] in the single–phase case, whereby $K = 0$, and eliminate ε by using the time derivative of [6.1] in [6.2]. The result is $\ddot{k} = C_{\varepsilon 2}(\dot{k}^2/k)$, so the standard coefficient $C_{\varepsilon 2}$ just expresses the proportionality between second derivative and the first; it sets the decay rate. If one can manage to obtain data for $k(t)$ associated with a fixed mass of material, and differentiate the data twice, then the coefficient is obtained. Such a thing has been done for a single fluid, both by observing the decay of grid–generated turbulence in a channel flow, and by DNS. (See Mansour and Wray 1994 for an excellent summary, including discussion of the spectral theory.) It is seen that the coefficient varies with intensity of the turbulence, but not too much, relatively speaking. If a universal form of the energy spectrum is assumed, one can expect values in

the range of about $1.4 \leq C_{\varepsilon 2} \leq 1.8$ depending on the particular parameters taken for the spectral distribution function. (A variation of $C_{\varepsilon 2}$ in the range of about 1.4–2.0 is more or less what is observed, and that is typically taken to be a validation of the spectral theory.) We shall use here the historical value listed in Table 6.1, partly in deference to the early workers (Launder & Spalding 1974) but mostly because we know that the collection of choices form a set – and changing one parameter independently of the others is ill advised. For the purposes of this section, we employ an old set assuming the peculiarities of the set are well known, on account of their antiquity.

There is an important point to be made in regard to the use of the standard single–phase coefficients here: the new coefficients are dependent on the old ones. This means that we are gauging what we have called multiphase turbulence in a way that is relative to what is called single–phase turbulence. If one's definition of the latter changes, so does the former. Hence what may have seemed, early on, to be a perfectly arbitrary definition of multiphase turbulence is suddenly made definite – in the act of choosing $C_{\varepsilon 1}$ and $C_{\varepsilon 2}$.

Before going on to our task here, it is instructive to observe the large–time behavior of the standard single–phase model. To make the point most simply we write [6.1–6.2] in terms of the log change rate

$$\dot{k}/k = -(\varepsilon/k) \quad , \quad \dot{\varepsilon}/\varepsilon = -C_{\varepsilon 2}(\varepsilon/k) \quad .$$

By inspection, one can observe the (inverse) relaxation rate for the k is (ε/k) and the rate for ε is $C_{\varepsilon 2}(\varepsilon/k)$; so if $C_{\varepsilon 2} > 1$ then ε goes to zero faster than does k, and the ratio k/ε goes to infinity for large time. Thus the integral scale becomes infinite which it should; when the fluctuations are all zero they are perfectly correlated over all space. Recall the discussion on similarity back in § 4 where it was pointed out that one might expect the C_{ε} coefficients to lie in the range between one and two, depending on whether a time scale, length scale, or viscosity scale is preserved in the microdynamical processes. So far that line of thinking has been holding up for the single–phase theory, we shall see if it continues for the multiphase case.

Now consider [6.2]. If we suppose that a fixed value for $C_{\varepsilon 5}$ is selected, then the only items left to gauge are $C_{\varepsilon 4}$ and the coefficient in the model for the partition functions β.

Let us begin by assuming a unit value of $C_{\varepsilon 5}$, which implies that we are guessing that the exchange rate given by K is about right, so that we do not need to raise or lower it by the magnitude of the C's. Hence as we raise or lower $C_{\varepsilon 4}$, we are just raising or lowering the importance of gaining energy versus loosing it, by way of the exchange term.

For the partition functions $\beta_{\rm r}$ we consider [4.2], which for a zero mean relative motion, gives the limit $\beta_{\rm p} = \beta_{\rm f} = \frac{1}{2}$; this means the energy partitioning is 50–50 between the two materials.

Let [6.1] define $\varepsilon_{\rm r}$ and its time derivative, for $r = 1, 2$. Then [6.2] can be written specifically for r–material

$$\rho_{\rm r} C_{\varepsilon 4}[r] = \frac{\rho_{\rm r} C_{\varepsilon 2}(\varepsilon_{\rm r}^2/k_{\rm r}) - \rho_{\rm r}\ddot{k}_{\rm r} + KC_\beta(\beta_{\rm r}\dot{k}_{\rm s} - \beta_{\rm s}\dot{k}_{\rm r} + \beta_{\rm s}\varepsilon_{\rm r})}{KC_\beta\beta_{\rm r}\varepsilon_{\rm s}}$$

which we display only to make the point that the unknown coefficient can be found from *either* [6.2] for r–material, or for s–material, or for that matter any of the N materials in the general case. The validity of our theory depends on the sameness of the coefficients – among the collection of materials. Hence we shall find $C_{\varepsilon 4}[r]$ as defined by the Sundaram–Collins data for both materials, in the two–phase case, and just for good measure we shall display its mass–mean $\overline{C}_{\varepsilon 4} = (\rho_1 C_{\varepsilon 4}[1] + \rho_2 C_{\varepsilon 4}[2])/(\rho_1 + \rho_2)$.

Briefly the numerical data used here were obtained by considering a periodic box filled with fluid and stirred up by forcing function. At time zero, the forcing function was terminated, and solid grains were randomly distributed (in noncontacting positions) having been assigned the local fluid velocity. The full dynamics of the system were then followed for a length of time assumed much larger than that required for a relevant spectral equilibria to be established (Sundaram & Collins 1999).

For us to conduct the calculation, we need to set values for the densities ρ, the energies k, and the momentum exchange rate K, using the corresponding Sundaram–Collins conditions. Table 6.2 lists the initial conditions for the fluid in the box of volume $(2\pi)^3$. For our calculations we shall presume that $k_{\rm f} = k_{\rm p} = \frac{3}{2}u'^2$ all at time zero. The Stokes number is defined (in Sundaram & Collins 1999) as the ratio of the Stokes time scale $\tau_{\rm p} = \rho_{\rm p}^{\circ} d^2/18\rho_{\rm f}^{\circ}\nu_{\rm f}$ to the Kolmogorov time scale $\tau_\eta = (\nu_{\rm f}/\epsilon)^{\frac{1}{2}}$. (Also the Taylor microscale is $\lambda_T = (15\nu_{\rm f}u'^2/\epsilon)^{\frac{1}{2}}$, and $Re_\lambda = u'\lambda_T/\nu_{\rm f}$.) Using the standard force

model, these definitions permit us to deduce that $K = \rho_{\rm p}/\tau_p$. Finally the densities can be determined by extracting volume fraction from the definition of the mass fraction, which gives $\theta_{\rm p} = 1.808 \cdot 10^{-4}$; a grain diameter of $d = 0.01374$ (in consistent units); and a mean separation distance of about 18 grain diameters. The parameters suggest very dilute large grains of solid in a turbulent gas, as was desired.

Dimensional	$\rho_{\rm p}^{\rm o}$	$\nu_{\rm p}$	$u'(0)$	$\epsilon(0)$	$l_e(0)$
Value	1.0	$7.854 \cdot 10^{-3}$	0.9362	0.22282	1.6223
Nondimensional		ϕ	$\rho_{\rm p}^{\rm o}/\rho_{\rm f}^{\rm o}$	St	$Re_\lambda(0)$
Value		0.14	900	6.41	81.145

Table 6.2. Parameters for isotropic decay calculation of Sundaram & Collins (1999). Dimensional quantities are respectively the material density of the (pure) fluid, kinematic viscosity of the fluid, initial turbulence intensity, initial dissipation per unit of (mixture) mass, and initial integral scale. (Note that the u', ϵ and l_e are all integrals over the energy spectrum; their u' should be our $(\frac{2}{3}k)^{\frac{1}{2}}$, but their ϵ may or may not have anything to do with our ε, consequently their l_e may not be related to our $k^{\frac{3}{2}}/\varepsilon$.) Nondimensional quantities are respectively the particle mass fraction, ratio of particle to fluid material densities, Stokes number, and turbulence Reynolds number based on the Taylor microscale.

If we obtain values for the $k(t)$ by placing a graduated scale on the page displaying the Sundaram & Collins data and differentiate twice, the results are noisy, owing to the crudeness with which the numbers are obtained. Nevertheless they are the only numbers available, and so we are compelled to use them. The result of placing them into [6.1–6.2] are summarized in Fig. 6.1 for the coefficient $C_{\varepsilon 4}$, and for $C_\beta = 2$. The findings illustrated here are encouraging. To the extent that anything is indicated at all, Fig. 6.1 suggests a comparatively small variation of $C_{\varepsilon 4}$ among the model equations that use it, and a small variation with time (and therefore turbulence intensity), and that $C_{\varepsilon 4} \sim 1$ for $C_\beta = 2$. (Smaller values of C_β produce a larger difference among the materialwise $C_{\varepsilon 4}$; larger C_β values bring them together. We shall henceforth suppose that $C_\beta = 2$ is reasonable.)

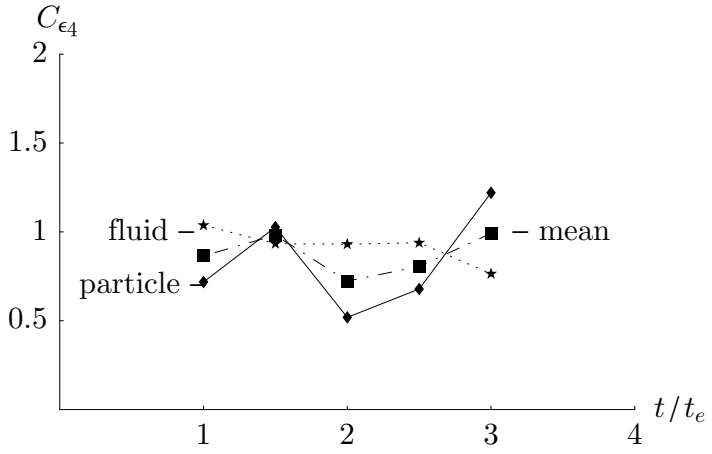

Figure 6.1. Isotropic decay for a fluid with suspended solid grains in a gas, for the case $St = 6.4$ of Sundaram & Collins (1999). The conditions (given in Table 6.2) correspond to a grain size of 0.014 cm, a volume fraction of $1.5 \cdot 10^{-4}$, and separation number of about 18 diameters.

We regard the foregoing findings as important in the following way. Despite the highly idealized nature of the isotropic decay experiment, it represents a critical first step in the qualification of a general, useful turbulence model. There are plenty of occurrences in practice where the flow has a sudden removal of the forces causing generation of the turbulence; flow in a pipe with a sudden expansion is a homely example, but a common one. Hence one must be sure that the model equations have a proper limiting behavior – if only in a clumsy fashion. So it would appear that the model proposed here passes the first test.

It is instructive to observe the large–time behavior of the multiphase equations in a fashion similar to the way it was observed for the single–phase case. For large time it is clear that the two energies tend to become equal, owing to the exchange terms. In a similar way the decay rates become similar, and everything is headed toward zero; the question is how fast. Let $\rho = \rho_{\rm p} + \rho_{\rm f}$ be the mixture density, and let k and ε be the corresponding mixture energy and total decay rates. If we sum [6.1] for both materials, and sum [6.2] for both materials, and express the two equations in terms of log rates the result is

$$\dot{k}/k = -(\varepsilon/k) \quad , \quad \dot{\varepsilon}/\varepsilon = -C_{\varepsilon 2}(\varepsilon/k) + (KC_\beta/\rho)(C_{\varepsilon 4} - 1) \quad .$$

So for $C_{\varepsilon 4} < 1$ as time increases it is a very good bet that the $\varepsilon_{\rm r}$ will vanish faster than the $k_{\rm r}$; and again the integral scales become infinite. In fact we see that the multiphase relaxation rates are increased over the single–phase rates by the last term, which represents the modification to the energy spectra as a result of local relaxation of velocity differences. This is a relaxation process that Sundaram and Collins correctly pointed out as a purely dissipative one, for a system lacking any energy sources.

For a system containing a source to the fluctuational energy (considered next) there is a catch in connection with $C_{\varepsilon 4}$, which requires an important modification. To see it consider [6.4], displayed for both materials r and s:

$$0 = \frac{\varepsilon_{\rm r}}{k_{\rm r}} \left[-C_{\varepsilon 2} \rho_{\rm r} \varepsilon_{\rm r} + (\lambda_{\rm r}/D - C_{\varepsilon 3}) \mathcal{P}_{\rm r}^S \right] + K C_\beta (C_{\varepsilon 4} \beta_{\rm r} \varepsilon_{\rm s} - \beta_{\rm s} \varepsilon_{\rm r}) \ ,$$
$$0 = \frac{\varepsilon_{\rm s}}{k_{\rm s}} \left[-C_{\varepsilon 2} \rho_{\rm s} \varepsilon_{\rm s} + (\lambda_{\rm s}/D - C_{\varepsilon 3}) \mathcal{P}_{\rm s}^S \right] + K C_\beta (C_{\varepsilon 4} \beta_{\rm s} \varepsilon_{\rm r} - \beta_{\rm r} \varepsilon_{\rm s}) \ .$$

Observe that if the exchange rate K becomes very large compared to everything else, then the equations contradict one another unless $C_{\varepsilon 4} \to 1$. To reconcile this we recall that there could be a dependence of $C_{\varepsilon 4}$ on the mean relative Reynolds number, which is not apparent in the present case of isotropic decay. We recognize that generally as the mean relative Reynolds number gets small, the momentum coupling becomes strong. To permit such a dependence, and retain our current result we shall consider the form

$$C_{\varepsilon 4} = a + (1 - a)/(1 + Re_p^b) \ , \qquad [6.5]$$

where a is a number between zero and one, and b is an unknown power. This form allows $C_{\varepsilon 4}$ to take on values less than one for finite Reynolds number cases. In the next section, we find that the values $a = \frac{1}{2}$ and $b = 2$ give quite adequate representation of the data.

6.2. Homogeneous sedimentation

Once again the literature is good to us by providing excellent data from the laboratory for gravity–driven homogeneous sedimentation, whereby the fluctuational statistics for velocity of the sedimenting material, and of the displaced fluid, are measured by either laser–Doppler anemometry, or by particle imaging velocimetry. Recall that the main

task at hand is to determine the coefficient $f_{\rm r}$ for the modewise partitioning of the slip production rate in the k equations. This task will be accomplished by comparing model results to an experimental database for homogeneous sedimentation. This database consists of four widely differing test conditions: (1) glass spheres falling in water (Parthasarathy and Faeth 1990); (2) air bubbles rising in water (Lance and Bataille 1991); (3) glass spheres falling in air (Mizukami, Parthasarathy and Faeth 1992); and (4) polystyrene (colloidal) grains falling in water (Segrè et al. 1997).

We use the term homogeneous to characterize the experiments as being free of mean velocity gradients (as measured on the scale of the device). The local velocity gradients (in regions small compared to the device) have been averaged away. We note too the well–known fact that the sedimentation of a suspension is highly susceptible to nonhomogeneity of the phase distribution (Weiland et al. 1984). As discussed in the Introduction, this nonhomogeneity is caused by the very nonlinear dynamical behavior of what we are calling the DKT instability. Recall too from our discussion in the Introduction, that these nonlinear phenomena arise no matter how slow the flow may be, which caused Lhuillier (and others) to call the motions "pseudo–turbulence". Because these motions may have a profound influence on the large–scale (averaged) behavior of the suspensions, we call these motions multiphase turbulence – and have set out to find an appropriate model for it.

Our model for multiphase turbulence is supposed to account for the effect of nonhomogeneous phase distribution on the macroscopic behavior of a suspension; this spatial nonhomogeneity is smoothed out in the ensemble averaging process in exactly the same way that local velocity nonhomogeneity gets averaged out – the net effect being expressed by the model equations. Because the Reynolds stress represents the consequences of a difference between averaged and local velocities, the force density must represent the consequences of differences between averaged and local densities – local spatial nonhomogeneity and all. This is our motive for selecting what is included in our experimental database. A high–level summary of the database is given in Table 6.3.

We remark that the database (consisting of sets 1–4) is selected partly to span a large range in particle separation, material density ratio, and particle size (indicated by Reynolds number), and partly because this is about that all there is. Note that the span in material

density ratio is six orders of magnitude. The range of particle spacing depends only on the mean volume fraction, and the range there is clearly two orders of magnitude. The range in Reynolds number is the impressive number here; as a practical matter it goes from zero to infinity. What is conspicuously absent, however, is a set of measurements taken at around $Re_{\mathrm{p}} \sim \mathcal{O}(1)$, the point at which a crossover begins from viscous dominated drag over to a drag force dominated a pressure deficit in the wake (often called form drag); good data in this regime would be very helpful.

Investigators	$\rho_{\mathrm{p}}^{\mathrm{o}} : \rho_{\mathrm{f}}^{\mathrm{o}}$	θ_{p}	D/d	Re_{p}
(1) Parthasarathy & Faeth (1990)	2:1	10^{-5}–10^{-4}	50–20	40–500
(2) Lance & Bataille (1991)	10^{-3}:1	10^{-3}–10^{-2}	10–5	1000
(3) Mizukami et al. (1992)	2:10^{-3}	10^{-7}–10^{-6}	200–100	100–700
(4) Segrè et al. (1997)	2:1	10^{-3}–10^{-1}	20–2	10^{-4}

Table 6.3. Summary of homogeneous sedimentation database. Columns after the investigators are respectively the ratio of particle to fluid material densities, range of particle volume fractions studied, mean particle separation in particle diameters, and Reynolds number based on single–sphere settling speed. The numbers are given to one–digit accuracy in order to provide a rough picture of the range of the database. (All experiments were performed at room temperature and under normal earth gravity.)

Generally the database is fairly complete in that it contains fluctuational energies measured for both the particle and the fluid fields, as well as correlations representing the associated integral scales. The fluctuations and integral scales are given in both the direction parallel to the gravity vector, and perpendicular to it. The only exceptions are for the water in the bubbly case (2) for which gas–phase fluctuational data could not be obtained and for the gas–solid case (3), where fluctuations in the particle velocities were below the sensitivity of the measuring apparatus. (These defects are not critical. For (2) we suspect from the work of Tryggvason (2000) that the gas–phase fluctuational energy is roughly of the same order as that of the fluid; and for (3) we can get an estimate of the particle fluctuational energy from the analytical work of Koch (1990). So there are reasonable ways to fill the holes in the data, and we make use of them.)

The complete data set as extracted from the literature is listed in Appendix B, along with some commentary on how the numbers were interpreted from the various references.

Finally, before commencing our gauging task for this subsection, we observe that the mixture settling speed for the data sets used here is very close to the settling speed of a single particle in an infinite fluid given the standard representation of the drag coefficient for a sphere. This observation is, of course, made in reference to those cases that are sufficiently dilute. This is very good news from the viewpoint of the present task; we do not have to fuss with modeling of the force to represent the deviations in averaged drag force density, compared to that of a single–sphere, which surely result from the multiphase turbulence itself. This means that we can use the model equations as if there were only a one–way coupling between the momentum equation and [6.3–6.4], for the special case of homogeneous sedimentation. That is, we can assume that the drag force density is fully responsible for production of the turbulence energy, but that the fluctuational energy has no effect on the drag force density. This is surely untrue in general, so the decoupling is clearly only a low–order approximation, but the simplification here is helpful at the present stage of these developments.

We now turn to the nonlinear algebraic equations [6.3–6.4] which is our model system in the limit of homogeneous sedimentation of a suspension, expressed in functional form. Owing to the high order of nonlinearity (typically fourth–order), a solution cannot be expressed in closed form. Nevertheless it is very instructive to observe an approximate solution, relevant for the case of slow momentum exchange (weak velocity coupling between fields). In the limit of zero coupling, the equations are simply

$$\begin{aligned} 0 &= -\rho_{\mathrm{r}}\varepsilon_{\mathrm{r}} + \mathcal{P}_{\mathrm{r}}^{S} \\ 0 &= -C_{\varepsilon 2}\rho_{\mathrm{r}}\varepsilon_{\mathrm{r}} + (\lambda_{\mathrm{r}}/D - C_{\varepsilon 3})\mathcal{P}_{\mathrm{r}}^{S} \ , \end{aligned}$$

and whose solution can be seen by inspection, namely

$$\lambda_{\mathrm{r}}/D = C_{\varepsilon 2} + C_{\varepsilon 3} \ .$$

This can be back substituted into [6.3] to yield an approximate solution for the energy. Again using subscripts f (fluid) and p (particle) the approximate solution for the fluid, normalized by the relative velocity w, is

$$k_{\mathrm{f}}/w^2 = [(\lambda_{\mathrm{f}}/D)\tfrac{3}{4}C_d f_{\mathrm{f}}\beta_{\mathrm{f}}(\theta_{\mathrm{f}}\theta_{\mathrm{p}})^{\frac{2}{3}}\rho_{\mathrm{fp}}^{\circ}/\rho_{\mathrm{f}}]^{\frac{2}{3}} \ , \qquad [6.6]$$

where we have used the standard force density, and $\mathcal{P}_{\rm f}^S = f_{\rm f}\beta_{\rm f}Kw^2$. (Recall that $C_{\varepsilon 2}$ is to be taken from the single–phase theory, and survives in both the equations for energy and length scale: this is precisely where the link is made to the single–phase meaning of turbulence.) Now observe that in the dilute regime the fluid density and $\rho_{\rm fp}^{\rm o}$ are the same, so if $\beta_{\rm f}$ can be estimated then everything is known except for the modewise energy partitioning coefficient $f_{\rm f}$ which multiplies the rate at which mean flow energy is converted into fluctuational energy (slip production).

Let us suppose that the fluctuational energy is produced (by slip) at a length scale comparable to the entity scale d, and the energy enters the energy spectra at a corresponding wave number. Because the wake size of a single particle scales with the particle size (and relative Reynolds number), this is not an unreasonable thing to suppose. Further, if the spectra have a fairly universal form, then the energy corresponding to wave number $1/d$ is roughly a fraction $d/(\lambda + d)$ of the mean energy, as was shown in § 4. If we suppose that the fluid β is one–half, and use the database to compare the $f_{\rm f}$ implied by [6.6] to the fraction $d/(\lambda_{\rm f} + d)$ the values (given in Appendix B, Table B2) are amazingly close. The only exception is the case for the colloidal suspension, which has a very small Reynolds number. By observing that the drag coefficient is large in that case, the flaw is easily corrected by using a function of the Reynolds number to scale diameter. For simplicity we propose the general model

$$f_{\rm r} = \left(\frac{d}{\lambda_{\rm r} + d}\right)\left(\frac{Re_{\rm p}}{1 + Re_{\rm p}}\right) \ , \qquad [6.7]$$

which becomes small for small $Re_{\rm p}$. Note that the product $C_d f_{\rm r}$ in [6.6] effectively removes the Reynolds number dependence of k for both large and small $Re_{\rm p}$, so that it only has an importance for Reynolds numbers near one – a regime for which we find no data for homogeneous sedimentation. Thus we are forced to leave the model as a prediction, until such data can be obtained.

The last item of the closure business here is to devise a function for the ratio of integral scale to mean separation $C_{\varepsilon 3}$, and again we turn to the database for guidance. In the colloidal suspension it was clear to Segrè et al. (1997) that the integral scale varied in direct proportion to the mean separation distance. If this were true for all

Reynolds numbers then $C_{\varepsilon 3}$ would be a fixed constant (fully determined by the data) and we would be done. However, this is in contrast to the data for higher $Re_{\rm p}$ which suggest both a smaller value of $C_{\varepsilon 3}$, and a greater–than–unit variation with separation distance. To understand this behavior, we turn to the microphysical picture as follows, which is immediately suggestive of a model.

Let us suppose that mechanism by which particles in the colloidal suspension can communicate with one another over large distances (compared to their mean separation) is a viscous lift force combined with Einstein's mixture viscosity. The mechanism works as follows. Any perturbation causing nonuniformity in particle concentration is accompanied by a change in the buoyancy surrounding a group of particles, causing dense regions to fall slightly faster than the less dense ones; this creates a shear region in between light and heavy spaces. Because particles can move away from a shear region by viscous lift (Saffman 1965) there is created a separation potential that increases the nonuniformity; and it is all aggravated by the fact that the less dense regions are less viscous, so the shear gets even stronger. This action is the definition of instability: the original perturbation must grow, and it only stops when enough viscous dissipation is created to stop it. The result in the colloidal suspension is to produce fingers and spikes resembling a Taylor instability between separated fluids of different density, in a gravity field. For the polystyrene–water system studied by Segrè et al. (1997) the result is to produce structures having a height that is about ten or so mean spacings, and a width that is about one–third of the height.

Now consider the high Reynolds number case, where it has also been observed that particles tend to congregate with each other (called "preferential concentration" by Squires & Eaton 1991) as a result of an entirely different mechanism. When the momentum transfer rate is slow (weak coupling) then as the fluid spins and contorts the particles have trouble following; so they simply wind up hanging around flow spaces that are more quiescent (relatively speaking, of course). These quiescent spaces are the stagnation zones where in fact the shear is the highest; and furthermore because the coupling–force density increases with concentration the congregation effect *enhances* the quiescence. Furthermore if the particles are fluctuating in such a way that they collide in the high concentration areas, then they may dissipate the fluctuational energy which enhances even more the tendency

to remain congregated. Finally it is known that a potential flow force exists that tends to move an immersed body toward higher shear (Drew 1983, Zhang & Prosperetti 1994). So inertia, coupling, collisions, and potential effects all add up to yet another instability.

Both the viscous and nonviscous effects are wrapped up in creating what we have called the DKT instability, which is our catchall term for describing these highly nonlinear, complex dynamics.

In the case of glass spheres falling in water the particles tend to "cluster" into groups roughly five D in height by about one D in width; for glass spheres in air the groups are about two D in height by about one–half D in width. (See data in Appendix B.) The picture generated by the foregoing is shown schematically in Fig. 6.2, where the particles are shown by small circles.

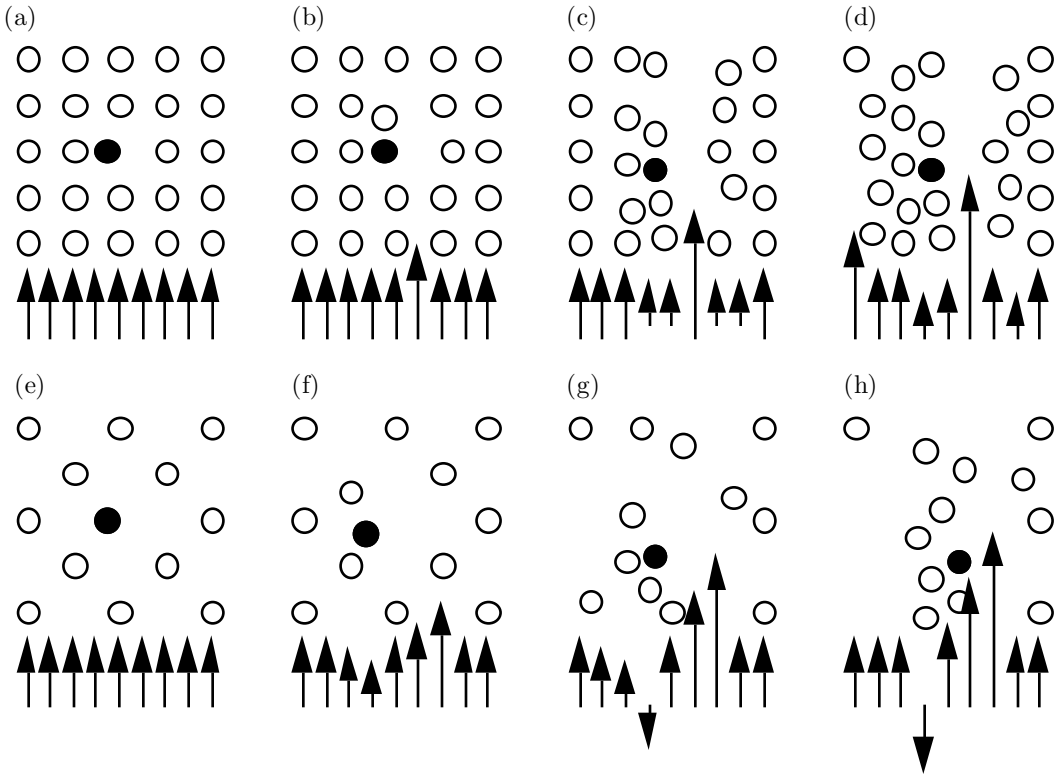

Figure 6.2. Schematic of the DKT instability developing clusters. Time increases from left to right. Row (a)–(d) show development at very small Re_{p}, where particles tend to avoid the shear region due to the viscous lift force; (e)–(h) show development at large Re_{p}, in which case particles congregate in regions of relative stagnation which typically reside in spaces in between fluid eddies – a sort of potential flow effect.

Given a knowledge of the mechanisms that compete with one another to create the instabilities leading to the integral scales observed, one can easily imagine the successful stability analysis that would give the two scales (vertical and horizontal), replete with the dependencies on entity scales, gravity, material densities, viscosities, elasticities, and other relevant parameters. We have not done the analysis, but it should be no great surprise that parts of the analysis have not been completed. The reader can consult Göz (1993) to see that the work is far from done, but that there exists some encouragement that it *could* be done. For the purposes of this work we shall be content to suppose that such an analysis could be carried through to completion, with a result that would agree with the experimental data. Hence we shall settle for a simple correlation with which to plug the last remaining hole in the present theory, leaving the unfinished stability matter as interesting future work for a rainy day.

The settling velocity in a homogeneous suspension is typically a simple function of the densities, entity scale, gravity and viscosity:

$$w^2 = \frac{gd|\rho_{\mathrm{f}}^{\mathrm{o}} - \rho_{\mathrm{p}}^{\mathrm{o}}|}{\frac{3}{4}C_d\rho_{\mathrm{f}}^{\mathrm{o}}}$$

which contains everything expected to influence the stability except for the separation distance and elasticity. If we elect to make a correlation based on mean relative Reynolds number, then we are probably at least getting the majority of the physical parameters into the expression. Our present model involves only a single scalar length $k^{\frac{3}{2}}/\varepsilon$, so we cannot distinguish between vertical and horizontal integral scales. (Extension to a tensor integral scale is future work too.) Hence we need but one relation for $C_{\varepsilon 3}$ which shows a decrease with Re_{p}. A function that does this is

$$C_{\varepsilon 3} = 1 + 5/(1 + Re_p^{\frac{1}{2}}) \qquad [6.8]$$

which is used in the following calculations.

Solutions for the closed system [6.3–6.4] are shown in Fig. 6.3 for the conditions given in the data set for homogeneous sedimentation.

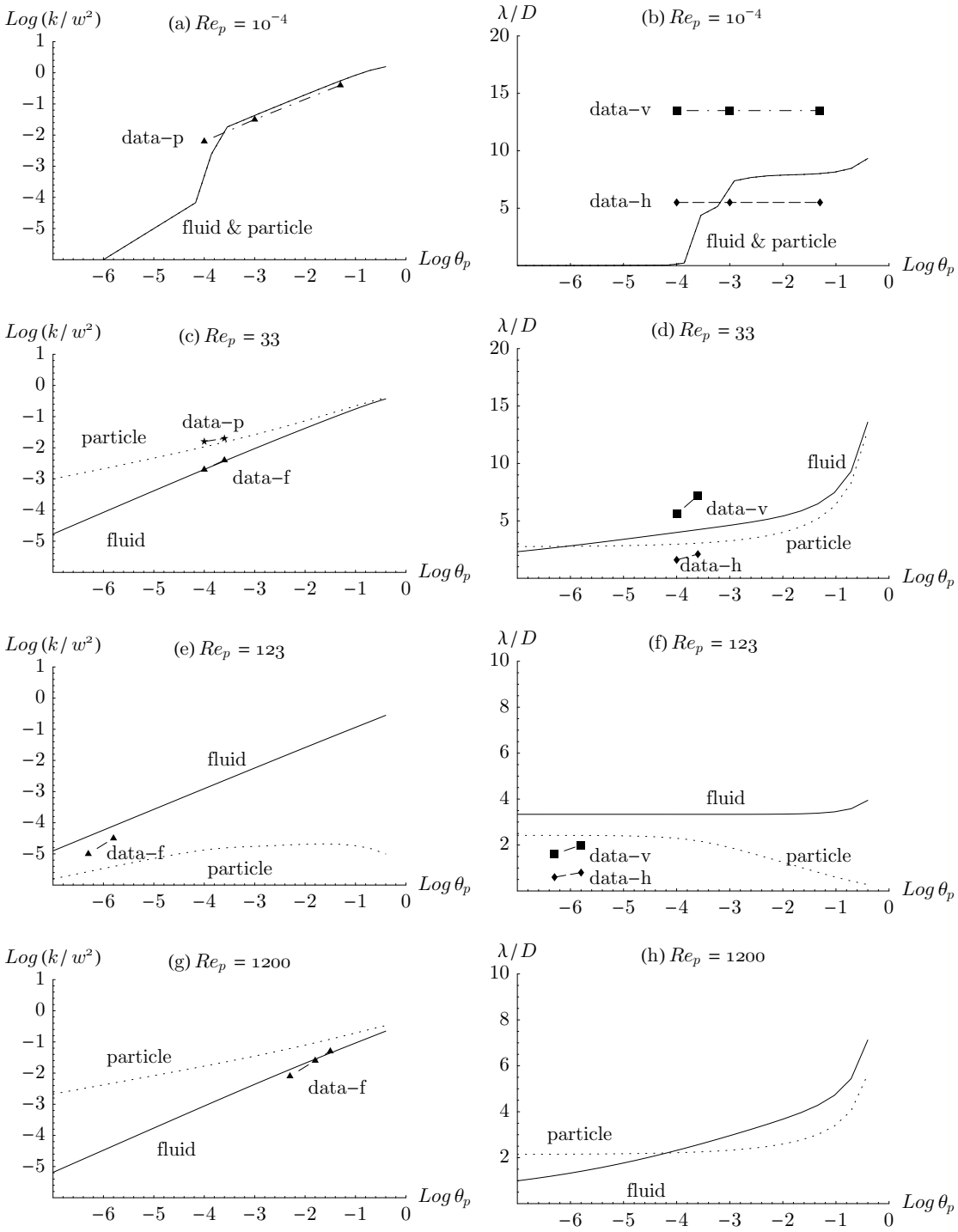

Figure 6.3. Homogeneous sedimentation solutions for the conditions corresponding to Table 6.2. The left column has $\mathrm{Log}(k/w^2)$ versus $\mathrm{Log}(\theta_\mathrm{p})$; the right column has (λ/D) versus $\mathrm{Log}(\theta_\mathrm{p})$. Row (a)–(b) is for the $Re_\mathrm{p} = 10^{-4}$ colloidal polystyrene in water; (c)–(d) is for the $Re_\mathrm{p} = 33$ glass beads in water; (e)–(f) is for $Re_\mathrm{p} = 123$ glass beads in air; and (g)–(h) is for $Re_\mathrm{p} = 1200$ bubbles rising in water.

There are several things that are supposed to be noteworthy in Fig. 6.3, one of the most prominent of which is the breadth of the data. The cases are arranged in order of increasing Re_{p}, with the lowest relative Reynolds number at the top.

The top row has the result for the colloidal suspension (Segrè et al. 1997) in which the fluid and particle properties have been driven together by the strong momentum coupling. The flat integral scale for the colloidal suspension is a direct consequence of the model for $C_{\varepsilon 3}$, and reflects the linear increase in λ with separation D (recall that we are plotting λ/D). What is somewhat of a pleasant surprise, however, is that for very low concentrations the integral scales still get small (as would be expected) – and rapidly so, below a volume loading of around 10^{-4}; the scale also tends to increase rapidly above volume fractions of about 10^{-1}. Both trends are quite plausible but as yet unmeasured.

The second row in Fig. 6.3 has the results for glass beads falling in water, which clearly shows that the beads have a higher fluctuational energy than does the water, as was measured (Parthasarathy and Faeth 1990). The fluid integral scale falls between the measured values for the horizontal and vertical directions, and shows an increase with loading, although perhaps not as rapid an increase as the data would indicate. In this case the theory gives a particle integral scale (not measured) that is typically smaller than that of the fluid, except at extremely small particle loading.

The third row has the result for glass beads falling in air (Mizukami et al. 1992). In this result the beads clearly have a lower energy than does the air, but just about one order of magnitude in the range of the measurements. This is in contrast to the theory of Koch (1990) which suggests that the beads should have an energy about two orders of magnitude less than that of the air, under these conditions. Again the integral scales are about in correspondence with the measured values for the fluid; however now the fluid exhibits a larger scale than does the particle field.

Finally, the bottom row of Fig. 6.3 has the result for bubbles rising in water, and shows bubble fluctuational energies (not measured) greater than the water energies, for small bubble concentrations. Again the model suggests a bubble integral scale is greater than the fluid integral scale, neither of which were reported (Lance and Bataille 1991).

These results for the scalar parts of the homogeneous sedimentation are encouraging in the sense that there exists, so far, one set of coefficients that permit the model equations to exhibit a behavior that is qualitatively sensible and in most cases quantitatively correct.

Now we must go on to explore what the formalism may have to say about the anisotropy. Since mean flow gradients are absent from the homogeneous sedimentation problem, the zeroth–order approximation [5.5] gives the full anisotropy. The r–material anisotropy is

$$\mathbf{b}_{\mathrm{r}}^{(0)} = g'_{\mathrm{s}}\boldsymbol{\kappa}_{\mathrm{r}} + \xi'_{\mathrm{r}}\boldsymbol{\kappa}_{\mathrm{s}}$$

where the nondimensional factors $\boldsymbol{\kappa}$, g and ξ, defined in § 5, contain the last remaining coefficients to be established. Recall too that the anisotropy tensor has one nonzero component in the case of homogeneous sedimentation, and again let that component be the one associated with the $\mathbf{e}_3$ direction. In § 5 we showed that the functional form of the model equations dictates $\gamma = R_{33}/R_{11} > 1$. The data set given in Table 6.2 (and fully described in Appendix B) contains data for this ratio, and we shall use it to help gauge the constants C_5, C_6, and C_7. By definition of the anisotropy, it turns out that the foregoing ratio of stress components is simply

$$\gamma_{\mathrm{r}} = 1 + 3b_{\mathrm{r}33} \ , \qquad \gamma_{\mathrm{s}} = 1 + 3b_{\mathrm{s}33} \ .$$

To gauge the coefficients, we start by fixing one value and varying the others while comparing γ to the experimental data. In this case it is convenient to set C_5, which multiplies the slip production rate in the coefficients $\boldsymbol{\kappa}$, while varying C_6 and C_7 (which appear only in the factors g and ξ). Inspection of the terms into which these coefficients are placed shows that a unit value of C_5 removes all of the anisotropy, and unit values for C_6 and C_7 take away all influence of the energy exchange process. Results from this procedure are summarized in Fig. 6.4, where again the cases are arranged in order of increasing Re_{p}. In these calculations, the standard single–phase value of $C_1 = 2$ has been used, along with $C_5 = \frac{1}{2}$.

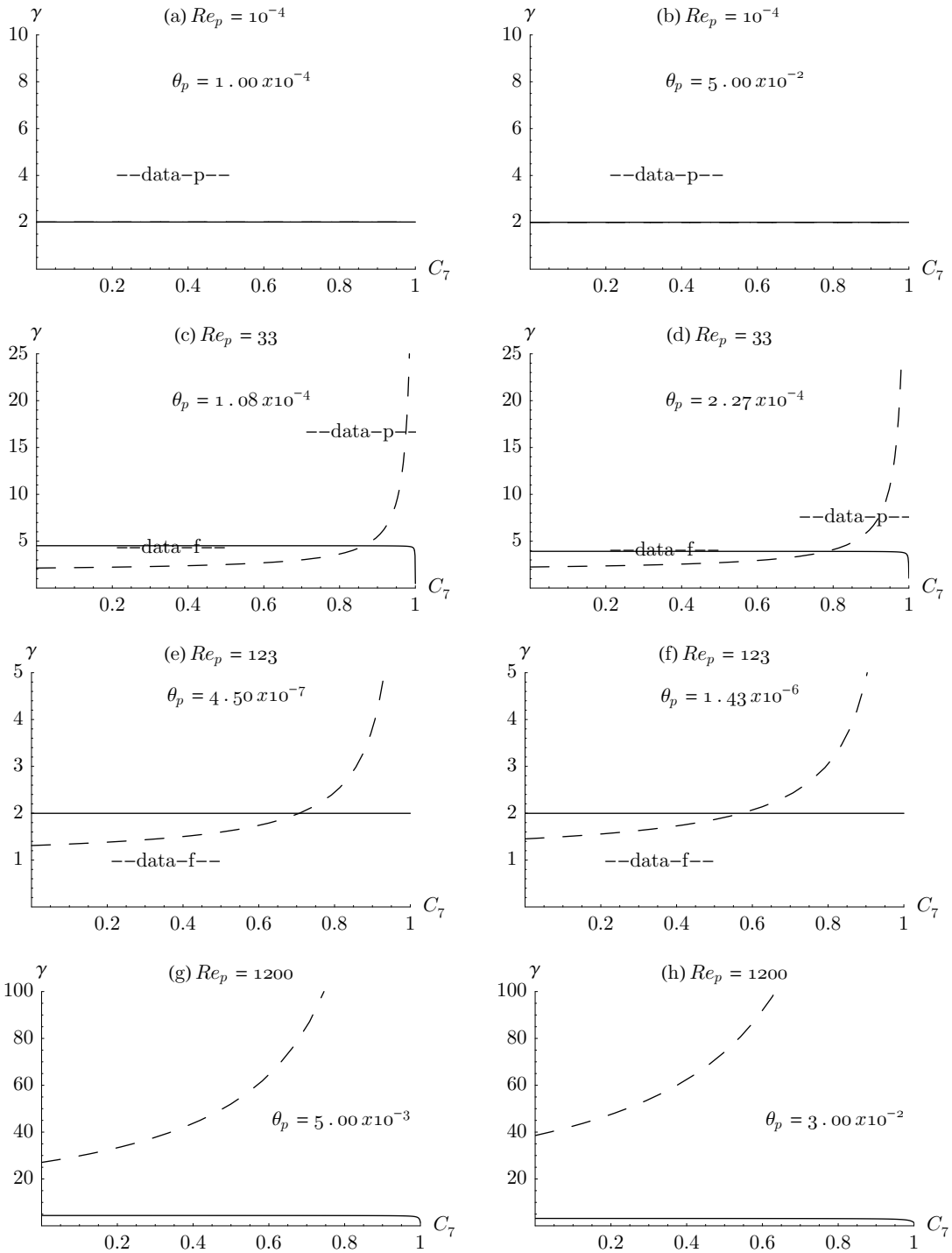

Figure 6.4. Stress ratio γ versus coefficient C_7 for the homogeneous sedimentation database. These results are for a fixed value of $C_5 = 0.5$, and $C_6 = C_7$. The left column shows that result for the lowest volume fraction cases, and the right column has the highest volume fraction cases for each of the various experiments, listed in the same order as in Fig. 6.3.

In Fig. 6.4 (a–b) the fluid and particle results are the same; in (c–h) the solid (flat) curves are associated with the fluid field and the dashed curves are for the particle field. Note that in Fig. 6.4, the first row (colloidal polystyrene) indicates that the anisotropy is independent of the value used for C_6 (because of the strong momentum coupling), and the model value lies below the data in the range of volume fractions studied; however the model does show a small change with θ_p that was not observed in the experiments.

The second row from the top ($Re_{\rm p} = 33$), shows that $\gamma_{\rm f}$ is slightly above the data, until suddenly dropping near $C_6 = 1$, while $\gamma_{\rm p}$ does the opposite, but not so drastically. These results would indicate a value of C_6 somewhere above about 0.9 but certainly below 1.0 where both γ's undergo a very sudden change.

The third row ($Re_{\rm p} = 123$) shows the model $\gamma_{\rm f}$ at about half of the value indicated by the data ($\gamma_{\rm p}$ could not be measured in this experiment).

There were no γ data for the bubble–water case, but the very high $\gamma_{\rm p}$ shown in row four could be a consequence of the possibly high bubble energies seen earlier.

We conclude that the theory is in reasonable (but certainly not perfect) agreement with the data for $C_5 = 0.5$, $C_6 = C_7 = 0.9$, on the basis that the γ is below that data for the colloidal case and above the (fluid) data for the higher $Re_{\rm p}$ cases; so the data is at least bracketed by the model. The very rapid variation of $\gamma_{\rm f}$ near the unit value of C_6 is reduced if we permit C_7 to approach a unit value more slowly than does C_6 (so the equations decouple slightly before the exchange process is completely removed). Such behavior would perhaps be more favorable, but rather than increase the complexity yet another level, we prefer to leave $C_6 = C_7$ until much more testing can be done.

7. Boundary conditions at a solid wall

The present modeling approach to turbulence in the single–phase limit belongs to the class of so–called high–Reynolds number models, in which the Reynolds number is based on the characteristic mean flow speed and on the characteristic device dimension. In the case of pipe flow, "high" Reynolds numbers are above 10^4 or so, using the pipe diameter for the device scale. For such conditions the most common (and practical) scheme for conducting device–scale numerical calculations is to use a wall–stress boundary condition in lieu of

attempting to resolve the very steep velocity gradient in the wall boundary layer in the fluid. In this approach, the boundary condition on velocity amounts to $\mathbf{n}\cdot\mathbf{u}=0$, $\boldsymbol{\nabla}_{\rm n}\mathbf{u}=0$; the normal velocity is zero, and the gradient in the local normal direction $\mathbf{n}$ is zero. (These two conditions are sufficient to permit construction of a full velocity vector, positioned at the wall, in a discrete manner using data from the flow field a finite distance away from the wall.) Typically the assumption for the turbulence quantities that accompanies the wall stress model, is that in the space nearest the wall, $\boldsymbol{\nabla}_{\rm n}k=0$, $\mathcal{P}^G-\varepsilon=0$; the normal gradient in fluctuational energy is zero and there is a state of local equilibrium where the gradient production is exactly balanced by dissipation. These assumptions regarding the fluctuational energy balance are exactly equivalent to specifying the local integral scale as a function of the local k and some fraction of the local device scale, that fraction being determined by the discrete spatial resolution used in the calculation (grid size).

The purpose of this section is introduce the necessary extensions to the wall–stress, and integral scale models, required to make the multiphase turbulence model compatible with the high–Reynolds number single–phase turbulence model. In the single–phase case, there are many different ways of furnishing specific wall–stress functions, and specific wall–integral scale functions (which vary according to the particular tastes of the analyst). Hence we shall have to select one way for demonstration of the approach here. What should be clear, however, is that the extensions represent a scheme for making the multiphase case compatible – so that the practitioner with a different taste toward handling these matters can use whatever single–phase model may be their favorite, and extend it in the manner shown here. We shall begin with the wall–stress model, and finish with the wall–integral scale model extensions.

7.1. Wall stress for a fluid phase

The main goal of a wall–stress model is to represent the mean flow energy loss to wall friction in some reasonable way. Owing to the huge number of ways that fluid properties and wall (roughness) properties can be combined, the practical way of making this representation is with a correlation to experiment. A good correlation is one having a functional form that has one or two parameters that can be used to tailor the wall

function to a large collection of specific fluid–wall combinations, with a single set of parameters. For single–phase turbulence, there exists a substantial variety for such functional forms, and one that suits our taste is the one–seventh power law, which relates the averaged (tangential) velocity to the distance from the wall, along the local normal. In nondimensional form it is (Kays 1966)

$$u^+ = 8.7(y^+)^{\frac{1}{7}}$$

in which the velocity $u^+ = u\sqrt{\rho/\tau}$ and the distance $y^+ = (y/\nu^o)\sqrt{\tau/\rho}$ are both nondimensionalized by that wall stress. (The superscript o is used on the kinematic viscosity as a reminder that it is a material constant, rather than a turbulent viscosity.) In dimensional terms, the wall stress is

$$\tau = \pm 0.023(\nu^o/uy)^{\frac{1}{4}}\rho u^2 \ , \qquad [7.1]$$

where the sign is taken such that the stress acts to slow the tangential flow. Note the functional form. The wall stress is the tangential dynamic pressure times a simple function of the local Reynolds number (based on the local discretization scale y). This model has been used extensively for time–dependent, three–dimensional device–scale calculations (Amsden et al. 1989) at various flow speeds. It can be used here for the fluid phase in our multiphase model, provided the coefficients are modified according to whatever may be the effect of the particle phase on the structure of the boundary layer.

7.2. Wall stress for a particulate solid phase

For the particle phase–wall interaction, a similar functional form can be developed, using only elementary principles. Like the fluid–wall interaction, we are interested in finding a functional form that expresses the flow loss in a way that can be readily tailored to a specific set of particle–wall material pairs. Recall from elementary kinetic theory, that

the pressure exerted by molecules impacting the wall of a container (a cube, say, with wall length ℓ) can be estimated by

$$\begin{aligned} p = \frac{1}{\ell^2} &\cdot [\text{momentum change for one molecule} - \text{wall collision}] \\ &\cdot [\text{number of molecules}] \\ &\cdot [\text{wall} - \text{collison rate for one molecule}] \\ = \frac{1}{\ell^2} &\cdot [2mc_1] \cdot [n] \cdot \left[\frac{c_1}{2\ell}\right] \end{aligned}$$

for n molecules of equal mass m in the container, and mean molecular velocity c_1 in the direction normal to the wall. Let $mn/\ell^3 = \rho$ and use $\frac{1}{3}(c_1^2 + c_2^2 + c_3^2) = \frac{1}{3}c$ in place of c_1^2 because the pressure is the same in all directions, and this is (Vincenti & Kruger 1982)

$$p = \tfrac{1}{3}\rho c^2 \ ,$$

which is fairly accurate for monatomic molecules (which have only three degrees of freedom; one each associated with the possible directions of motion).

Now consider a flowing macroscopic system, with mean velocity u tangential to the wall, and fluctuational speed $\sqrt{\frac{2}{3}k}$ associated with a discrete collection of r–material solid particles undergoing occasional collisions with the wall. Let the coefficient $\mathrm{e_t}$ be the ratio of tangential velocity just after a wall collision, to the tangential velocity just before. Then the change in tangential momentum is $-mu(1-\mathrm{e_t})$ for a single collision between a particle of mass m and the wall, on average. (Here we suppress r–material indices for simplicity.) For a volume of space with one side adjacent to the wall (again a cube with side length ℓ) the stress would be

$$\tau = \pm\frac{(1-\mathrm{e_t})}{\sqrt{6}}\left(\frac{\sqrt{k}}{u}\right)\rho u^2$$

which assumes that the incoming particles are unaffected by the outgoing ones (no particle–particle collisions near the wall), meaning there is no normal gradient in tangential particle velocity. Clearly there can be sufficiently high particle densities to create a good likelihood that particle–particle collisions will take place, and fluid drag will be present; both of which will generate a normal gradient in u. To allow for such real effects we can express

the fluctuational energy in terms of the local turbulent viscosity, which is $C_\mu^{\circ}\sqrt{k}y = \nu$ (to lowest order). Now the stress becomes

$$\tau = \pm C_\tau (\nu / yu)^\eta \rho u^2 \qquad [7.2]$$

in which the coefficient would be $C_\tau = (1 - \mathrm{e_t})/C_\mu^{\circ\,\frac{1}{4}}\sqrt{6}$ if this relationship were exact. The power η would be $\frac{1}{4}$ if the velocity profile were to be like the one–seventh power law for the fluid, nondimensionalized by the turbulent viscosity ν, in which case the functional form is identical to the fluid wall stress [7.1], but using the turbulent viscosity. Specific values for the coefficient and the power can be interpreted, for certain limited conditions, from analytic work in the literature (see for example, Sinclair & Jackson 1989). For cases lacking a trustworthy analytic theory, the foregoing model can be related to experimental data reported in the form of a friction coefficient (for such data see any of the handbooks, such as Hetsroni 1982). One could also boldly use results from DNS such as those performed by Thakurta et al. (1998), taking appropriate caution.

This completes our model for the wall stress. For a fluid phase the expression [7.1] is used, typically with the standard values for the pure–fluid coefficients; for the particle phase, whatever it may be, we propose [7.2] with coefficients determined on a case–by–case basis using either analytic theory or available experimental data relevant to the materials making up the system. (The practitioner should exercise some caution here, because the data typically are all for steady state situations, and often are correlated for the total stress; which includes both fluid–wall and particle–wall contributions.)

7.3. Boundary condition on ε

The multiphase model for the wall integral scale requires two extensions beyond the standard single–phase model. These extensions are given in the following discussion, beginning with a review of the standard single–phase model. The standard model is a solution to the steady state equations for k and ε, written for a discrete region of space, spanning the distance between a point on the wall and a point y units away in the normal direction (Launder & Spalding 1974). The situation is sketched in Fig. 7.1 where k_y and ε_y give the state at the point y; k_w and ε_w give the state at the wall.

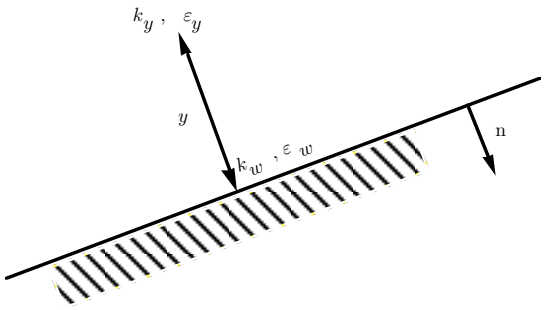

Figure 7.1. Sketch of the coordinate system near an arbitrary solid wall. The point at y units from the wall is the origin of a local coordinate system, with the normal coordinate increasing toward the wall.

The corresponding equations are, using $\mathcal{P}_y^G$ for the gradient production rate, per unit of mass, at y

$$0 = \mathcal{P}_y^G - \varepsilon_y$$

$$0 = \frac{\nu}{\sigma_\varepsilon y}\left[\varepsilon'_w - \varepsilon'_y\right] + \frac{\varepsilon_y}{k_y}\left[C_{\varepsilon 1}\mathcal{P}_y^G - C_{\varepsilon 2}\varepsilon_y\right]$$

where the first part of the ε equation is a one–dimensional discretization of the diffusion term, with gradients ε' at the wall, and at y respectively. The diffusive loss of energy near the wall is neglected; the assumption implied is that the second derivative of the energy distribution in the normal direction is zero (or at least negligible as a higher–order effect). The model assumes $\varepsilon'_w = 0$, and uses the discrete approximation $\varepsilon'_y = (\varepsilon_w - \varepsilon_y)/y$, with $\varepsilon_w = 0$. Using $\nu = C_\mu^{\text{o}} k_y^2/\varepsilon_y$, the only unknown is ε_y. The solution is the boundary condition. It is

$$\varepsilon_y^2 = \frac{C_\mu^{\text{o}}}{\sigma_\varepsilon(C_{\varepsilon 2} - C_{\varepsilon 1})}\left(\frac{k_y^3}{y^2}\right) \ , \qquad [7.3]$$

which is a standard result.

The first multiphase extension is to include the slip production term in the energy equation, while neglecting the exchange term, the idea being that both energy diffusion and exchange are higher–order effects. Now the model equations are, using $\mathcal{P}_y^S$ for the r–material slip production rate, per unit of r–material mass,

$$0 = \mathcal{P}_y^G - \varepsilon_y + \mathcal{P}_y^S$$

$$0 = \frac{\nu}{\sigma_\varepsilon y}\left[\varepsilon'_w - \varepsilon'_y\right] + \frac{\varepsilon_y}{k_y}\left[C_{\varepsilon 1}\mathcal{P}_y^G - C_{\varepsilon 2}\varepsilon_y + C_{\varepsilon 3}\mathcal{P}_y^S\right] \ ,$$

where again the indices on material type are suppressed for simplicity. The second multiphase extension arises with a slightly higher approximation for ε'_y. In this we

recognize that there may be a reduction in the local dissipation in some materials, if the material is only partially elastic. Let $\mathrm{e_n}$ be the ratio of normal velocity magnitude after and before a particle–wall collision (the normal restitution coefficient as opposed to the tangential one needed for the particulate wall stress). Then we may suppose that $k_w \sim \mathrm{e_n^2} k_y$ for this material, which means that $k_y' \sim -(1-\mathrm{e_n^2})k_y/y$. By similarity we expect $\varepsilon_y' \sim -(1-\mathrm{e_n^2})\varepsilon_y/y$. Again we set the wall gradient of dissipation to zero by analogy to the single–phase case, and eliminate the gradient production term between the model equations. The result is the multiphase model for the boundary condition on ε:

$$\varepsilon_y^2 - \varepsilon_y \left(\frac{C_{\varepsilon 3} - C_{\varepsilon 1}}{C_{\varepsilon 2} - C_{\varepsilon 1}} \right) \mathcal{P}_y^S = \frac{C_\mu^{\mathrm{o}} (1 - \mathrm{e_n^2})}{\sigma_\varepsilon (C_{\varepsilon 2} - C_{\varepsilon 1})} \left(\frac{k_y^3}{y^2} \right) \ . \qquad [7.4]$$

Equation [7.4] is identical to [7.3] for $\mathrm{e_n} = 0$ and $\mathcal{P}_y^S = 0$, which is what would be expected in the case of a pure fluid. For particles having finite elasticity ($0 < \mathrm{e_n} < 1$) this is probably a reasonable approximation as well; it recognizes that the integral scale is influenced by both elastic effects in the material, and by the rate of energy production via momentum coupling. If the volume fraction of discrete material is nonzero, then the production rate will likewise be nonzero for any amount of relative motion. Solution of the quadratic [7.4] is straightforward, and the nature of the parameters guarantees ε_y to be a nonnegative real number. Finally, because wall values are typically needed for evaluation of the diffusive fluxes, the wall values consistent with the foregoing (either [7.3] or [7.4]) are

$$k_w = k_y \quad \text{and} \quad \varepsilon_w = \varepsilon_y \ ,$$

which effectively sets a zero diffusive flux (normal) to the wall for both k and ε. The is correct because the eventual effects of a diffusive loss to the wall have been taken into account by the calculation of ε_y.

We close this section by remarking that the boundary conditions given here are to be regarded as the lowest–order approximations for stress and integral scale, consistent with the model for the field variables. One could certainly improve on these boundary conditions by introducing non–steady state effects, for example. It is not unreasonable, nor is it unusual to make the boundary conditions themselves into time–dependent functions.

We settle for the low–order functions given here only to show the means by which the model is made consistent with what is typically done in turbulence work that is considered to be both general and useful; referring once again to our discussion in the Introduction. Hence our goal is to include in our formalism the basic steps one would take to formulate boundary conditions that fit the model equations.

8. Summary and discussion

To begin our summary, let us briefly recap the developments of this report. In § 3 we showed how an exact set of dynamical equations for multiple materials, each having arbitrary compressibility, could yield a set of field equations by way of ensemble averaging. Multiple mass conservation equations emerged naturally, and because we neglect a transfer between material types, these mass equations look identical to a single–phase mass conservation equation written for each material using the material–specific velocity. The momentum equations for each field likewise resemble the single–phase momentum equation, with two additions: (1) a conservative acceleration coming from averaged deviations between the material stress and the mixture stress; and (2) an interaction force representing thrusting of one material upon another. (As an aside we discussed the closure of the equation system ignoring the Reynolds stress, in order to make clear the meaning of pressure in the equations, with special emphasis on the incompressible limit.) The equation developed for the multiphase Reynolds stress resembles the analog in single–phase turbulence, plus two effects: (1) a production term arising from differences between the material stress and the mixture stress, and (2) a jump density that has been modeled here as a positive production plus a conservative exchange in stress. We pointed out that the work in § 3 was primarily organizational in nature, consisting of preparatory steps needed to separate out that which is new from that which is commonly known about multiphase flow.

In § 4 we focused on developing the closure approximations unique to this approach to multiphase turbulence. These mainly consisted of partitioning the rate at which flow energy is diverted from the mean kinetic energy, into a combination of heat energy and fluctuational energy. We also developed the evolution equation for the materialwise

dissipation rate, using classical similarity methods. One unique aspect of this similarity method is that the mean flow energy diverted into fluctuational energy is expected to influence the energy spectra by causing a shift in the integral scale toward one that is characteristic of the process creating the diversion, namely the momentum interaction force density. For this behavior a new model is introduced. Finally, in order to superimpose the effects of grain–grain collisions, we decompose the fluctuational energy spectrum for a grainlike material in order to select the probable energy associated with collisions, called the collisional temperature.

Section 5 was devoted to the business of invoking the structural equilibrium approximation, finding the appropriate (linear) closure expression for the isotropization tensor, and obtaining an approximate solution for the Reynolds stress. The perturbation expansion method for obtaining the approximate solution is new, and applies equally well to the single–field case. The result for the stress is also new, and we showed how uniquely multiphase features are embedded in the solution. One effect is the anisotropy arising from the mean relative motion; another is the depression of turbulent viscosity coming from the energy exchange process. The equations limit smoothly to the single–phase equations as the volume fraction of one field approaches a unit value, in which case the model becomes essentially equivalent to the standard k–ε model of Launder & Spalding (1974).

Having obtained a fully closed set of model equations in § 3–5 in their functional form, we turned to the task of gauging the undetermined coefficient functions in § 6. By using a standard set of coefficients known to be reliable (in a sense) for single–phase flow, we showed that all of the new coefficients could be determined by using data for two ideal circumstances: (1) isotropic two–fluid decay of turbulence; and (2) homogeneous sedimentation. A satisfactory set of functions was shown to exist, that appears capable of describing the available data over a seven order of magnitude range in relative Reynolds number.

This summarizes what has been done here. Next we need to discuss the range of applicability of the theory, and some of the many things still remaining to be done.

8.1. Range of validity

There are a variety of issues concerning the range of validity for the model equations developed here. Some high–level issues are, in no particular order: (1) validity of local structural equilibrium approximation, and attendant solution for the stress; (2) validity of combining fluctuational energy produced by mean flow gradients with the energy produced by slip between materials; and (3) validity of the continuum assumption implied by the averaged equations. The first issue has to do with the model for the Reynolds stress; the second has to do with the marriage of gradient–generated turbulence with our multiphase turbulence (Lhuillier's pseudo–turbulence); and the third has to do with the multiphase model equations themselves – with or without the Reynolds stress. We shall attempt a rational discussion of these items in that (arbitrary) order.

The first validity question can be dispensed with immediately: we really do not know what to expect for the range of validity for the Reynolds stress model developed here. Qualitatively the main premise is that if the spatial gradients in the flow are not too large, then the turbulence can adjust itself so that it would appear to be in structural equilibrium. Quantitatively, the goodness of this approximation has to be determined by careful and extensive testing in practical situations; if the progress in single–phase turbulence is any indication, this testing will take a good many years to accomplish. We hope, of course, that the outcome would be a valid multiphase model at least as useful as the popular k–ε model has been for engineering studies in single–phase turbulence (whose limitations are still becoming better defined).

The second question can be settled to some degree of satisfaction by considering the relative magnitude of the length scales associated with different physical effects in the problem. For the single–phase turbulence problem the success of all existing theories depends upon the large disparity between the integral scale of motion λ, which is typically comparable to the device scale L, and the smallest–scale motions where the actual viscous dissipation is supposed to take place. The smallest scale is known as the Kolmogorov length scale $\eta = (\nu^3/\varepsilon)^{\frac{1}{4}}$. According to the very convincing presentation by Tennekes & Lumley (1972), the reason that one can model fluid turbulence with any success at all is because the motions at the Kolmogorov scale are statistically independent from the integral

scale motion. This means that for $\eta/\lambda \ll 1$ the behavior of the fluid turbulence becomes independent of the material properties, in particular the fluid viscosity. Crudely speaking it means that the small–scale motions organize themselves in such a way that they can furnish whatever dissipation may be called for by the macroscopic flow conditions – so the large–scale (inertially dominated) motions can behave in a fairly universal way. The typical measure of relevance is the Reynolds number $Re = UL/\nu$ based on the convective flow speed, system dimension, and fluid viscosity. For Re greater than a couple of thousand the length scales are generally far enough apart to permit universal description for many flow situations. Apart from a long list of very ugly details, the single–phase turbulence picture is, in a sense, rather tidy.

Now we want to introduce another material into the problem by placing discrete "particles" in the fluid, and to permit them to move around with the fluid, but not quite with exactly the same mean flow velocity. Incredibly just placing these particles in the flow brings in a whole laundry list of new length scales: the momentum–exchange–size d, mean separation D, mean free path λ_c, integral scale associated with particle fluctuational motion $\lambda_{\rm p}$, wake momentum diameter d_w, wake length d_l, particle boundary layer thickness $\ell_{\rm p}$, and even the space between clusters of particles δ_c. In addition to the previous two scales, this makes a list of ten length scales in the problem (at least). We shall suppose that validity of superimposing the turbulence produced by slip production with that produced by mean flow gradients still depends on separation of the Kolmogorov from the integral scales. Hence our task is to show how the newly introduced scales do not upset the applecart with respect to $\eta/\lambda \ll 1$, which validates the high Reynolds number theory.

Consider first the case of particles having a high relative Reynolds number $Re_{\rm p} = wd/\nu$, where w is a characteristic relative flow speed, like the settling speed of a single grain in an ocean of fluid. The boundary layer thickness at the surface of the distributed particles varies like $\ell_{\rm p} = d \cdot Re_p^{-\frac{1}{2}}$, which is a dissipation scale; if the Kolmogorov scale is not already this small it becomes $\ell_{\rm p}$ by definition. Hence all we need for scale separation is $d/\lambda \ll 1$ which is typical because the integral scale is generally like the device scale L. So for $Re_{\rm p} > 1$ the scales apparently separate. The difficult part has to do with the very small $Re_{\rm p}$ where the boundary layer thickness can become as large as the system

dimension. In this case nature steps in and creates another small scale, and indeed the one where additional dissipation takes place: this is the thin region between the spikes and bubbles created as a consequence of the DKT instability. We showed in § 6 how the integral scale and cluster size are the same item, in the very slow sedimentation of a colloidal suspension. The only way that these features can exist is if there is a thin space between them where most of the shearing is taking place. This thin space is tantamount to a fracture plane in a solid material, or a fault plane in the earth's upper crust: in most places in the mixture the motion is nearly that of a rigid body, with isolated (small volume) spaces in between where the fluid is getting sheared like crazy. (The only area of uncertainty here is if Re_{p} is only slightly less than one; then it is not clear whether the slip planes get created, throwing the validity of the scale separation once again into question. To settle the issue in that regime, either experiments or some kind of convincing stability study is required.) Hence for now we conclude that in general the principle of separation between the dissipative scale and the integral scale is preserved; so the concept of combining the energy produced by mean–field slip and that produced by mean–field gradients is always valid.

The third and last validity question is much deeper and has never really been afforded a proper analysis (at least as far as we have been able to determine). The formalism used here results in what others have called "continuum" equations, and so the tendency is to suppose that some kind of continuum approximation conditions should be imposed, thereby determining the range of validity of the averaged equations. Indeed this is a helpful concept, so it will be instructive to review what is meant by the continuum approximation in its original context. That review in turn leads to a useful validity test for the multiphase equations.

Classically the continuum approximation, as the term is typically used in the kinetic theory of gases, is tested by comparing the molecular mean free path λ_c to the macroscopic scale of the device L. The ratio λ_c/L is called the Knudsen number, which must be small compared to one for the continuum approximation to be valid. The mean free path is a measure of how far molecules are thought to fly through space before striking one another; a small Knudsen number just means that molecules hit each other much more often than

they tend to strike the device boundary. Very frequent molecular collisions cause individual molecules to lose their identity, so that one molecule looks like any other from the statistical point of view. This loss of individuality essentially validates *moments* of the Boltzmann equation, which are the continuum conservation equations for mass, linear momentum, and total energy. Again it is primarily the moment (averaged) equations that are considered valid when the Knudsen number is small; when it is not small the flow regime is often referred to as "free molecular flow". Modeling free molecular flow is often approached by finding approximate (numerical) solutions to the collisionless Boltzmann equation itself, and is sometimes called the "kinetic" approach in plasma physics. The kinetic approach amounts to evolving the statistical distribution function directly, rather than taking for granted that a suitable probability distribution exists and will yield good averages.

Now let us consider the multiphase flow case, and first take on the validity question for a continuous field, like a fluid, in which some set of discrete particles (droplets, bubbles, grains, whisps, parachutes, Volkswagens) are submerged. It should be clear that the mean free path for molecules in the fluid, under most industrial conditions of interest (excluding plasma processing) is generally such that the pure fluid should qualify for a continuum. When its exact equations are averaged, there is no added restriction on the validity; regardless of the size of the particles compared to the flow domain (perhaps with the exception of Brownian motion problems, which we shall exclude here). This is a nice feature of the ensemble average – it just produces an expectation, and in our case uses the **H** function to select certain materials out of the list of possible ones that might occupy a point at any instant. So for a fluid we expect that the equations are always valid (but clearly subject to whatever inaccuracy the model may possess). That leaves the question of validity for the equations for the discrete (particle) material and now we have to get serious about invoking the right kind of test concerning the relationship of scales that will describe the multiphase analog to the Knudsen number.

For this there is some precedence, although not entirely adequate. Part of the required background is furnished by Crowe et al. (1998) who provide an extensive discussion of the relationship of time scales in multiphase flow – but without pinpointing the conditions of validity for the continuum (averaged) equations. The important point here is that the

dispersed entities in a multiphase mixture must undergo some process that permits them to lose their individuality so that the statistical averages that we compute become meaningful. It can be shown that the ensemble averaged equations that we use can be derived from a Boltzmann–like equation for the evolution of an ensemble probability distribution function (Travis et al. 1976); the conditions of validity for this Boltzmann–like equation are the same as for the molecular one. The same goes for its moments, which are our averaged equations.

There are two processes that our particles can undergo causing them to lose their individuality, and therefore behave in a statistically uniform fashion: interactions with the fluid; and interaction with each other via direct collisions. Particle–fluid interaction is by far the most important. The idea is that the discrete entities can behave as a *field* if they communicate in some consistent (predictable) fashion with the fluid. Hence the fluid furnishes a sort of *background* field that normalizes the behavior of the separated entities, in much the same way that an imposed magnetic field normalizes the dynamics of a collection of ions and electrons in a plasma. Direct collisions are important in some cases, so we need a measure of both processes. With these we can construct two multiphase Knudsen numbers.

To obtain the proper length scale for the particle–fluid interaction, consider the dynamics of a single sphere of mass M, and radius a in a fluid having material density $\rho_{\mathrm{f}}^{\mathrm{o}}$. The relaxation equation for its velocity w, relative to that of the surrounding fluid is given by

$$M\dot{w} = -(\pi a^2) C_d \tfrac{1}{2} \rho_{\mathrm{f}}^{\mathrm{o}} w^2$$

where the drag coefficient depends on the relative velocity itself, the size of the sphere, and the viscosity of the fluid (relative flow regime). Let us assume that the relative flow regime is fairly constant. (If the pressure deficit in the wake dominates the drag, then $C_d \sim \frac{1}{2}$, for example.) Given an initial relative velocity, say $w(t=0) = w_{\mathrm{o}}$, this constitutes an initial value problem whose solution (a rare one for nonlinear equations) is, with $M = \frac{4}{3}\pi a^3 \rho_{\mathrm{p}}^{\mathrm{o}}$

$$w(t) = \frac{w_{\mathrm{o}}}{1 + w_{\mathrm{o}} b t}$$

where the coefficient is $b = \frac{3}{8} C_d \rho_{\mathrm{f}}^{\mathrm{o}} / \rho_{\mathrm{p}}^{\mathrm{o}} a$. Clearly as $t \to \infty$ the relative velocity goes to zero. By inspection, the characteristic relaxation time scale is $\tau_R = 1/w_{\mathrm{o}} b = \rho_{\mathrm{p}}^{\mathrm{o}} a / \frac{3}{8} C_d \rho_{\mathrm{f}}^{\mathrm{o}} w_{\mathrm{o}}$. The distance travelled by the sphere in the time τ_R is (with $d = 2a$),

$$\lambda_R = \int_0^{\tau_R} w(t) dt = Ln(2)/b \approx \left(\frac{\rho_{\mathrm{p}}^{\mathrm{o}}}{\rho_{\mathrm{f}}^{\mathrm{o}}} \right) \frac{d}{C_d} \, ,$$

so for solid grains in a gas the relaxation length can be as large as a thousand grain diameters; for bubbles in a liquid the relaxation length is a small fraction of a bubble diameter – both owing to the ratio in material densities. For solid grains in a liquid, where the density ratio is of order one, the relaxation length depends mainly on the flow regime, as it influences the drag coefficient.

Now we need to estimate the mean free path associated with particle–particle collisions, which is not at all a free path because all along the way between collisions the particle is interacting with the fluid – so much so that collisions may be altogether precluded. Nevertheless an estimate can be obtained as follows. Let λ_c be the distance between collisions, and suppose that it is composed of a frequency for actual collisions and a fluctuational speed that scales potential collisions. The frequency is given by classical kinetic theory thinking; it is $\sqrt{2} \pi d^2 n \sqrt{\frac{2}{3} \Theta}$ where n is the number density, and $\sqrt{\frac{2}{3} \Theta}$ is a mean fluctuational speed associated with the collisional temperature. This is just the actual rate of collision, based purely on geometry. It says that if a particle were to have the sustained speed $\sqrt{\frac{2}{3} \Theta}$, then it would be capable of hitting some number of others in a unit of time, where the number is based on the mean spacing. The distance between collisions has to be computed with the realization that not all of the fluctuational energy is available to drive collisions – it may be driving the integral scale motions (large eddies) instead. This was our development in § 4 where we found a model for collisional temperature Θ, which was estimated by [4.9]

$$\Theta = k \left(\frac{D}{D + \lambda} \right)^{\eta} \, , \qquad [4.9]$$

where as usual $D = d(\theta_{\mathrm{p}} \theta_{\mathrm{f}})^{-\frac{1}{3}}$ is the symmetric separation distance. The corresponding potential collisional speed is $\sqrt{\frac{2}{3} k}$. The collisional speed divided by the frequency of

potential collisions is the length between collisions. Apart from some constant factors of order one, this is

$$\lambda_c = \left(\frac{d}{\theta_{\rm p}}\right)\left(\frac{\lambda + D}{D}\right)^{\frac{2}{3}\eta}$$

which indicates that if the integral scale λ is large compared to the mean spacing D then the collision length can be large. Now we can display the two multiphase Knudsen numbers, $N_R = \lambda_R/L$ and $N_c = \lambda_c/L$:

$$N_R = \left(\frac{\rho_{\rm p}^{\rm o}}{\rho_{\rm f}^{\rm o}}\right)\frac{d}{C_d L} \quad \text{and} \quad N_c = \left(\frac{d}{\theta_{\rm p} L}\right)\left(\frac{\lambda + D}{D}\right)^{\frac{2}{3}\eta}$$

at least one of which must be small compared to one for the averaged equations for the dispersed phase to be valid. Amazingly many industrial cases are such that the relaxation number $N_R \ll 1$, with the notable exception of solid grains in a gas, with a small system dimension (gas–solid jet); then the continuum validity depends on the collisional number N_c which can only save the day if the volume fraction is large enough, and the integral scale is not too large compared to the mean grain spacing. Clearly this will not always be attained. Recall from the discussion in the previous section, concerning the integral scale λ. There we saw that the experimental data for homogeneous sedimentation suggest that the integral scale is typically one to five times the mean entity spacing D. If the exponent in the expression for N_c is of order two then the part of N_c involving the integral scale is of order one. Now consider the case of ten micron solid grains in a one centimeter diameter gas jet; then $N_R \sim \mathcal{O}(1)$ and $N_c \sim \mathcal{O}(10^{-3}/\theta_{\rm p})$. Hence the model equations will only be valid for volume fractions greater than 10^{-3} where the mean grain spacing is less than ten grain diameters.

For problems failing to satisfy the continuum condition [$N_r \ll 1$ or $N_c \ll 1$] the averaged equations for the particle phase should not be used. Instead it would be more appropriate (and is common practice) to use the so–called "spray" equation for the dispersed phase, which is a Boltzmann–like equation for the evolution of a probability function for velocity, size, temperature, and whatever other variables may be needed to describe the state of an individual (or representative) particle in the spray (Crowe et al. 1977, Dukowicz 1980, Amsden et al. 1989). The spray equation regime is the macroscopic

analog of the free molecular flow regime in plasma physics. Unfortunately the spray equation method is cumbersome if conditions are such that interaction between individual entities are dominant (collisional effects), in which case the continuum method is once again appropriate, due to collisional relaxation molecular style. Evidently, a satisfactory formalism for making the transition back and forth between spray and continuum regimes has not yet been devised. This leads us to the final subsection, where we list a collection of other items that would make excellent follow–on work.

8.2. Next steps

The largest and most important item of follow–on work is the testing of the theory presented here. This testing will undoubtedly uncover oversights and errors in our thinking relative to the phenomenology, and will (hopefully) suggest ways to remedy those errors. The testing will surely define the limits of applicability for the local structural equilibrium assumption, which is wide open for discovery (in the multiphase case at least).

Another important area that has only been hinted at here, is the proper formulation of the momentum exchange force density for cases of large nonhomogeneity in the local volume fractions. We are confident that the equations are self–consistent, so long as the practitioner uses a force density that is consistent with what is called the averaged velocity. If so, a consistent Reynolds stress should automatically emerge. The bubbling regime in fluidized bed technology is an excellent example of where the force density, based on the averaged relative velocity, is far different from the local–instantaneous force density, because of the extreme nonhomogeneity (large gas bubbles in an otherwise packed bed); the appearance of so–called "clusters and streamers" in a fast–fluidized gas–solid pipe flow is another example of the manifestations of a nonhomogeneous volume fraction.

The velocity fields in a multiphase flow are typically nonsolenoidal. Because the turbulence field variables are transported along the separate material trajectories, the turbulence will be subjected to compression and expansion. In single–phase turbulence the "Rapid Distortion Theory" (Reynolds 1987) gives rise to an additional term in the equation for ε which has been ignored here. RTD could provide an important improvement in the present theory by determining the proper variation in the integral scale

associated with multiphase compression and expansion, which has nothing to do with the material compressibility of the components making up the mixture. In this connection, an examination of the "realizability" (Reynolds 1987) of the model equations should be taken up as well, an exercise that should provide physical limits on the coefficients finally selected in the model.

In the present theory, the isotropic form of the dissipation tensor leads to a scalar integral scale. The data for homogeneous sedimentation show that the integral scale is itself anisotropic. Some kind of extension that permits anisotropic dissipation might improve on the generality of the present model. Apart from the anisotropic nature of the integral scale, we found it necessary to include the physical effect of the DKT instability on the energy spectra, which was introduced in § 4 in the discussion of the evolution equation for ε. The coefficient for the scale–relaxation model was postulated in § 6 as a function of Re_{p} only, which may be inadequate in general. For this it would be much more satisfactory to obtain, say, the proper scaling of this relaxation law from a proper stability analysis. Such analysis would hopefully include the main features that lead to the DKT instability, which was shown to be instrumental at all values of Re_{p}.

The goal here has been to develop a turbulence model capable of predicting the averaged flow fields directly. This means that bubbles and slugs in devices such as fluidized beds, risers and bubble columns are all averaged over. The result is typically time–steady, which is supposed to equate to the time–averaged statistically stationary state characteristic of the bubbling device. It is well known that the net chemical reaction rate can be greatly affected by the instantaneous bubbling (intermittency) of this kind of device. To round out the general usefulness of this theory, a companion theory is needed for relating net (averaged) chemical reaction rates to the mean flow and turbulent flow variables. This is the analog to computing the force density for the (instantaneous) nonhomogeneous volume fraction field.

Finally, and certainly not lowest on the list, is the idea of using a spectral approach to fine–tune the present theory – and perhaps even to place some of the more intuitive parts onto a more solid (or even correct) foundation. This is where we would hope that the

present work could eventually lead; so that some of the guesswork, or even the dependence on experiment, might be removed from the theory.

Acknowledgments

Support for this work from The Procter & Gamble Company is gratefully acknowledged. Joseph Kitching and John McKibben of P&G were very helpful users during the formative stages of the theory. The authors thank the many members of Los Alamos National Laboratory, Theoretical Division Group T–3 for helpful discussions that are ongoing; notably Tim Clark, Frank Harlow, Rick Rauenzahn, Chuck Zemach, and Duan Zhang.

Appendix A. Expression for the Collisional Contribution to the Stress

An additional contribution to the isotropic part of the Reynolds stress arises as a result of direct grain–grain collisions due to fluctuational motion. This additional contribution is often called the granular pressure. The kinetic theory of gases, applied to granular materials, provides a model for this effect giving a pressure departure

$$2\rho_{\mathrm{p}}^{\mathrm{o}}\left(1+e_{\mathrm{p}}^{\mathrm{o}}\right)g_{\mathrm{o}}\theta_{\mathrm{p}}\Theta_{\mathrm{p}}$$

where $e_{\mathrm{p}}^{\mathrm{o}}$ is the coefficient of restitution, g_{o} is a so–called radial distribution function and Θ_{p} is the so–called granular temperature of the granular media (Savage & Jeffrey 1981, Gidaspow 1994). The radial distribution function is usually assumed to be a function of the solids volume fraction, a function which is one for low volume fractions and very large for volume fractions approaching the close–packing limit, denoted θ_{cp}. A simple model often used is

$$g_{\mathrm{o}}=\left[1-\left(\frac{\theta_{\mathrm{p}}}{\theta_{cp}}\right)^{\frac{1}{3}}\right]^{-1}$$

The granular temperature is a measure of the fluctuational kinetic energy driving the grain–grain collisions. It will typically be some fraction of the turbulence kinetic energy, as is shown in § 4.

An additional contribution to the solids phase deviatoric stress arises from grain–grain collisions as well. Again, we can turn to the kinetic theory of granular materials for a closure model. The simplest result is of the form

$$2\mu_{\mathrm{p}}^{\mathrm{o}}\mathbf{S}_{\mathrm{p}}$$

where $\mathbf{S}_{\mathrm{p}}$ is the traceless rate–of–strain tensor for the grain phase, based on the mean grain phase velocity. The granular viscosity coefficient is given by

$$\mu_{\mathrm{p}}^{\mathrm{o}}=\frac{4}{5\sqrt{\pi}}\theta_{\mathrm{p}}\rho_{\mathrm{p}}^{\mathrm{o}}dg_{\mathrm{o}}\left(1+e_{\mathrm{p}}^{\mathrm{o}}\right)\sqrt{\Theta_{\mathrm{p}}}$$

where d is the diameter of the grains.

Appendix B. Homogeneous Sedimentation Database

Here we display the data collected from the literature, and placed into a database for our use in § 6.2. Table B1 contains the dimensional quantities cited directly from the various publications, and Table B2 has the same numbers in nondimensional form.

d (cm)	theta_p	w (cm/s)	k_f (cm/s)^2	k_p (cm/s)^2	gamma_f	gamma_p	l_v (cm)	l_h (cm)
Parthasarathy & Faeth (1990) J. Fluid Mech. **220**, 485-514.								
	glass beads in water (2.45:1.0)							
5.00E-02	1.08E-04	6.50E+00	8.01E-02	6.78E-01	4.25E+00	1.66E+01	5.90E+00	1.70E+00
5.00E-02	2.27E-04	6.50E+00	1.83E-01	9.26E-01	4.03E+00	7.56E+00	5.90E+00	1.70E+00
1.00E-01	2.86E-05	1.47E+01	4.32E-02	1.51E+00	4.00E+00	4.62E+01	5.90E+00	1.50E+00
1.00E-01	1.63E-04	1.47E+01	1.83E-01	2.95E+00	4.92E+00	8.75E+00	5.90E+00	1.50E+00
2.00E-01	3.40E-05	2.62E+01	9.74E-02	2.41E+00	4.74E+00	5.93E+00	5.70E+00	2.10E+00
2.00E-01	9.92E-05	2.62E+01	2.82E-01	3.06E+00	3.87E+00	4.38E+00	5.70E+00	2.10E+00
Lance & Bataille (1991) J. Fluid Mech. **222**, 95-118.								
	air bubbles in water (0.001:1.0)							
5.00E-01	5.00E-03	2.40E+01	4.95E+00	a	-	-	-	-
5.00E-01	1.60E-02	2.40E+01	1.59E+01	a	-	-	-	-
5.00E-01	3.00E-02	2.40E+01	2.97E+01	a	-	-	-	-
Mizukami, Parthasarathy, & Faeth (1992) Int. J. Multiphase Flow **18**, 397-412.								
	glass beads in air (2.45:0.001)							
5.50E-02	4.50E-07	3.36E+02	1.14E+00	b	9.60E-01	-	1.17E+01	4.01E+00
5.50E-02	1.43E-06	3.36E+02	3.90E+00	b	2.28E+00	-	9.80E+00	3.82E+00
5.50E-02	2.87E-06	3.36E+02	-	b	-	-	-	-
1.00E-01	3.90E-07	4.97E+02	5.28E-01	b	1.63E+01	-	1.23E+01	1.25E+00
1.00E-01	9.70E-07	4.97E+02	1.84E+00	b	8.22E+00	-	9.70E+00	2.00E+00
1.00E-01	2.20E-06	4.97E+02	5.67E+00	b	5.74E+00	-	-	-
2.00E-01	4.00E-07	5.64E+02	1.40E+00	b	1.97E+00	-	1.43E+01	2.49E+00
2.00E-01	8.20E-07	5.64E+02	1.75E+00	b	3.61E+00	-	1.76E+01	2.32E+00
2.00E-01	2.45E-06	5.64E+02	4.24E+00	b	3.02E+00	-	-	-
Segrè, Herbolzheimer & Chaikin (1997) Phys. Rev. Lett. **79**, 2574-2577.								
	polystyrene beads in water (1.05:1.00)							
1.56E-03	1.00E-04	6.50E-04	c	2.73E-09	-	4.00E+00	4.54E-01	1.85E-01
1.56E-03	1.00E-03	6.50E-04	c	1.27E-08	-	4.00E+00	2.11E-01	8.58E-02
1.56E-03	5.00E-02	6.50E-04	c	1.72E-07	-	4.00E+00	5.72E-02	2.33E-02
constants used: gravity magnitude=980 cm^2/s; water viscosity=0.01 cm^2/s; air viscosity=0.15 cm^2/s								

Table B1. Dimensional data for homogeneous sedimentation, taken from the literature. Notes: (a) Bubble–phase fluctuational data were not taken, and only the vertical component of fluctuational velocity was measured; (b) fluctuational velocity in the glass beads was below the sensitivity of the instrumentation, and the apparatus was too short to permit the beads to achieve the terminal velocity; (c) fluid velocity data were not taken, but owing to the very low Reynolds number the fluid statistics and the polystyrene statistics should be quite similar. Also, l_v and l_h are respectively the vertical and horizontal integral scales for the fluid phase.

Re_p	D/d	C_d	W/w	Log(k_f/w^2)	Log(k_p/w^2)	l_v/D	l_h/D	Log(theta_p)
Parthasarathy & Faeth (1990) J. Fluid Mech. **220**, 485-514.								
	glass beads in water (2.45:1.0)							
33	21	2.1	1.0	-2.7	-1.8	5.6	1.6	-4.0
33	16	2.1	1.0	-2.4	-1.7	7.2	2.1	-3.6
147	33	1.1	0.9	-3.7	-2.2	1.8	0.5	-4.5
147	18	1.1	0.9	-3.1	-1.9	3.2	0.8	-3.8
524	31	0.8	0.8	-3.8	-2.5	0.9	0.3	-4.5
524	22	0.8	0.8	-3.4	-2.4	1.3	0.5	-4.0
Lance & Bataille (1991) J. Fluid Mech. **222**, 95-118.								
	air bubbles in water (0.001:1.0)							
1200	6	0.7	1.3	-2.1	-	-	-	-2.3
1200	4	0.7	1.3	-1.6	-	-	-	-1.8
1200	3	0.7	1.3	-1.3	-	-	-	-1.5
Mizukami, Parthasarathy, & Faeth (1992) Int. J. Multiphase Flow **18**, 397-412.								
	glass beads in air (2.45:0.001)							
123	130	1.2	1.1	-5.0	-	1.6	0.6	-6.3
123	89	1.2	1.1	-4.5	-	2.0	0.8	-5.8
123	70	1.2	1.1	-	-	-	-	-5.5
331	137	0.9	1.2	-5.7	-	0.9	0.1	-6.4
331	101	0.9	1.2	-5.1	-	1.0	0.2	-6.0
331	77	0.9	1.2	-4.6	-	-	-	-5.7
752	136	0.7	1.6	-5.4	-	0.5	0.1	-6.4
752	107	0.7	1.6	-5.3	-	0.8	0.1	-6.1
752	74	0.7	1.6	-4.9	-	-	-	-5.6
Segrè, Herbolzheimer & Chaikin (1997) Phys. Rev. Lett. **79**, 2574-2577.								
	polystyrene beads in water (1.05:1.00)							
1.0E-04	22	2.4E+05	1.0	-	-2.2	13.5	5.5	-4.0
1.0E-04	10	2.4E+05	1.0	-	-1.5	13.5	5.5	-3.0
1.0E-04	3	2.4E+05	1.0	-	-0.4	13.5	5.5	-1.3

Table B2. Nondimensional display of the data in Table B1.

In Table B2 the length scales are normalized by our 'symmetric' separation distance $D = d(\theta_{\rm p}\theta_{\rm f})^{-\frac{1}{3}}$; and the observed relative velocity (settling speed) is normalized by the Stokes speed for a single sphere, W, given by

$$W^2 = \frac{gd|\rho_{\rm p}^{\rm o} - \rho_{\rm f}^{\rm o}|}{\frac{3}{4}C_d\rho_{\rm f}^{\rm o}} \ .$$

Finally we illustrate the efficacy of the energy partitioning model given in Eq. [6.7], by comparing to the value implied by the experimental data. For this we use the approximate solution for the homogeneous sedimentation problem given by Eq. [6.6], solved for f_f with the energy, relative velocity, and integral scale coming from the experimental data. The comparison is given in Table B3, in which a value of $\beta_f = \frac{1}{2}$ has been assumed. Notice

that at moderate relative Reynolds numbers there is only about one percent of the slip energy production that goes into the generation of fluctuational energy – the rest goes directly into heat energy; at the very small Reynolds number of the colloid almost none of the available work goes into fluctuational energy.

Re_p			Eq. [6.6]	Eq. [6.7]	[6.6]/[6.7]	
Parthasarathy & Faeth (1990) J. Fluid Mech. **220**, 485-514.						
6935			8.10E-03	8.15E-03	9.93E-01	
6935			1.33E-02	8.15E-03	1.63E+00	
16470			3.99E-03	1.66E-02	2.41E-01	
16470			6.10E-03	1.66E-02	3.68E-01	
41760			5.84E-03	3.38E-02	1.73E-01	
41760			9.86E-03	3.38E-02	2.91E-01	
Lance & Bataille (1991) J. Fluid Mech. **222**, 95-118.						
82601			-	-	-	
82601			-	-	-	
82601			-	-	-	
Mizukami, Parthasarathy, & Faeth (1992) Int. J. Multiphase Flow **18**, 397-412.						
978			7.51E-04	4.64E-03	1.62E-01	
978			1.78E-03	5.54E-03	3.22E-01	
978			-	-	-	
1955			1.96E-04	8.04E-03	2.44E-02	
1955			6.51E-04	1.02E-02	6.40E-02	
1955			-	-	-	
3725			1.16E-03	1.38E-02	8.41E-02	
3725			6.42E-04	1.12E-02	5.72E-02	
3725			-	-	-	
Segrè, Herbolzheimer & Chaikin (1997) Phys. Rev. Lett. **79**, 2574-2577.						
2.4E+03			2.01E-07	3.47E-07	5.79E-01	
2.4E+03			4.34E-07	7.46E-07	5.82E-01	
2.4E+03			1.65E-06	2.69E-06	6.14E-01	

Table B3. Energy partition function using the experimental data in the approximate solution from Eq. [6.6], compared to the model Eq. [6.7].

References

Amsden, A. A., O'Rourke, P. J. & Butler, T. D. 1989 KIVA–II: A computer program for chemically reactive flows with sprays. Los Alamos National Laboratory report LA–11560–MS.

Besnard, D. C. & Harlow, F. H. 1988 Turbulence in multiphase flow. *Int. J. Multiphase Flow* **14**, 679–699.

Bolio, E. J. & Sinclair, J. L. 1995 Gas turbulence modulation in the pneumatic conveying of massive particles in vertical tubes. *Int. J. Multiphase Flow* **21**, 985–1001.

Buyevich, Y. A. 1999 Particulate stresses in dense disperse flow. *Ind. Eng. Chem. Res.* **38**, 731–743.

Cao, J. & Ahmadi, G. 1995 Gas–particle two–phase turbulent flow in vertical duct. *Int. J. Multiphase Flow* **21**, 1203–1228.

Crowe, C. T. & Gillandt, I. 1998 Turbulence modulation of fluid–particle flows – a basic approach. In Proceedings of the Third International Conference on Multiphase Flows, Lyon France, June 8–12.

Crowe, C. T., Sharma, M. P., & Stock, D. E. 1977 Particle–source–in cell (PSI Cell) model for gas–droplet flows. *Trans. ASME, J. Fluids Eng.* **99**, 325–332.

Crowe, C., Summerfield, M. & Tsuji, Y. 1998 *Multiphase Flows with Droplets and Particles*, CRC Press.

Crowe, C. T., Troutt, T. R., & Chung, J. N. 1996 Numerical models for two–phase turbulent flows. *Annu. Rev. Fluid Mech.* **28**, 11–43.

Dasgupta, S., Jackson, R. & Sundaresan, S. 1994 Turbulent gas–particle flow in vertical risers. *AIChE J.* **40**, 215–228.

Drew, D. A. 1983 Mathematical modeling of two–phase flow. *Annu. Rev. Fluid Mech.* **15**, 261–291.

Drew, D. A. & Passman, S. L. 1999 *Theory of Multicomponent Fluids.* Springer–Verlag.

Dukowicz, J. K. 1980 A particle–fluid numerical model for liquid sprays. *J. Comput. Phys.* **35**, 229–253.

Elghobashi, S. E. & Abou–Arab, T. W. 1983 A two–equation turbulence model for two–phase flows. *Phys. Fluids* **26**, 931–938.

Fan, L. S. & Zhu, C. 1998 *Principles of Gas–Solid Flows.* Cambridge University Press.

Gatski, T. B. & Speziale, C. G. 1993 On explicit algebraic stress models for complex turbulent flows. *J. Fluid Mech.* **254**, 59–78.

Gidaspow, D. 1994 *Multiphase Flow and Fluidization – Continuum and Kinetic Theory Descriptions.* Academic Press.

Göz, M. F. 1993 Instabilities and the formation of wave patterns in fluidized beds. In G. Gouesbet and A. Berlemont, eds. *Instabilities in Multiphase Flows*, Plenum Press.

Hetsroni, G. 1982 *Handbook of Multiphase Systems.* Hemisphere.

Hwang, G.–J. & Shen, H. H. 1993 Fluctuation energy equations for turbulent fluid–solid flows. *Int. J. Multiphase Flow* **19**, 887–895.

Ishii, M. 1975 *Thermo–fluid dynamic theory of two–phase flow.* Direction de Etudes et Recherches d'Electricité de France.

Joseph, D. D. 1993 Finite size effects in fluidized suspension experiments. In M. C. Roco, ed. *Particulate Two–Phase Flow*, Butterworth–Heinemann.

Joseph, D. D. & Lundgren, T. S. 1990 Ensemble averaged and mixture theory equations for incompressible fluid–particle suspensions. *Int. J. Multiphase Flow* **16**, 35–42.

Kays, W. M. 1966 *Convective Heat and Mass Transfer*, McGraw–Hill.

Kashiwa, B. A. 1987 Statistical theory of turbulent, incompressible, multimaterial flow. Los Alamos National Laboratory report LA–11088–T.

Kashiwa, B. A. & Gore, R. A. 1991 A four equation model for multiphase turbulent flow. Los Alamos National Laboratory document LA–UR–90–2273. Also in Proceedings, First Joint ASME/JSME Fluids Engineering Conference, June 23–26, 1991, Portland, OR.

Kevorkian, J. 1974 First order partial differential equations. In C. E. Pearson, ed. *Handbook of Applied Mathematics. Selected Results and Methods.* Van Nostrand Reinhold Company.

Kim, S.–W. & Chen, C.–P. 1989 A multiple–time–scale turbulence model based on variable partitioning of the turbulent kinetic energy spectrum. *Numerical Heat Transfer, Part B* **16**, 193–211.

Koch, D. L. 1990 Kinetic theory for a monodisperse gas–solid suspension. *Phys. Fluids A* **2**, 1711–1723.

Kulick, J. D., Fessler, J. R. & Eaton, J. K. 1994 Particle response and turbulence modification in fully developed channel flow. *J. Fluid Mech.* **277**, 109–134.

Lance, M. & Bataille 1991 Turbulence in the liquid phase of a uniform bubbly air–water flow. *J. Fluid Mech.* **222**, 95–118.

Launder, B. E. & Spalding, D. B. 1974 The numerical computation of turbulent flows. *Computer Methods in Applied Mechanics and Engineering*, **3**, 269–289.

Launder, B. E. 1990 Phenomenological modeling: present and future. In J. L. Lumley, ed. *Lecture Notes in Physics* **357**, 439–485, Springer.

Lhuillier, D. 1996 Macroscopic modelling of multi–phase mixtures. In U. Schaflinger, ed. *Flow of Particles in Suspensions.*, Springer–Verlag.

Lundgren, T. S. 1971 Slow flow through stationary random beds and suspensions of spheres. *J. Fluid Mech.* **51**, 273–299.

Ma, D. & Ahmadi, G. 1988 A kinetic model for rapid granular flows of nearly elastic particles including interstitial fluid effects. *Powder Technology* **56**, 191–207.

Mansour, N. N., & Wray, A. A. 1994 Decay of isotropic turbulence at low Reynolds number. *Phys. Fluids* **6**, 808–814.

Mizukami, M., Parthasarathy, R. N., & Faeth, G. M. 1992 Particle–generated turbulence in homogeneous dilute dispersed flows. *Int. J. Multiphase Flow* **18**, 397–412.

Parthasarathy, R. N. & Faeth, G. M. 1990 Turbulence modulation in homogeneous dilute particle–laden flows. *J. Fluid Mech.* **220**, 485–514.

Reynolds, W. C. 1987 Special course on modern theoretical and experimental approaches to turbulent flow structure and its modelling. AGARD–R–755, North Atlantic Treaty Organization.

Roco, M. C., ed. 1993 *Particulate Two–Phase Flow.* Butterworth–Heinemann.

Saffman, P. G. 1965 The lift force on a small sphere in a slow shear flow. *J. Fluid Mech.*, **22**, 385–400.

Saffman, P. G. 1971 On the boundary condition at the surface of a porous medium. *Studies in Appl. Math.* **50**, 93–101.

Savage, S. B. & Jeffrey, D. J. 1981 The stress tensor in a granular flow at high shear rates. *J. Fluid Mech.* **110**, 255-272.

Schiestl, R. 1987 Multiple–time–scale modeling of turbulent flows in one point closures. *Phys. Fluids* **30**, 722–731.

Segrè, P. N., Herbolzheimer, E. & Chaikin, P. M. 1997 Long–range correlations in sedimentation. *Phys. Rev. Lett.* **79**, 2574–2577.

Sinclair, J. L. & Jackson, R. 1989 Gas–particle flow in a vertical pipe with particle–particle interactions. *AIChE J.*, **35**, 1473–1486.

Soo, S. L. 1990 *Multiphase Fluid Dynamics.* Science Press, Beijing.

Sundaram, S. & Collins, L. R. 1999 A numerical study of the modulation of isotropic turbulence by suspended particles. *J. Fluid Mech.* **379**, 105–143.

Squires, K. D. & Eaton, J. K. 1991 Preferential concentration of particles by turbulence. *Phys. Fluids A* **3**, 1169–1178.

Tennekes, H. & Lumley, J. L. 1972 *A First Course in Turbulence.* The MIT Press.

Thakurta, D. G., Chen, M., McLaughlin, J. B., & Kontomaris, K. 1998 Thermophoretic deposition of small particles in a direct numerical simulation of turbulent channel flow. *Int. J. Heat and Mass Transfer* **41**, 4167–4182.

Travis, J. R., Harlow, F. H. & Amsden, A. A. 1976 Numerical calculation of two–phase flows. *Nuclear Science and Engineering* **61**, 1–10.

Tryggvason, G. 2000 Private communication.

Vincenti, W. G. & Kruger, C. H. 1982 *Introduction to Physical Gas Dynamics.* Robert E. Krieger Publishing Co.

Viollet, P. L., Simonin, O., Olive, J. & Minier, J. P. Modelling turbulent two–phase flows in industrial equipments. In C. Hirsch, ed. 1992 *Computational Methods in Applied Sciences.* Elsevier Science Publishers.

Weiland, R. H., Fessas, Y. P. & Ramarao, B. V. 1984 On instabilities arising during sedimentation of two–component mixtures of solids. *J. Fluid Mech.* **142**, 383–389.

Zhang, D. Z. & Prosperetti, A. 1994 Averaged equations for inviscid disperse two–phase flow. *J. Fluid Mech.* **267**, 185–219.

Los Alamos
NATIONAL LABORATORY
Los Alamos, New Mexico 87545